Variation in *Pseudotsuga menziesii* foliar fungal endophyte community composition over a growing season.

by

Callah McCarroll

A Thesis Submitted in Partial Fulfillment of the
Requirements for the Degree of

BACHELOR OF SCIENCE (HONS.)

in the Department of Biology

University of Victoria

Variation in *Pseudotsuga menziesii* foliar fungal endophyte community composition over a growing season.

by

Callah McCarroll

Supervisory Committee

Dr. Jürgen Ehlting, Supervisor
Department of Biology

Dr. Barbara Hawkins, Honours Advisor
Department of Biology

Dr. Terri Lacourse, Honours Advisor
Department of Biology

Abstract

Plants host a diverse array of micro-organisms referred to as endophytes, which reside primarily in the interstitial spaces between plant cells. Endophytes often exist in complex communities composed of multiple species from multiple kingdoms, although fungi are the most common colonizers of plant tissues. These micro-organisms interact with each other and with the host, sometimes resulting in altered phenotypes for the host plant which can be beneficial or detrimental. Determining what drives the structure of these community assemblages is a key prerequisite for understanding the overall nature of microbial ecology. Douglas-fir trees (*Pseudotsuga menziesii*) are a keystone species threatened by disease, climate change, and human development, and like all plants, they harbour a diverse suite of fungal endophytes. In this research, the temporal dynamics of Douglas-fir foliar fungal endophyte communities was systematically characterized over an entire growing season. This was done by collecting Douglas-fir needles from 16 trees in a single location six different times over a calendar year. High-throughput sequencing-based metabarcoding was employed to amplify fungal ITS1 sequences for identification of fungal endophyte community members within Douglas-fir leaf tissue at different times of the year. Using both Alpha and Beta diversity measures, this research was able to show significant community dissimilarity between sampling months. This research also described a dominant unknown endophyte within the order of Mycosphaerellales appearing to have a negative relationship with *Nothophaeocryptopus gaeumannii*, a well studied Douglas-fir endophyte and causal agent of Swiss needle cast disease. This is the first seasonal description of fungal endophytes within Douglas-fir needles using meta-barcoding analyses.

Table of Contents

Supervisory Committee ………………………………………………………………..……….. ii

Abstract ……………………………………………………………………..…………... iii

Table of Contents …………………………………………………………...………… iv

List of Tables ……………………………………….……………………………….…….. vi

List of Figures ……………………………………….………………..…………….….. vi

Acknowledgements ……………………………………………………………………... ix

Introduction ………………………………………………………………….………….... 1

Endophytes ……..……..………………….……...…………………………..…... 1

Drivers of Fungal Endophyte Infection……………..……………………...…... 4

Pseudotsuga menziesii …….……………….……………………………….……………... 5

Douglas-fir Needle Endophytes……………………………………………….……… 5

Seasonal Changes in Endophyte Communities of Douglas-fir Needles………..……….. 7

Materials and Methods ……...…………………………………………….………………... 8

Results …………………………………………………………………….………………. 15

DNA extraction & sequence processing ……………...…………………………... 15

Phylogeny & taxonomic resolution …………………...…………………………….. 17

Alpha Diversity…………………………………………………………………...….. 20

Beta Diversity………………………………………………………….…..………… 21

Relative Abundance & Seasonal Fluctuation…………………………………………… 25

Nothophaeocryptopus gaeumannii & Mycosphaerellales sp3………………………….. 29

Fungal Traits Assignment……………………...……………………………….. 29

Discussion ……………………………………………………………………..………... 31

Seasonal Drivers of Endo-Mycobiome Diversity ……...…………………...….. 31

Basidiomycetes ………...…………………………...……………………….…. 33

Nothophaeocryptopus gaeumannii & Mycosphaerellales sp3………………………….. 34

Fungal Traits……………………………………...……………………………….. 35

The OTUs Driving Seasonal Community Variation……………….……………………… 36

Filtering……………………………………………………………….……………………… 38

Future Outlook………………………………………………………………………….. 39

Conclusion ………………………………………………..…………………….……….... 40
References ………………………………….…………...…………………….……….... 41
Appendix A: Metadata …………………………………………………………………. 53
Appendix B: Culture Based Taxonomy…..….…………………………………………. 56
Appendix C: Fungal Traits Assignments…………………………………..………………... 58
Appendix D: Full OTU Taxonomy List………………………………………………... 60
Appendix E: Stomatal Occlusion by Month…………………………………………… 69

List of Tables

Table 1. Quality processing of fungal ITS1 rRNA short read amplicons performed in QIIME2 for 94 samples collected from 16 Douglas-fir trees semi-monthly over the 2025 growing season... 17

Table 2. Fungal OTUs with significant differential abundance between sampling months as determined by ANCOM analysis in Qiime2…………………………………….…………...…. 28

Appendix A, Table 1. Brush species composition adjacent 16 trees at the West45 research site collected over the 2025 growing season. Crown closure (cc) and heights (cm) are listed for each brush species at each tree ………………………………………………………………… 53

Appendix A, Table 2. Metadata collected from year 2 needles of 16 trees at the West45 research site over 2025 growing season …………………….………………………………………..... 55

Appendix B, Table 1. Douglas-fir needle fungal endophyte taxonomy acquired through culture-based methods using Sanger sequencing to compare against fungal endophyte taxonomy acquired through Illumina sequencing…………………………………….…………….... 56

Appendix C, Table 1. Annotated functional traits for fungal endophytes of Douglas-fir needles ……………….…………………………………………………………...………………….. 58

Appendix D, Table 1. Full list of OTU taxonomic assignments for fungal endophytes found in Douglas-fir needles collected from 16 trees at the West 45 research site over the 2025 growing season (n = 94)……………………………………………………...………………….. 60

List of Figures

Figure 1. West45 B.C. Ministry of Forests Douglas-fir breeding research site located ~ 10 km West of Jordan River on Vancouver Island, British Columbia.……………..……..…………..… 8

Figure 2. Collection dates, total precipitation, and temperatures with seven-day averages accompanied by likely Douglas-fir phenological events for the 2025 growing season ……..…. 15

Figure 3. DNA quality assessments and gel electrophoresis images for 94 samples…..………. 16

Figure 4. Krona plot showing the overall percent of sequence reads represented by taxa present in 93 samples of Douglas-fir needle DNA……………………………...…………………… 19

Figure 5: Phylogenetic tree constructed using ITS fungal sequences from 16 Douglas-fir trees depicting only lineages resolved to the class of Dothideomycetes within the phylum Ascomycota……………………………………………………………………………….. 20

Figure 6: Boxplot showing Shannon's Diversity Index for fungal endophyte communities of Douglas-fir needles grouped into sampling months……………………………………….. 21

Figure 7: Beta Diversity measures showing pairwise distance values for within-month sample comparisons and between-month sample comparisons using Bray-Curtis, Weighted UniFrac, & Unweighted UniFrac………………………………………………………………………. 23

Figure 8: Beta Diversity determined using distance matrices show significant pairwise dissimilarity between fungal endophyte communities grouped by sampling month using Bray-Curtis, Weighted UniFrac, & Unweighted UniFrac……………………………………….. 23

Figure 9: PERMDISP comparison of fungal community dispersion among months based on unweighted UniFrac distances comparing fungal endophyte communities of Douglas-fir needles……………………………………………………………………………………….. 24

Figure 10: Relative abundance of fungal endophytes of Douglas-fir needles from 16 trees grouped by sampling month. Relative abundance is displayed both with and without dominant taxa…………………………………………………………………………………..….. 26

Figure 11: Boxplot showing Basidiomycete endophytes increase in mean relative abundance as the 2025 growing season progresses………………….……..……………………………. 27

Figure 12: Top 12 most fluctuating individual OTUs from Douglas-fir needles collected semi-monthly from 16 trees over a growing season ………………………………………………. 27

Figure 13: ANCOM volcano plot showing differential abundance of taxa among sampling months……………………………………………………………………………………... 28

Figure 14: Negative correlation between *Nothophaeocryptopus gaeumannii & Mycosphaerellales sp3;* line graph showing relative abundance of *Nothophaeocryptopus gaeumannii & Mycosphaerellales sp3* over the sampling period and a **s**catterplot showing *N. gaeumannii* relative abundance on the y-axis and *Mycosphaerellales sp3* relative abundance on the x-axis……………………………………………………………………………………... 29

Figure 15: Annotated functional traits for fungal endophytes of Douglas-fir needles collected over a growing season. Trophic modes are grouped by month showing relative abundance on the y-axis……………………………………………………………………………..….. 30

Appendix E, Figure 1: Monthly average of proportion of stomata occluded by N. gaeumannii pseudothecia. Data were acquired from needles 16 Douglas-fir trees collected eight times over the 2025 growing season…………………………………………………………………..…. 69

Acknowledgements

I would like to thank Jürgen Ehlting for allowing me this opportunity to engage in meaningful research. I would also like to thank Randi Church and Olivia Osborne for helping with Douglas-fir needle collection, and Eve Kenny and Declan McIntosh for SNC metadata acquisition. I would also like to extend my gratitude to honours advisors Terri Lacourse and Barbara Hawkins. Funding for this research was granted through the GeneSolve project "Genetic and biotic factors influencing tolerance of Douglas-fir to Swiss Needle Cast" from Genome British Columbia.

Introduction

Endophytes

Microorganisms provide some of the most diverse ecosystem services on a global scale; phytoplankton (microalgae) produce half of the Earth's oxygen, fixing an equal amount of carbon (Field *et al*., 1998), mycorrhizal fungi draw down 13 billion tonnes of CO_2 every year (Hawkins *et al*., 2023), fungi are primarily responsible for degrading lignocellulose, effectively clearing massive quantities of wood debris from landscapes and recycling carbon (Andler *et al*., 2018), and *Rhizobium* bacteria fix atmospheric nitrogen into forms usable by food crops (Masson-Boivin & Sachs, 2018). Microorganisms are also behind some of the most important discoveries in human history; secondary metabolites produced by the fungus *Penicillium chrysogenum* revolutionised modern medicine (Ligon, 2004), yeasts have been providing essential services in the making of bread and our much-cherished alcoholic beverages for over 9000 years (Phillips, 2014), the discovery in 1890 that microbes were responsible for many illnesses turned medicine into a science, and we are now just realising that microbial diversity is essential for holistic health (Chen *et al*., 2019). We owe much to microbes, least of which is general curiosity towards the microbial world.

Plants and microorganisms engage in symbiotic relationships dating back to plant terrestrial colonization over 430 million years ago (Berbee & Taylor, 2007), and possibly dating back a billion years according to phylogenomic analysis (Berbee *et al*, 2020). This long history of co-evolution has led to a diverse spectrum of symbioses spanning the entire plant kingdom. In fact, microbe infection is so ubiquitous that it appears to be the rule, while existing microbe-free is the exception (Sieber, 2007; Partida-Martínez & Heil, 2011). Endophytes are microorganisms that live within plant tissues for part or all of their life cycle, and comprise the microbiome of a plant, along with epiphytes and mycorrhizae (Liao *et al*., 2025). The definition for endophyte is hotly debated and, while I prefer the simple definition as being "any organism living within plant tissues" (de Bary, 1866), endophytes are currently described as "asymptomatic microbial partners that are intimately associated and co-inhabit within healthy internal plant tissues with the ability to confer benefits, co-evolve and alter their lifestyle depending upon plant life stages and adverse conditions" (Liao *et al*., 2025). However, this later definition reflects an idealism common in endophyte research, in which speculative benefits are emphasized for potential commercial value. Epiphytes occupy the outer surfaces of plants, and some can transition to being endophytes at certain life stages, while mycorrhizae are fungi that colonize root systems and are defined separately from endophytes due to differing lifestyles (Liao *et al*., 2025). Bacteria, archaea, fungi, viruses, and protists have all been observed as endophytic microbes (Hardoim *et al*., 2015; Chow *et al*., 2022; Liao *et al*., 2025; Santoyo *et al*., 2025), and I believe it is important to enhance our understanding of the roles these endophytes play in order to better understand the wildly complex interconnectedness of nature and ecosystems.

It has been shown that microorganism communities can differ greatly between the inside and outside of a plant, between plant species, between plant tissues, and between ecosystems (Sieber, 2007; Liao *et al*., 2025), although exceptions to this pattern exist (Massoni *et al*., 2020). Clear differences are often observed between foliar, seed, fruit, stem and root endophyte communities, which may reflect variation in environmental exposure. For example, roots are more likely to be colonized by soil-associated microbes, flowers can acquire microorganisms from pollinators, seed endophytes are frequently transmitted vertically from the mother (Newcombe *et al*., 2018), and leaves are more likely to intercept wind-dispersed spores (Hardoim *et al*., 2015; Fitzpatrick *et al*., 2020). Microbial colonisation is also reliant on host species, and specific mechanisms are at play in both plants and microbes to facilitate infection (Zipfel & Oldroyd, 2017). Plants have sophisticated immune response systems to keep most microbes out and a selection process in place to allow entry to beneficial endophytes, conversely, many infecting microbes have mechanisms to avoid plant defense systems (Zipfel & Oldroyd, 2017). Immune signalling and metabolite biosynthesis vary depending on host and/or microbe genetics, which creates host dependent endophyte communities (Redman *et al*., 2001; Ludwig-Müller, 2015; Zipfel & Oldroyd, 2017).

Microbial infection spans the range of symbioses from mutualism to parasitism (Sieber, 2007), although the majority of endophytes reside in plants in a commensal manner, wherein the plant host suffers no harm, nor gains any benefit (Hardoim *et al*., 2015; Brader *et al*., 2017). Many commensal endophytes become saprobes, degrading dead plant tissue upon senescence (Promputtha *et al*., 2010). Some endophytes can adopt a pathogenic or parasitic lifestyle, causing disease symptoms or depleting plant resources (Brader *et al*., 2017). Disease symptoms caused by fungal pathogens can depend on multiple factors, including interactions among fungal endophytes; for example, mango malformation disease involves a complex of six *Fusarium* species (Freeman *et al*., 2014). Le May *et al*. (2009) demonstrated that fungal establishment in plant tissues is strongly influenced by the order of colonization, showing that co-inoculation of two fungal pathogens reduced disease symptoms on pea leaves, whereas successive inoculation increased symptom severity. Fungal endophytes can also be mutualists, offering great advantages to hosts by producing secondary metabolites that deter herbivores, or confer tolerance to biotic and abiotic stressors (Sieber, 2007; Aghai *et al*., 2019; Watts *et al*., 2023). Native endophyte *Phiocephala scopiformis* was found to reduce spruce budworm damage in *Picea glauca* (white spruce) trees in eastern Canada (Quiring *et al.,* 2019) resulting in the commercial production of Rugulosin as a biocontrol agent. Redman *et al*. (2002) showed that *Dichanthelium lanuginosium* (rosette grass) and its fungal symbiont were mutually dependent, as neither species could survive the extreme temperatures of their geothermal habitat in Yellowstone National Park when cultivated alone. Research also shows that fungal endophytes previously designated as mutualists can alter their lifestyle to become pathogens, and vice versa. Redman *et al*. (2001) showed *Colletotrichum* species to be either pathogenic, mutualist, or commensal depending on plant host family. This display of plasticity is not only regulated by host species, life stages, and environmental cues, but also by specific microbes or microbial communities (Redman *et al*., 2001). Inter-microbe interactions, as well as plant-microbe interactions, lead to co-regulation of gene expression, resulting in phenotypic plasticity for both host and endophyte (Goh *et al*., 2013; Ludwig-Müller, 2015; Raza *et al*., 2024).

A popular example of endophyte contribution to pharmacological advances is Taxol from Pacific Yew; a bark-inhabiting fungal endophyte was shown to produce Taxol (Stierle *et al*., 1993), and later research showed that Taxol production increased eightfold in the presence of a second unique fungus (Soliman & Raizada, 2013), showing that metabolite biosynthesis can be triggered by multiple actors. To make things more complicated, even endophytes can have endosymbionts; pathogenic fungus *Rhizopus,* known to cause rice seedling blight, owes its toxicity to its own endosymbiotic bacterium (Partida-Martinez & Hertweck, 2005). The holobiont community appears to work as a consortium, engaging in inter-domain and inter-kingdom communication via chemical signalling (Ludwig-Müller, 2015; Geetha *et al*., 2020), and understanding these interactions would be the ultimate goal in a holistic approach to endophyte research, but this study focuses only on fungal endophytes. Fungi appear to make up the majority of endophytes (Rana *et al.,* 2020), and have been shown to confer a range of benefits to hosts. Drought tolerance could have major implications for crop species in the face of climate change, and conifer seedlings inoculated with a specific consortium of fungal endophytes showed greater survival in drought and stress conditions (Aghai *et al*., 2019). Substantial benefits can come from a deeper understanding of fungal microbes.

Drivers of Fungal Endophyte Infection

Environmental factors that influence fungal endophyte infection can vary greatly over a growing season. It has been shown that dry, hot conditions are conducive to higher concentrations of airborne fungal spores (Katial *et al*., 1997; Pakpour *et al*., 2015) while precipitation reduces airborne fungal load, presumably by 'washing' spores from the air (Katial *et al*., 1997; Pakpour *et al*., 2015). Peak airborne fungal spore concentrations were observed mid to late summer (Katial *et al*., 1997). Species diversity in sporulation timing influences aerial spore composition (Katial *et al*., 1997), and it has been shown that foliar mycobiome composition changes from season to season and from year to year (Solheim *et al*., 2021; Gervers, 2024; Brodski *et al*., 2025; Szymanski & Miles, 2025). Solheim *et al*. (2021) found fungal endophyte richness of *Pinus sylvestris* (Scots pine) needles to be highest in fall. In a three-year trial, Broski *et al.* (2025) also reported higher fungal endophyte species richness in *Betula pendula* (silver birch) leaves in fall for two consecutive years, while year three did not show higher richness in fall, likely reflecting yearly seasonal variation.

Many fungal endophytes were found to be geographically bound by environmental conditions and landscape fragmentation (Bowman & Arnold, 2021), and sampling site had the highest influence on fungal endophyte community composition in Northern European Scots pine (Solheim *et al*., 2021). Wet leaf surfaces promote fungal infection (Bradley *et al*., 2003) therefore humidity fluctuations may drive mycobiome composition and load as well. Brodski *et al.* (2025) showed a shift in silver birch foliar fungal community structure with increased humidity treatment. Mobilization of non-structural carbohydrates between plant inner tissues occurs throughout the growing season (Wong *et al*., 2003) which may impact fungal communities as well. Conifer needles accumulate starch at the onset of spring with levels remaining higher throughout early summer, while soluble sugars increase in fall and stay high over winter, then drop during summer months (Schoonmaker *et al*., 2021). Dynamic sugar distribution due to tree phenology may contribute to hyphal growth and fungal load, as endophytes are thought to acquire carbon from plant hosts (Lam *et al*., 1994; Cosner *et al*., 2025).

Pseudotsuga menziesii

Douglas-fir (*Pseudotsuga menziesii*) trees are evergreen conifer species in the pine family (Pinaceae) and are the tallest species of this family, growing up to 60m tall and with a life span of roughly half a millennium. There are two subspecies of Douglas-fir; a coastal variety (var *menziesii*) found across Vancouver Island and parts of the southern coast, and an interior variety called Rocky Mountain Douglas-fir (var *glauca*) found throughout much of southern British Columbia (Natural Resources Canada, n.d.). Douglas-fir trees are keystone species, shaping the biotic terrestrial landscape and serving as critical habitat to a diverse range of species and offering invaluable ecosystem services (Perry, 1996; Simard *et al.*, 2020). Unfortunately, coastal Douglas-fir ecosystems are currently impacted by human development (Flynn, 1999). As with the vast majority of plants (Partida-Martínez & Heil 2011), Douglas-fir trees harbour diverse communities of micro-organisms (Carroll & Carroll, 1978; Kiser *et al*., 2019; Gervers, 2024; Hayward, 2024) whose niche roles have yet to be parsed for the most part. Understanding this microbial ecology bolsters a holistic approach to future conservation of this ecosystem asset.

Douglas-fir Needle Endophytes

The mycobiomes within Douglas-fir needles have been previously studied through culturing methods, wherein hyphae grow from needles into media, and are subsequently isolated for identification. In this manner, Carroll and Carroll (1978) demonstrated that fungal endophytes are widespread and commonly occur as asymptomatic infections within Douglas-fir needles, showing that endophyte infection is a ubiquitous feature of conifer needles. Kiser *et al*. (2019) isolated and identified a diverse assemblage of culturable fungal endophytes from Douglas-fir needles, reporting 39 taxa from 215 needles. In her thesis, Hayward (2024) isolated and identified 38 species of fungal endophytes from 100 Douglas-fir trees on Vancouver Island, showing Sordariomycetes to be the dominant Class among culture sequences.

Recently, NextGen sequencing using high throughput meta-barcoding has been made available for microbiome analyses, wherein amplification of a specified non-conserved gene region is used for quantification and taxonomic identification of microbial community members.

The internal transcribed spacer (ITS) region of ribosomal DNA (rRNA) is amplified for fungal specimens (Abdelfattah *et al*, 2019). This method can identify previously un-culturable endophytes, offering great opportunities to better understand Douglas-fir microbiomes. Hayward (2024) complemented her culture-based work with NextGen meta-barcoding sequence analyses of needles from 60 Douglas-fir trees, and in this manner, found Dothidiomycetes to be the dominant Class, namely the species *Nothophaeocryptopus gaeumannii,* contrasting with her culture-based findings. Gervers (2024), through similar methods, found both *Nothophaeocryptopus gaeumannii* and *Rhabdocline parkerii* to dominate high-throughput sequencing data from Douglas-fir needle tissue. Gonan (2022) sampled recently abscised needles and found them to be dominated by *Rhabdocline parkerii* as well as *N. gaeumannii.*

N. gaeumannii is the causal agent of Swiss Needle Cast which is native pathogen of Douglas-fir trees. Incidence of this disease increases with warmer winter temperatures and with the forestry practice of planting trees outside their natural range (Manter et al., 2005). This fungus becomes pathogenic when pseudothecia, the fruiting bodies, grow through stomata blocking gas exchange. This causes eventual needle senescence when pseudothecia block a critical number of stomata (Stone *et al*., 2008). Hyphae of a single spore can continue to grow internally and externally, reinfecting through unoccupied stomata (Stone *et al*., 2008). *R. parkerii* is another ubiquitous fungal endophyte that persists in a latent state infecting a single cell, then spreading throughout leaf tissue only after needle abscission (Sherwood-Pike *et al*., 1986). In this manner, *R. parkerii* often dominates Douglas-fir needle culture sets (Kenny, unpublished). *R. parkerii* was also seen to reduce *Contarinia* (gall midge) larvae in Douglas-fir needles, displaying a mutualistic association (Sherwood-Pike *et al*., 1986).

Through their work using high-throughput meta-barcoding, Gonen (2020) demonstrated that foliar fungal and oomycete communities in Douglas-fir needles are strongly structured by both needle age and crown microenvironment, with older needles supporting more differentiated and diverse communities. Later work by Gervers (2024) supported these findings, showing that tree canopies represent complex environmental gradients. He also showed that relative abundance of dominant taxa differed between sampling years, site location, and tree ecotype (Montane vs Coastal). Hayward (2024) found no clear patterns associating the abundance of *Nothophaeocryptopus gaeumannii,* or specific endophyte community assemblages, to Swiss needle cast severity. However, she did observe a negative correlation between *N. gaeumannii* and *Rhizosphaera sp*.

Seasonal Changes in Endophyte communities of Douglas-fir Needles

Only three studies have described the endo-mycobiome of Douglas-fir needles using NextGen meta-barcoding sequencing techniques, and of these, Gonan (2020) collected samples once in April and once in May, Hayward (2024) collected samples once in June, while Gervers (2024) sampled his study trees for three consecutive years in either August or September. Douglas-fir research lacks a description of foliar fungal endophyte community succession over an entire growing season. Research of fungal endophyte communities of varied organisms has revealed that seasonal changes strongly influence community structure. Investigations into fungal endophytes of *Eucommia ulmoides* (hardy rubber tree) in China and *Pinus sylvestris* (Scots pine) in Northern Europe, found significant community differences between seasons (Solheim *et al*., 2021; Tang *et al*., 2024). I thus hypothesize that Douglas-fir needles harbor complex, seasonally structured fungal endophyte communities.

Vancouver Island is particularly well suited for studying seasonal variation because our growing season provides a range in temperature and moisture regimes, with cool wet winters and warm dry summers, offering diverse conditions for fungal infections and endophyte interactions within Douglas-fir needles. In this research, I aim to provide a description of the temporal variation of fungal endophyte community structure and composition over an entire growing season in a coastal location on Vancouver Island. To accomplish this, 16 trees were sampled from a location within the coastal fog belt six times over a growing season. Sampling dates were selected to represent major weather changes. This research will expand our understanding of fungal endophyte ecology and bolster knowledge to help further conservation efforts and improve forestry practices.

Materials & Methods

West 45 Research Site

Douglas-fir needles were collected from the West45 BC Ministry of Forests research site (48°27′30″N 124°08′49″W) located roughly 10 km northwest of Jordan River on Vancouver Island, British Columbia (Figure 1). The site is located ~ 2 km north/northeast of the Salish Sea within the fog belt, and is therefore heavily influenced by marine weather and humidity. The site is south/southwest facing, at an elevation of 230 m – 250 m with a ~20 m elevation gain, resulting in a gentle slope angle of ~ 12°. There is low to moderate brush competition (Appendix A, Table 1), primarily from cherry (*Prunus emarginata*) and huckleberry (*Vaccinium parvifolium*), and the site has been mechanically brushed twice to reduce competition. The site was planted at an inter-tree distance of 2m x 2m in 2019, with seedlings sown in 2017. The site was planted 95 families, and each family is comprised of full siblings produced through controlled fertilisation wherein the pollen (father) and megaspore (mother) were carefully selected through the Douglas-fir tree breeding program run by the BC Ministry of Forests (BC Ministry of Forests, 2024). The site was established to challenge Douglas-fir against Swiss Needle Cast and employed an Alpha-lattice design, which optimizes

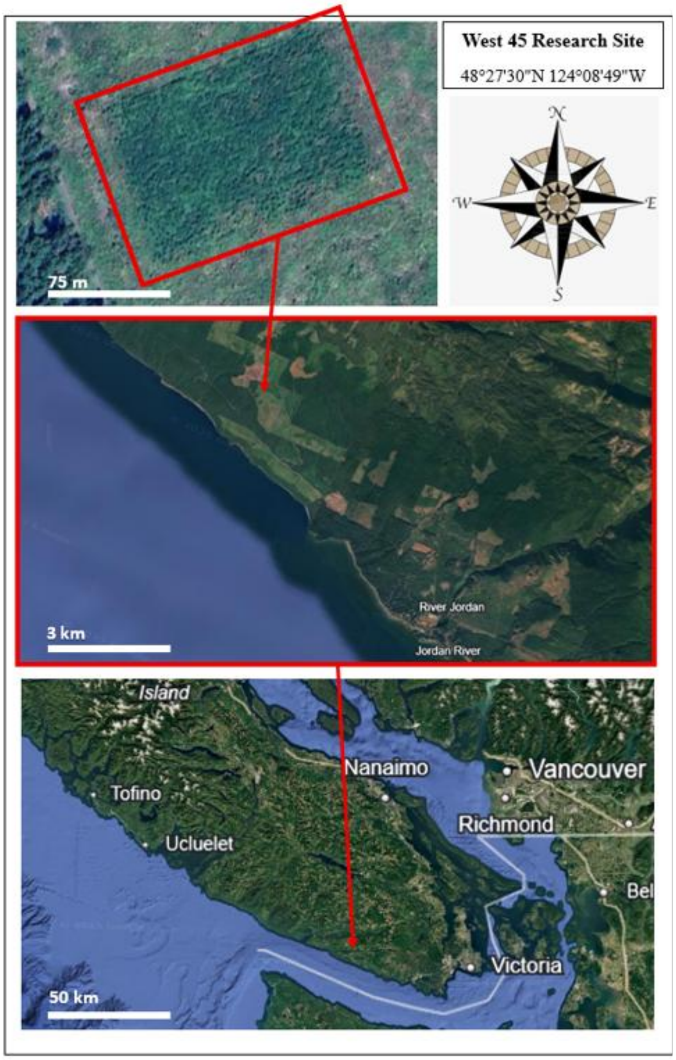

Figure 1: West 45 B.C. Ministry of Forests Douglas-fir breeding research site located ~ 10 km West of Jordan River on Vancouver Island, British Columbia.

treatment replication while minimizing environmental variation and maintaining balanced comparisons among treatments (Degner, J., personal communication, 2026).

Tree Selection, Controls, and Meta-Data

Of the families available for this research, three families of Coastal BC origin (Families 34, 46, & 14) and one family of Interior BC origin (Family 64) were chosen. The Interior BC and Coastal BC lineages represent two separate subspecies. From each family, 4 trees were selected for a total of 16 trees. All 16 trees were selected based on proximity to each other in the field to reduce microclimatic variability within the site. Tree heights ranged from 2 to 6 meters in the spring of 2025 (Appendix A, Table 2) and at each tree, one south facing branch was selected at mid-crown height and marked with ribbon for future identification. At each sampling event, ten needles were taken from year two growth only, and only taken from the marked selected branch. Needles were cut off with scissors rather than torn, to reduce induction of plant defense systems. All samples were kept cool until return to the lab and then stored at 4˚C. Needle collection was done in four-to-nine-week intervals, aiming to capture major weather changes. In spring and late fall, all trees were measured for height and stem diameter at breast height (DBH), neighboring plant and brush species and densities were recorded throughout the summer. Soil type and soil pH was recorded at each tree (Appendix A, Table 2). Swiss Needle Cast (SNC) signs and symptoms were assessed, including stomatal occlusion at each sampling date and needle loss for four dates during the 2025 growing season. SNC signs and symptoms were also assessed by BC Ministry of Forests staff for Swiss Needle Cast in 2025 and the West45 site was found to have high severity (Degner, J., personal communication, 2026).

Surface Sterilization & Cleaning

All needles were surface sterilized and washed to remove epiphytes and excess *N. gaeumannii* pseudothecia. Each set of needles was submerged in 0.01% Tween 20 for 5 minutes. Samples were then vortexed for 60 seconds to dislodge contaminants and then centrifuged for 30 seconds to pellet contaminants. Needles were then removed from the Tween solution using tweezers sterilized between each sample, and allowed to airdry on clean Kimwipes. Using another clean Kimwipe, each set of needles was rubbed to dry and remove any excess pseudothecia and epiphytes, then returned to new tubes and frozen at -20˚C until further steps.

DNA Extraction

Of the eight seasonal samples collected, six were chosen for DNA extraction and ITS sequencing; February 8, April 4, May 8, June 29, August 18, and November 4. These dates were selected based on phenological events and seasonal temperature changes (Figure 2). One study tree died in June and had no needles by August; therefore, a total of 94 samples were further processed (16 samples for each 4 sampling dates prior to August, and 15 samples each for August & November). One negative sample containing no needle tissue or sample DNA was processed using identical reagents and methods as all other samples. The negative control was carried through the extraction procedure to identify potential contaminants. Prior to extraction, 5 needles from each sample set were added to screw cap tubes with three sterilized 3.0 mm glass beads in each tube. These tubes were immediately frozen in liquid nitrogen, then homogenized in a Retsch® MM301 Mixer Mill (VERDER Group) for 30 seconds at 30 Hz, then immediately returned to liquid nitrogen for 60 seconds. These freeze and bead beat steps were repeated until all the needle material was reduced to powder, typically 3-4 cycles. DNA extraction was performed using the Mackery-Nagel NucleoSpin® Plant II Mini kit (MACHERY-NAGEL GmbH & Co KG) as per the manufacturer's protocol using the SDS based extraction buffer PL2 and with minor modifications; samples were incubated at 65˚C for 60 min on a heat block after addition of PL2 buffer also, and after incubation on ice for 5 minutes, the samples were centrifuged at 11,000 x g for 30 min to pellet debris. Clear supernatant was removed and the following steps were done following the manufacturers protocol. DNA was eluted in 75 µL of elution buffer PE.

DNA Sample Quality Assessments

Spectrophotometric quality assessment of DNA samples was performed using NanoDrop™ 2000 (Thermo Fisher Scientific™). Genomic DNA samples were assessed visually for DNA integrity using 0.9 % agarose gel electrophoresis. PCR reactions were performed to validate suitability of isolated DNA by amplifying the full internal transcribed spacer (ITS) region of fungal ribosomal DNA to confirm fungal material presence (Figure 3). The ITS primer set used was as follows; ITS1F-KY02 (TAG AGG AAG TAA AAG TCG TAA; Toju *et al*., 2012) and ITS4-KY01 (TCC TCC GCT TWT TGW TWT GC; Toju *et al*., 2012). PCR reactions contained 10% 10X Dream Taq Green buffer (Thermo Scientific), 47% sterile ddH$_2$O, 0.2 mM dNTPs, 0.5 μM ITS1F-KY02, 0.5 μM ITS4-KY01, 0.0125 mg/mL BSA, 0.25 % DMSO, 1% Dream Taq DNA Polymerase (Thermo Scientific), and 2.0 μL of diluted sample DNA per reaction. The Eppendorf Mastercycler Gradient model 5331 thermocycler was used for all reactions, and set to run as follows; 3 min at 94°C, then 35 cycles of 45 sec at 94°C, 30 sec at 55°C, and 40 sec at 72°C, with a final 10 min at 72°C, then held at 10°C after cycling. PCR samples were assessed visually for fungal DNA using 1.0% agarose gel electrophoresis. Low quality samples were identified by their spectrophotometric results; DNA concentration over 30ng/μL, 260/280 ratios above 1.8, and 260/230 ratios above 2.0 were considered acceptable. Low quality samples were re-extracted from the remaining surface sterilized needles stored at -20°C.

Illumina MiSeq Amplicon Sequencing

A total of 95 samples (20 μL each) were shipped on ice packs to Dalhousie University Integrated Microbiome Resource (IMR; Halifax, Nova Scotia, Canada) for ITS-amplicon library preparation and high throughput sequencing. For library preparation, DNA samples were split into two reactions; one at 1:1 dilution and one at 1:10 dilution. A single round of multiplexed PCR amplification was performed using fusion primers containing Illumina adaptors, library indices, and ITS1 custom primers ITS1F (5'- CTTGGTCATTTAGAGGAAGTAA-3'; Gardes & Bruns, 1993) and ITS2 (5'-GCTGCGTTCTTCATCGATGC-3'; White *et al.,* 1990) and using high-fidelity Phusion Plus polymerase. The PCR reactions of the two dilutions were then pooled, cleaned, then normalized following IMR standard protocols, and added to a pool of up to 380 other samples to generate a sequence library. The library was quantified fluorometrically and then sequenced using Illumina MiSeq i100 300+300 bp XLEAP kit targeting 30,000 paired-end reads per sample.

ITS Sequence Data Quality Processing and Taxonomic Assignment

All MiSeq sequence amplicon reads were prepared for downstream analyses using the QIIME2 2025.7 environment (Boylan *et al.,* 2019). FastQC Reports (v0.11.9; Brabraham Bioinformatics) were generated to assess sequence quality and representation prior to subsequent quality trimming. Primer sequences were removed from paired-end demultiplexed sequence reads using CutAdapt (Martin, 2011). Denoising, dereplication, chimera detection, and merging reads into ASVs (Amplicon Sequence Variants) was performed using DADA2 (Callahan *et al.*, 2016). Both forward and reverse reads were truncated at 260 bp and 240 bp respectively to remove poor quality read ends and optimize merging success. Taxonomic assignments were performed using the UNITE fungal ITS database (Abarenkov *et al.*, 2025) with an ITS sequence similarity threshold of 99% using a Naive Bayes classifier implemented in the QIIME2 q2-feature-classifier plugin (Bokulich *et al*., 2018) based on k-mer composition statistics through scikit-learn machine learning library (Pedregosa *et al*., 2011). ASVs were then clustered to representative sequences at 97% identity in QIIME2 using VSEARCH (Rognes *et al*., 2016) with centroid style clustering, creating OTUs (Operational Taxonomic Units). Filtering was done after OTU collapse. Any OTU not resolved as Fungi was filtered out, and all OTUs represented by less than 25 reads or presented in only one sample were removed from the data set to account for Illumina bleed through and contamination, and to focus subsequent analyses on consistently detectable fungal OTUs. All OTUs found in frequencies less than or equal to the negative control were also removed.

OTU taxonomic assignments were confirmed through sequence alignment statistics against the NCBI Core nucleotide database, containing compiled records from GenBank, RefSeq, and other International Nucleotide Sequence Database Collaboration repositories. (Camacho *et al.*, 2009). Taxonomic re-assignments were done manually and conservatively to resolve misclassifications or for higher resolution. All manual changes were documented and applied consistently across analyses. To confirm 97% clustering for highly repetitive taxonomic assignments, multiple sequence alignments were performed in MEGA12 (Kumar et al., 2024) using the MUSCLE algorithm (Edgar, 2004). Distance matrices were created in MEGA12 using a p-distance model, then exported to excel where percent identity was calculated using the following formula: % identity = (1 − p-distance) × 100. With this method, OTUs > 97% identical were grouped as one OTU. OTUs clustered with MEGA were denoted with an asterisk (*), but were not collapsed prior to statistical analyses, therefore this assignment is for discussion purposes only and are referred to as Biologically Unique Features. To expand identification efforts, dominant fungal OTUs with poor taxonomic resolution were aligned against a manually compiled database composed of full ITS Douglas-fir needle fungal endophyte sequences acquired through culture-based methods sourced from a site near Jordan River (Kenny, E., unpublished data; Appendix B). To do this, full ITS sequences were exported to QIIME2 to generate a reference database which was then aligned to taxonomically unresolved OTUs of my data using VSEARCH (Rognes *et al*., 2016).

All OTUs were assigned a species level taxonomy string wherein the species name was the highest resolved rank with multiples being assigned a species number, e.g.; k__Fungi;p__Ascomycota;c__Dothideomycetes;o__Mycosphaerellales;f__Unknown;g__Unknown;s__*Mycosphaerellales_sp3*. Multiple species resolved to the same species with < 97% similarity were assigned a variant number, e.g.; k__Fungi;p__Ascomycota;c__Dothideomycetes;o__Mycosphaerellales;f__Teratosphaeriaceae;g__Catenulostroma;s__*Catenulostroma_hermanusense_var2*. This was done to protect the integrity of fungal diversity.

Tree 555 was effectively dead for June sampling, with dry brown needles. This sample was removed from the dataset prior to statistical analyses (n = 93), as it would contain more saprotrophic fungi and not be a biologically accurate representative of living systems. Taxonomy was reimported into QIIME2, and a taxonomic tree was constructed from OTU sequences acquired through this research. OTU sequences were aligned using MAFFT v7 (Katoh & Standley, 2013) and a phylogenetic tree was inferred with FastTree 2 (Price *et al*., 2010). Taxonomic tree visualization using iTOL (Letunic & Bork, 2021) was used to infer general phylogeny for unresolved dominant taxa. Tree distances were used for downstream statistical analyses. Functional traits were assigned to taxa resolved to the genus or species level using the FungalTraits database (Põlme *et al*., 2020) in RStudio.

Statistical Analyses

Differential abundance between months was assessed using ANCOM (Mandal *et al*., 2015) implemented in QIIME 2. Alpha and Beta diversity PERMANOVA distance matrices were computed in QIIME2 using the Qiime2 diversity core-metrics-phylogenetic tool with rarefaction set to a depth of 29,000. A pooled taxonomy Krona plot was generated using the Krona visualization tool (Ondove *et al*., 2011). Distance matrices and relevant files were exported to R v4.5.1 (R Core Team, 2024) for further statistical analyses and figure generation using the RStudio integrated development environment (Posit Team, 2024). Unweighted UniFrac PERMANOVA results were tested using a PERMDISP comparison of dispersal. Relative abundance was calculated as ($\frac{Feature\ Count}{Total\ reads\ per\ sample}$) for each sample, then averaged over each month to show monthly variation. To test the fluctuation of Basidiomycete fungal endophytes over a growing season, a Kruskal-Wallis test for non-parametric categorical data was used accompanied with a pairwise Wilcoxon rank-sum test with Benjamini–Hochberg correction for multiple comparisons. To visualise which specific OTUs overall fluctuated over a growing season, relative abundance by month was used to calculate fluctuation scores for each OTU using $\sum | x_t - x_{t-1} |$ for total absolute change (x = OTU relative abundance, t = time point), creating an ordered list of most fluctuating OTUs. For analysing the relationship between the two dominant OTUs, a Spearman correlation for non-parametric continuous numerical data, was employed. Monthly trophic mode composition was calculated by averaging the relative abundance of taxa assigned to each functional category, as assigned through the FungalTraits database.

Results

DNA Extraction & Processing

Douglas-fir needles were collected from the West45 research site near Jordan river (Figure 1) over the 2025 growing season in an effort to describe temporal variation in foliar fungal endophyte communities using high-throughput meta-barcoding technology. Sixteen trees were selected representing four different families (4 trees/family), and two subspecies (Interior & Coastal). Sampling dates selected for DNA extraction were in February, April, May, June,

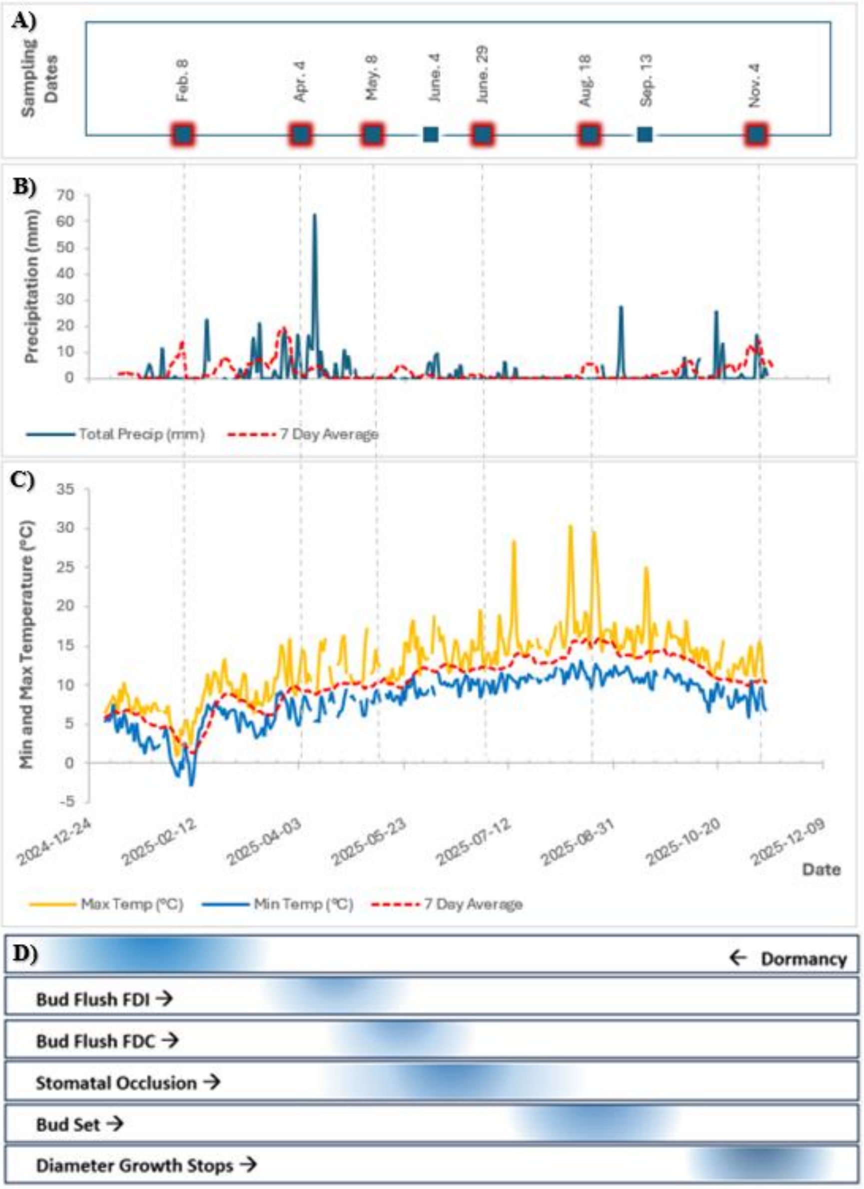

Figure 2: Douglas-fir needles were collected from the West45 BC Ministry of Forests research site near Jordan River BC. (A) Collection dates were February 8, April 4, May 8, June 4, June 29, August 18, September 13, & November 4. (B) Total precipitation, and (C) max & min temperatures with seven-day averages are for shown for the 2025 collection period. (D) Possible Douglas-fir phylogeny: dormancy occurs during the coldest period, bud flush occurs in May, stomatal occlusion by *N. gaeumannii* pseudothecia occurs in June & July, bud set occurs in August, and tree diameter growth ceases in November. Samples selected for DNA extraction were February 8, April 4, May 8, June 29, August 18, & November 4 highlighted in red (A).

August, & November (Figure 2-A). One tree died during the summer, resulting in a total of 94 samples. The February sampling date occurred during the coldest period, with temperatures below 0˚C. The highest precipitation occurred in early April. Rain events were reduced in May and June with steady temperature increases that peaked in August near 30˚C. Drought conditions were observed through July and August, and rains began again in October (Figure 2-A & C). Based on accounts through personal communication (Degner, 2026) bud flush began at the West45 site in May 2025, otherwise phenology at the West45 study site was not screened for this study, however, the phenological cycle for this site may be roughly as follows (Figure 2-D); dormancy occurs during the coldest period, bud flush occurs in May, stomatal occlusion by N. *gaeumannii* pseudothecia occurs in June and July, bud set occurs in August, and tree diameter growth stops in November (Gould *et al*., 2012; Degner, J., personal communication, 2026).

Genomic DNA was extracted successfully, passing quality thresholds based on spectrophotometric analyses, with DNA concentrations ranging from 28 – 300 ng/µL and purity ratios within acceptable parameters (Figure 3-A). Gel electrophoresis confirmed genomic DNA

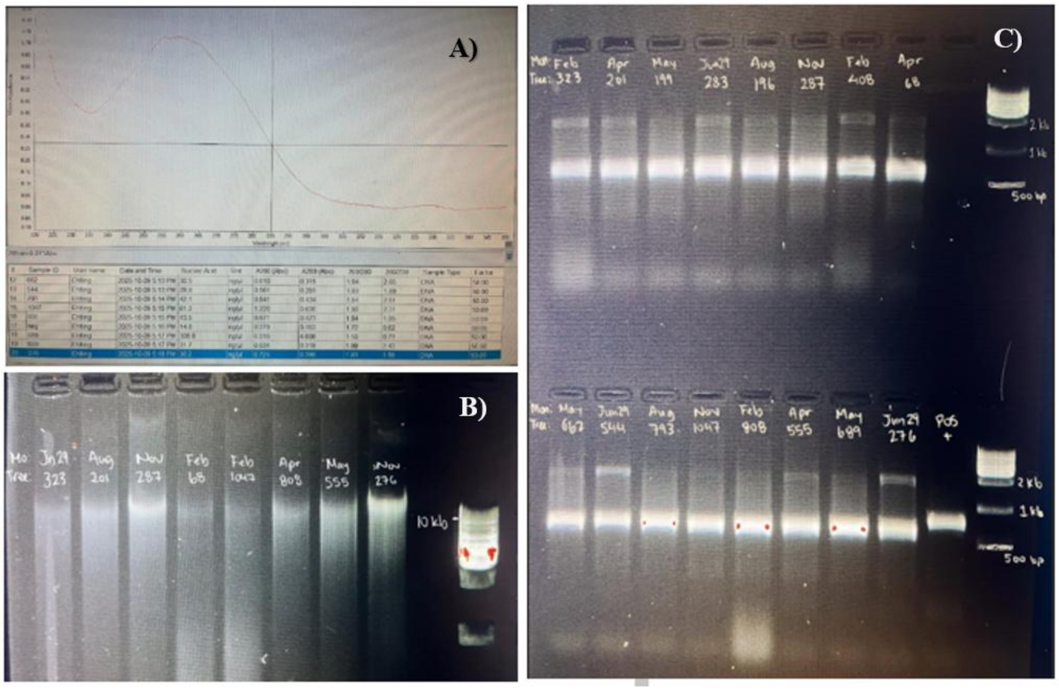

Figure 3: DNA quality assessments for 94 samples extracted from Douglas-fir trees over a growing season. A) Nanodrop spectrophotometric results indicating DNA concentrations and purity. B) Genomic DNA gel electrophoresis with sample date and tree ID indicated. C) PCR amplified fungal ITS sequence gel electrophoresis with sample date and tree ID indicated.

integrity (Figure 2-B) and fungal ITS sequence presence using PCR amplicons (Figure 2-C). All samples were thus sent for ITS1 amplicon metabarcoding using high-throughput DNA sequencing with a paired-end read length target of 300 bases.

All 94 samples were successfully sequenced resulting in a total of 14,368,544 reads prior to processing. After denoising and merging, total read count dropped to 13,569,293 and reads were assigned to 7,586 ASVs with a read length ranging from 260 – 451bp and a mean of 290 bp. Clustering ASVs at 97% identity resulted in 1980 unique Operational Taxonomic Units (OTUs), which were further reduced to 697 OTUs after low abundance filtering (Appendix C). Three taxa present in the negative control were removed from the dataset. The sample read depth ranged from 29,600 – 276,406 reads per sample, with a mean of 142,519. Rarefaction was set to a depth of 29,000 reads, which resulted in only the loss of the negative control sample. Manual alignments identified a further 58 OTUs collapsible at 97% identity, reducing OTUs to a total of 639 Biologically Unique Features (BUFs), however the feature table generated from this collapse was not used in statistical analyses.

Table 1: Quality processing of fungal ITS1 rRNA short read amplicon performed in QIIME2 for 94 samples collected from 16 Douglas-fir trees semi-monthly over a growing season.

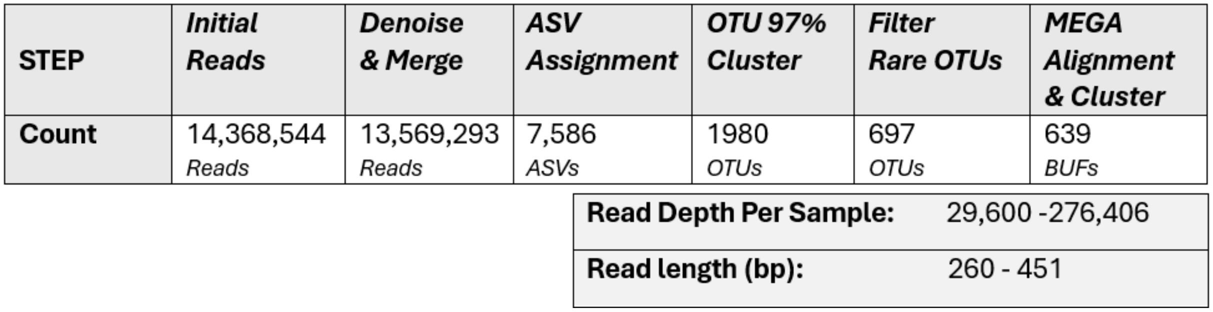

STEP	***Initial Reads***	***Denoise & Merge***	***ASV Assignment***	***OTU 97% Cluster***	***Filter Rare OTUs***	***MEGA Alignment & Cluster***
Count	14,368,544 *Reads*	13,569,293 *Reads*	7,586 *ASVs*	1980 *OTUs*	697 *OTUs*	639 *BUFs*

Read Depth Per Sample:	29,600 -276,406
Read length (bp):	260 - 451

ASV = Amplicon Sequence Variant, OTU = Operational Taxonomic Unit, BUF = Biologically Unique Feature

Phylogeny and Taxonomic Resolution

Features were assigned taxonomy with the UNITE fungal reference database through QIIME2 using k-mer frequency vectors, which allows for fast processing of large datasets. However, many features were poorly resolved, and therefore additional manual BLAST searches using sequence alignments against the NCBI Core nucleotide database were conducted to improve taxonomic resolution and, in some cases, to correct misassignments. For example, previous studies have consistently identified *Nothophaeocryptopus gaeumannii* as the dominant fungal taxon in Douglas-fir needles in Coastal areas (Stone *et al*., 2008: Gervers, 2024; Hayward, 2024), yet this taxon was initially indicated as representing only 35 sequence reads in my dataset. Instead, *Pallidocercospora ventilaginis* was recovered as the dominant taxon with 8,966,994 overall reads, and no further information could be found on this species. However, subsequent BLAST alignment of the representative dominant sequence indicated that this feature was in fact derived from *N. gaeumannii*. The majority of OTUs remained unresolved to species or genus level, but over half of the UNITE assigned taxa resolved to low rankings were assigned a higher ranking through NCBI Core nucleotide database alignments. Further attempts were made to manually refine the resolution of certain OTUs by aligning them to an in-house reference database composed of Sanger sequences from culture-based fungal isolates of Douglas-fir needles grown near Jordan River (Appendix B, Table 1). No matches with >86% identity were found for taxonomically unresolved OTUs. Among those OTUs from my data that were resolved to genus or species level, very few matched the in-house culture-based database (Appendix B). Approximately 10% of OTUs could not be assigned a rank higher than Fungi. Of those that received taxonomic assignments to phylum or higher, 38% (265 of 697 OTUs) were Basidiomycetes, yet Basidiomycetes accounted for only 1% of total sequence reads (Figure 4). Most Basidiomycetes were resolved to the genus or species level, while most Ascomycota were resolved to lower ranks.

N. gaeumannii was the dominant taxon, accounting for 66% of total pooled reads. *Mycosphaerellales sp3,* an unresolved species in the order of Mycosphaerellales, was the second most abundant, accounting for 23% of total reads. *N. gaeumannii* and *Mycosphaerellales sp3* together accounted for 90% of total reads while the remaining 695 OTUs accounted for ≤ 10% of reads, and the vast majority of OTUs were < 1% abundant (Figure 4). Ascomycota was the dominant phylum, accounting for ~ 98% of all fungal reads. Basidiomycetes and Unknown fungi (unresolved/undefined fungi) accounted for ~1 and 2 % of reads respectively. Dothideomycetes represented ~ 92% of class level abundance, Mycosphaerellales accounted for ~ 90% of order level abundance, and Mycosphaerellaceae accounted for ~ 67% of all family level abundance. *N. gaeumannii* is within the family Mycosphaerellaceae, while unresolved *Mycosphaerellales sp3* is within an unknown family (Figure 4). Phylogenetic reconstruction using sequences retrieved from this study inferred that *Mycosphaerellales sp3* may be within the family Teratosphaeriaceae, or may be closely related to families Dissoconiaceae and Cladosporiaceae

(Figure 5). *Mycosphaerellales sp3* does not appear to be closely related to *N. gaeumannii* (Figure 5). *Fungi sp37* was the third most abundant OTU representing ~ 1% of reads (Figure 4) and was situated in a clade including members of Teratosphaeriaceae (Figure 5). *Eurotiomycetes sp39* was the 4th most abundant OTU representing ~ 1% of reads (Figure 4) and was within the order Chaetothyriales (data not shown). *Dothideomycetes sp2* was the 5th most abundant OTU representing ~ 0.9% of reads (Figure 4) and was within the same clade as *Mycosphaerellales sp3* (Figure 5) and is therefor possibly also within the family Teratosphaeriaceae.

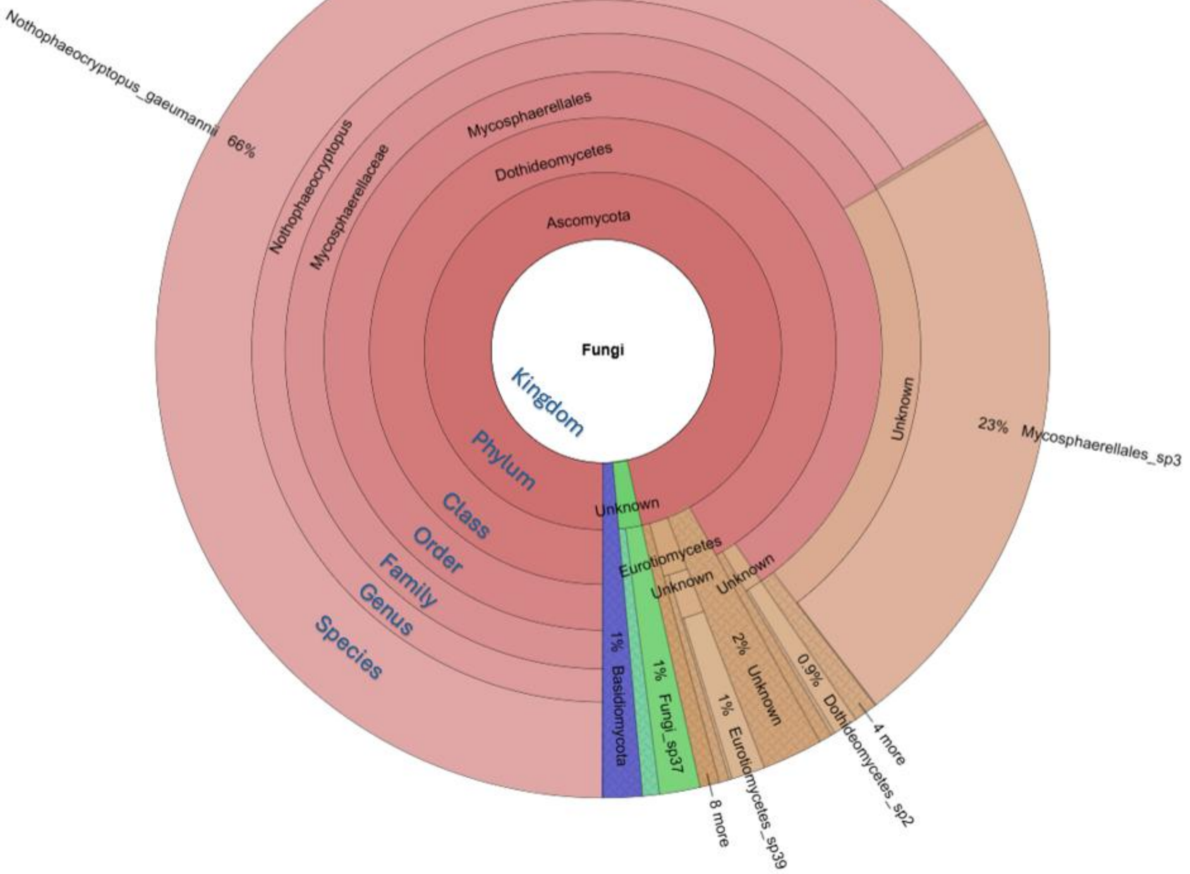

Figure 4: Krona plot showing the overall percent of sequence reads represented by taxa present in 93 samples collected from Douglas-fir needles over a growing season. *N. gaeumannii* represented 66% of reads, *Mycosphaerellales sp3* represented 23% of reads, and remaining OTUs were present at ≤ 2%. Phylum Ascomycota represented 98% of all fungal reads, and Phylum Basidiomycota and Unknown fungi each represented 2%. Mycosphaerellales, of the class Dothideomycetes, accounted for ~90% of all reads at order level. Blue labels indicate taxonomic rank. The full rank order for *N. gaeumannii* is k__Fungi; p__Ascomycota; c__Dothideomycetes; o__Mycosphaerellales; f__Mycosphaerellaceae; g__Nothophaeocryptopus; s__*Nothophaeocryptopus_gaeumannii*

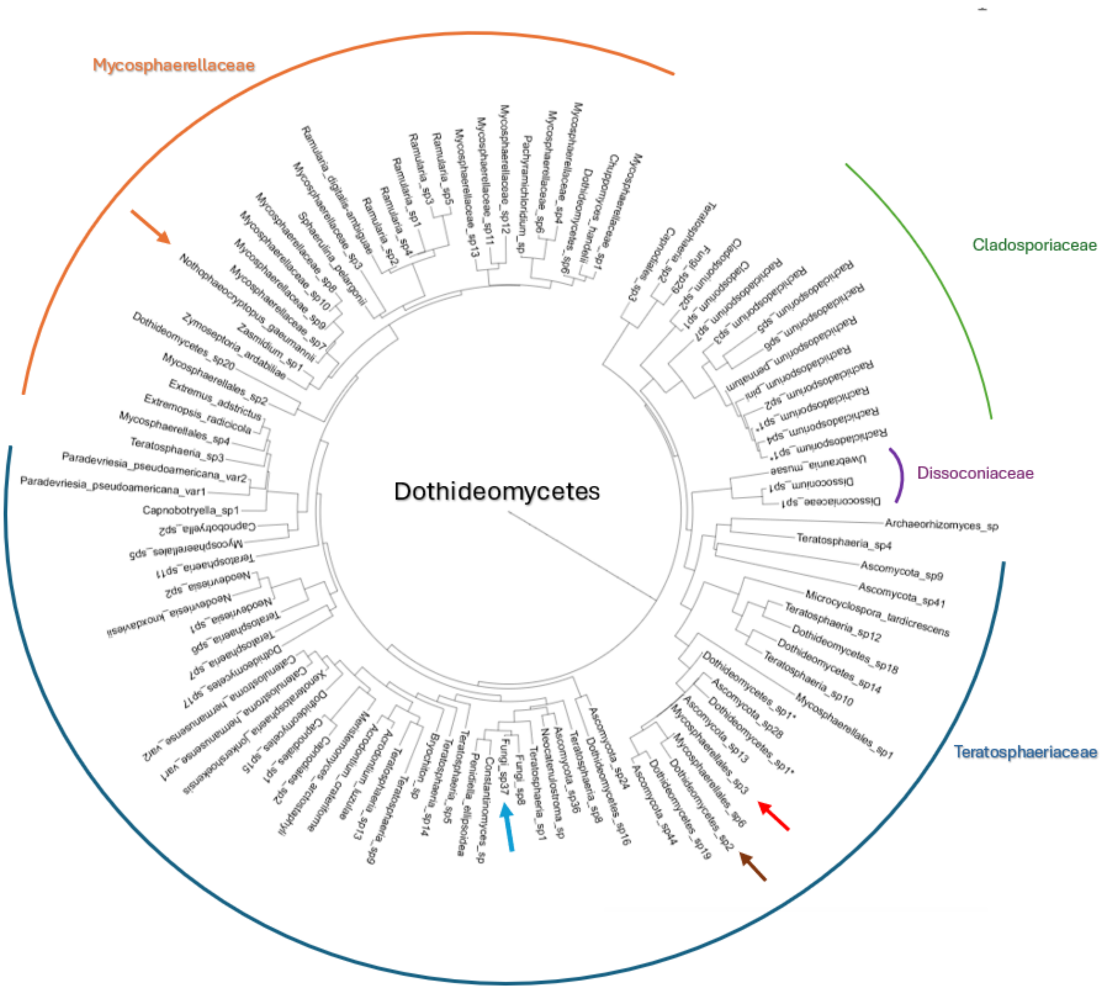

Figure 5: Phylogenetic tree constructed using ITS fungal sequences from 16 Douglas-fir trees depicting only lineages resolved to the class of Dothideomycetes within the phylum Ascomycota. This tree shows that *Mycosphaerellales sp3* (red arrow) may belong to Family Teratosphaeriaceae (dark blue), and may be closely related to Families Dissoconiaceae (purple) and Cladosporiaceae (green). *Mycosphaerellales sp3* does not appear to be closely related to *N. gaeumannii* (orange arrow). *Fungi sp37* (blue arrow) is the third most abundant taxon. *Dothideomycetes sp2* (brown arrow) is the 5th most abundant taxon. Dark blue semi-circle indicates members of the family Teratosphaeriaceae, purple semi-circle indicates members of the family Dissoconiaceae, orange semi-circle indicates members of the family Mycosphaerellaceae, and green semi-circle indicates members of the family Cladosporiaceae.

Alpha Diversity

To address the primary hypothesis, being that fungal endophyte communities shift in composition over a growing season, I initially disregarded host tree family information and other metadata. Samples from all trees were grouped into the months in which they were collected; February, April, May, June, August, & November. Each sampling date contained information from each of the 16 trees sampled. Shannon's Diversity Index is an Alpha diversity metric incorporating both the richness and evenness of taxa within each group. The data showed an overall progressive increase in Shannon diversity from February to November (Figure 6), with April appearing to have the lowest diversity and November appearing to have the highest. This observation was supported by a Kruskal-Wallis pairwise comparison which showed a significant difference between April and November (H = 9.025, p-value = 0.0027, q-value = 0.0399, α = 0.05), with Douglas-fir needles containing the most diverse fungal communities in November, and the least diverse communities in April.

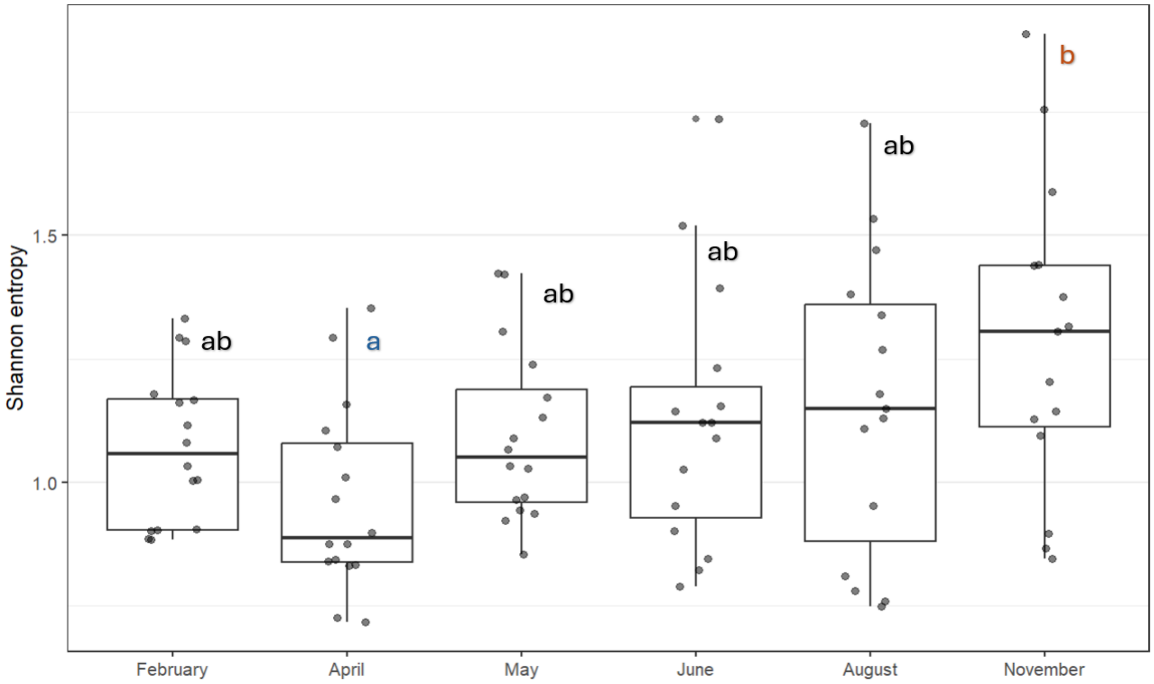

Figure 6: Shannon's Diversity Index for fungal endophyte communities of Douglas-fir needles collected on six separate sampling dates over a growing season (n = 93). Samples were grouped into months and Shannon Entropy for each sample is shown on the y-axis. Kruskal-Wallis test and pairwise comparisons were done using Qiime2. Letters represent significant differences between months ($p < 0.05$). Each dot represents one sample.

Beta Diversity

Beta diversity was measured to compare between-month variation of fungal endophyte communities, and each month supported a significantly different consortium of fungi. Using pairwise comparisons, community variation for each sample was assessed for between-month and within-month dissimilarity, and results were plotted for three beta diversity measures (Figure 7). Between month dissimilarity is greater for all three measures compared to within month dissimilarity, with unweighted UniFrac showing the greatest dissimilarity in fungal community composition between different months (Figure 7). Beta diversity dissimilarity distance measures between 0 – 1, with 0 being completely similar and 1 being completely dissimilar.

Bray–Curtis dissimilarity quantifies differences in community composition between samples based on shared OTU abundances. Pairwise comparisons using Bray-Curtis distance (Figure 8-A) showed dissimilarity in fungal OTU composition between samples grouped by month (PERMANOVA, $p = 0.001$). November fungal communities were significantly dissimilar from communities of all other months (mean distance ≈ 0.20–0.32; q-value = 0.003 vs. February, April, May, and June; q-value = 0.005 vs. August; $\alpha = 0.05$). Fungal communities in needles sampled in August were also significantly dissimilar from all other months (mean distance ≈ 0.20–0.25; q-value = 0.003 vs. February; q-value = 0.009 vs. April and May; q-value = 0.037 vs. June; $\alpha = 0.05$). In addition, communities sampled in Ju differed from communities sampled in February (mean distance ≈ 0.20; q-value = 0.037).

Weighted UniFrac is a quantitative Beta diversity measure that considers both phylogenetic relationships and OTU relative abundance. Pairwise comparisons using weighted UniFrac distances (Figure 8-B) confirmed dissimilarity of fungal communities in samples between sampling months (PERMANOVA, $p = 0.001$). November fungal communities were dissimilar from those of all other months (mean distance ≈ 0.09–0.15; q-value = 0.002 for all comparisons; $\alpha = 0.05$), August fungal communities were dissimilar from those of all other months (mean distance ≈ 0.09–0.15; q-value = 0.002 vs Feb & Apr, q-value = 0.004 vs May, q-value = 0.020 vs June, $\alpha = 0.05$), and community composition for June was dissimilar from February (mean distance ≈ 0.01; q-value = 0.013, $\alpha = 0.05$).

Unweighted UniFrac is a more qualitative approach to measuring between-group diversity, using only OTU presence/absence data rather than abundance while also taking into account phylogeny, which gives rare taxa more consideration. Pairwise comparisons using unweighted UniFrac distances (Figure 8-C) showed significant dissimilarity between communities (PERMANOVA, $p = 0.01$) with every month being significantly dissimilar (mean distance ≈ 0.45–0.60; q-value = 0.001 for all comparisons except q-value = 0.002 for Aug vs June, $\alpha = 0.05$).

Overall, the greatest dissimilarity was between communities sampled in November and February. Bray-Curtis and weighted UniFrac measures showed a distinction between early season and late season sampling dates, with dissimilarity increasing between later months. Mean distances were greatest for unweighted UniFrac (Figures 7-C & 8-C), showing strong support for dissimilarity in fungal community structure between each sampling date driven by rare taxa.

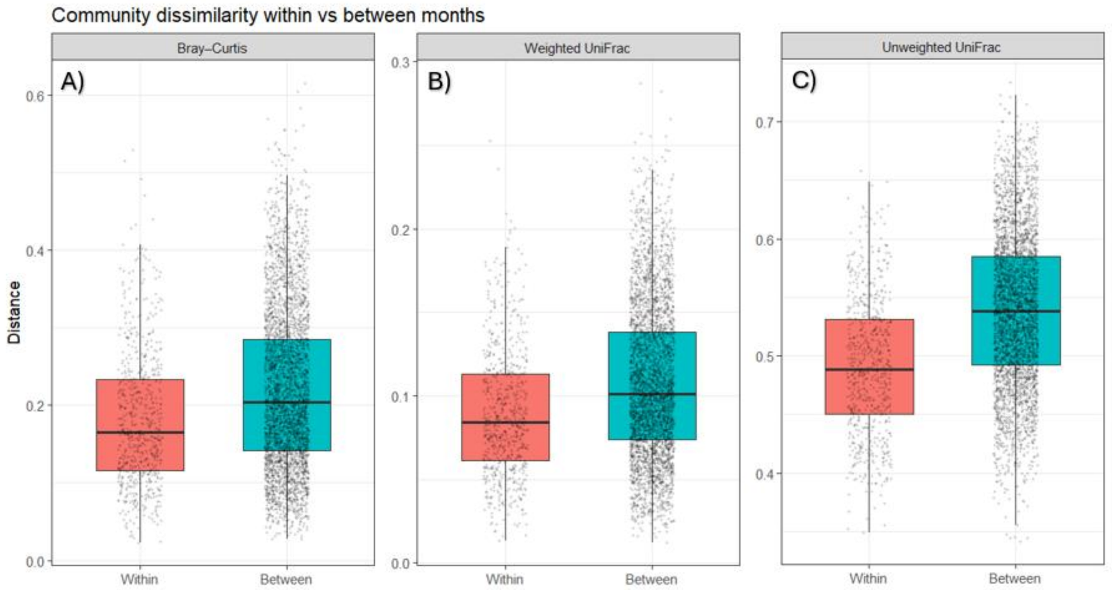

Figure 7: Beta Diversity was measured to show monthly dissimilarity between fungal endophyte communities of Douglas-fir needles collected from 16 trees over the 2025 growing season (n = 93). Samples were grouped by month and dissimilarity was measured using A) Bray-Curtis, B) Weighted UniFrac, & C) Unweighted UniFrac, with unique y-axes showing distances/dissimilarity determined using Qiime2. Dissimilarity in fungal endophyte community composition of samples within each month (orange box) is compared to dissimilarity of samples between each month (blue box) in each panel. Distance of 0 = groups are identical in composition. Distance of 1 = groups have completely different composition. Each dot represents one pairwise distance value between samples.

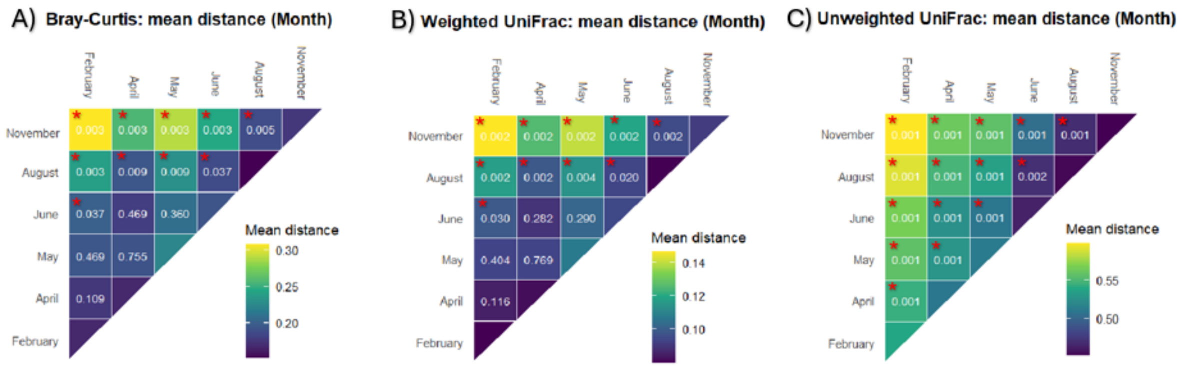

Figure 8: Beta Diversity determined using distance matrices show significant pairwise dissimilarity between fungal endophyte communities of Douglas-fir needles collected from 16 trees over a growing season (n = 93). Samples were grouped by month and dissimilarity was measured using A) Bray-Curtis, B) Weighted UniFrac, & C) Unweighted UniFrac. Colouring is coded by mean distance with yellow being most dissimilar in fungal community composition and dark blue being most similar. Q – values for each comparison are indicated inside each square. Significance is indicated with a red asterisk (*; $p < 0.05$).

PERMDISP in R is used alongside PERMANOVA to assess whether groups differ in the *dispersion* (i.e., variability) of community composition based on a distance matrix. It calculates the distance of each sample to its group centroid in multivariate space, providing a measurement for within-group variation among samples. PERMANOVA assumes homogeneity of dispersion, and significant PERMDISP results indicate that within-group samples display heterogeneity, indicating the potential to inflate PERMANOVA results.

For unweighted UniFrac, differences in community composition among months were accompanied by significant differences in dispersion (PERMDISP, $p = 0.001$), indicating that part of the observed temporal pattern may be driven by heterogeneity in fungal communities within months (Figure 9). Community dispersion differed significantly among months: February, April, and May exhibited greater within-month variability ($p = 0.001$, $p = 0.006$, $p = 0.005$,

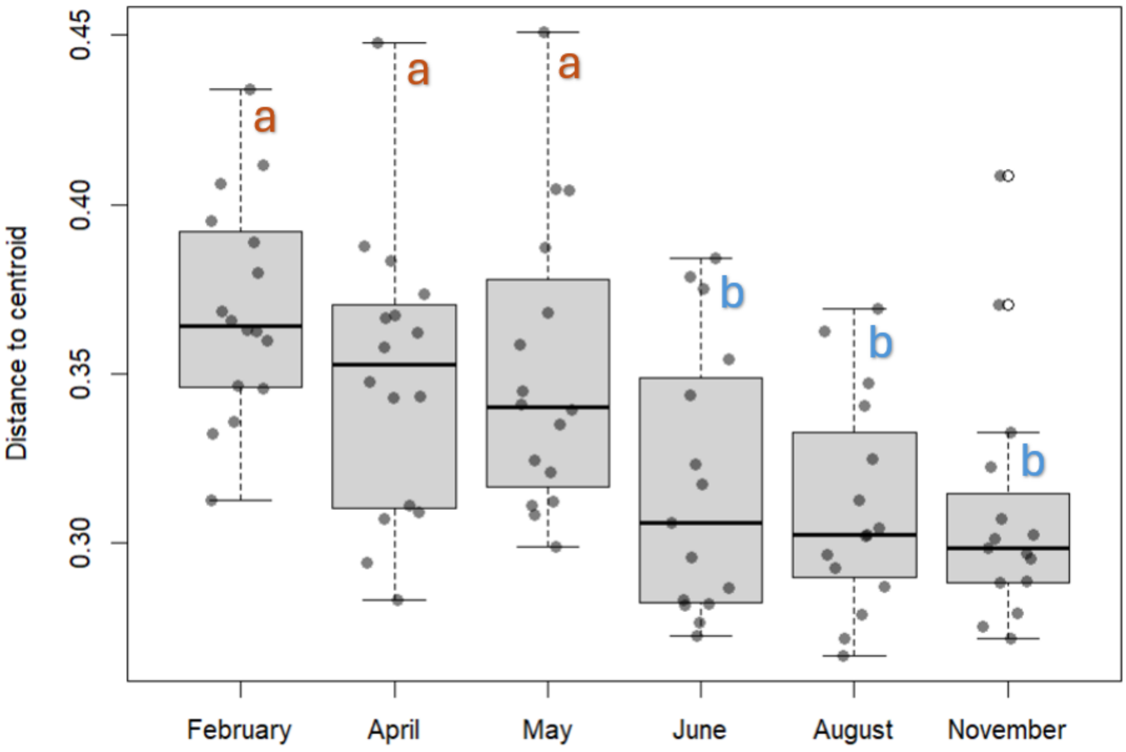

Figure 9: PERMDISP comparison of fungal community dispersion among months based on unweighted UniFrac distances comparing fungal endophyte communities of Douglas-fir needles collected from 16 trees over a growing season (n = 93). Dispersion reflects variability in fungal community composition among trees within each sampling month. Boxplots show the distance of individual samples to their group centroid, with each point representing a single tree with distance to centroid community on the y-axis and sampling month on the x-axis. Greater distances indicate higher variability in community structure within a given month. Letters indicate significant differences in dispersion between months based on pairwise permutational tests ($p < 0.05$).

respectively), whereas June, August, and November showed more consistent fungal assemblages with non-significant dispersion values.

Pairwise PERMDISP comparisons showed that early-season months (February, April, May) were significantly more dispersed than late-season months. February differed significantly from June, August, and November ($p = 0.0004$, $p = 0.00002$, $p = 0.0004$, respectively). April also differed from June, August, and November ($p = 0.04$, $p = 0.009$, $p = 0.009$, respectively), and May differed from these same months ($p = 0.03$, $p = 0.006$, $p = 0.007$, respectively). These results indicate a seasonal shift from highly variable fungal communities in early months to more stable and homogeneous communities later in the year.

Relative Abundance & Seasonal Fluctuation

OTU relative abundance was calculated to compare differences in fungal community structure between months. After grouping all OTUs present with < 1% relative abundance into one category, only 6 OTUs remained; *N. gaeumannii, Mycosphaerellales sp3, Fungi sp37, Dothideomycetes sp2, Eurotiomycetes sp39*, and *Cantharellales sp2* (Figure 10-A). *Fungi sp37, Eurotiomycetes sp39*, and *Cantharellales sp2* all appear to increase in relative abundance in November, while *Dothideomycetes sp2* appears to have higher relative abundance in February and May. *N. gaeumannii* increases consistently in relative abundance each month, showing a small spike in April. *Mycosphaerellales sp3* shows an opposite trend, with high relative abundance in February which decreases as the season progresses. With *N. gaeumannii* & *Mycosphaerellales sp3* removed and no abundance filter applied, the low abundant fungal diversity can be observed (Figure 10-B). November microbial composition appeared to contain more Basidiomycetes (Cantharellales & Sporobolomyces). This observation was supported in Figure 11 which shows the average relative abundance of Basidiomycetes for each month rising as the season progresses. Statistically significant differences in Basidiomycete relative abundance between months were observed using Kruskal-Wallis test ($\chi^2 = 28.53$, df = 5, p-value = 2.856e-05, $\alpha = 0.05$) accompanied by pairwise comparisons showing significantly different relative abundance of Basidiomycetes in later months (June, August, November) compared to early months (February, April, May). A Wilcoxon rank-sum test was employed with November set as the intercept ($W = 832$, p-value = 0.01003, $\alpha = 0.05$). The Wilcoxon rank-sum test statistic

(W) represents the sum of ranks for observations in one group and is used to assess differences in distributions between groups.

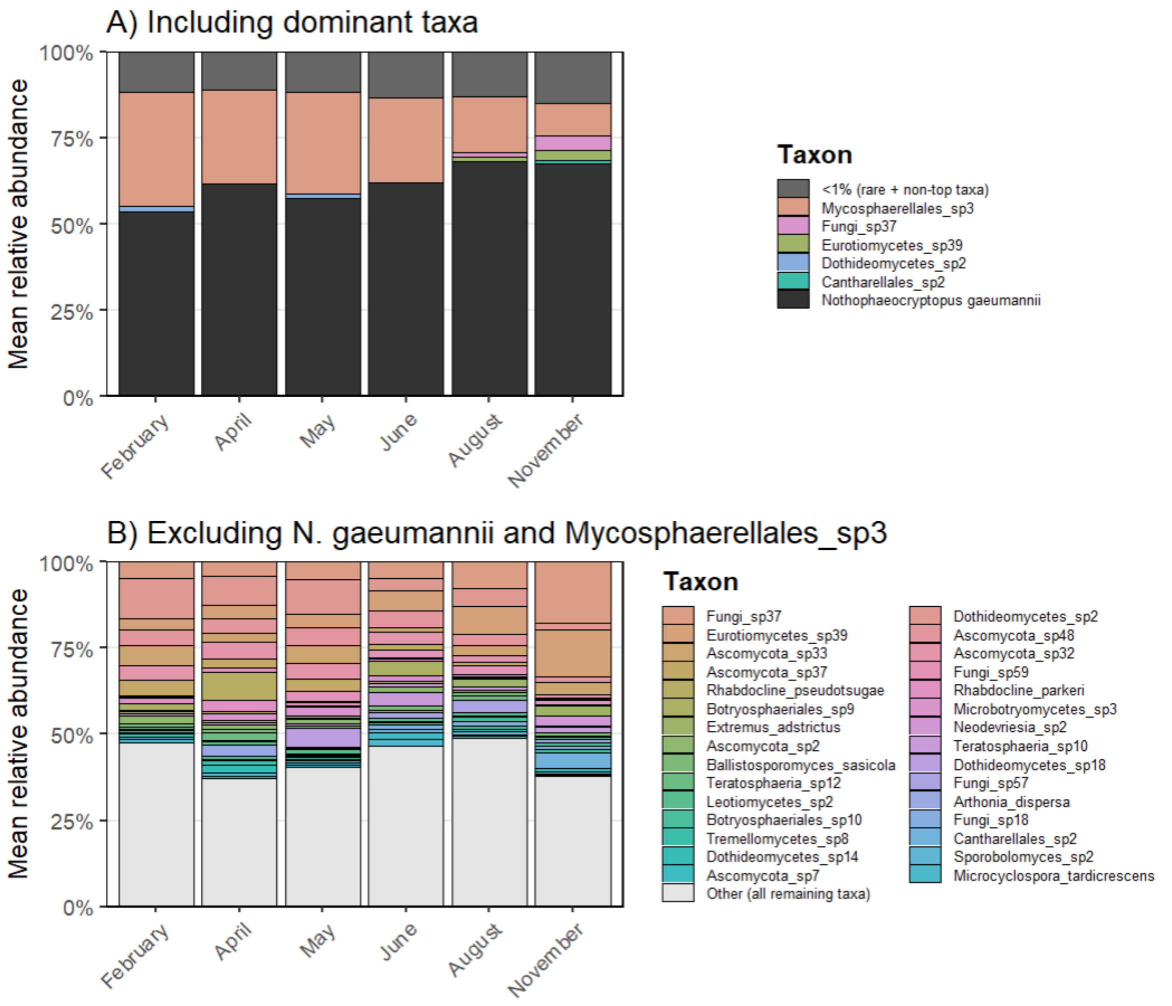

Figure 10: Relative abundance of fungal endophytes of Douglas-fir needles from 16 trees sampled over the 2025 growing season (n = 93). Samples were grouped into months and abundances were normalised to show mean relative abundance on the y-axis. **A)** Relative abundance of high abundance taxa: All OTUs in abundance of < 1% are grouped together. **B)** Relative abundance of low abundance OTUs*:* This panel selects for the top 30 most abundant taxa excluding both *N. gaeumannii* & *Mycosphaerellales sp3.* All remaining OTUs are grouped as Other. Colours are assigned in a descending zig-zag pattern from left to right.

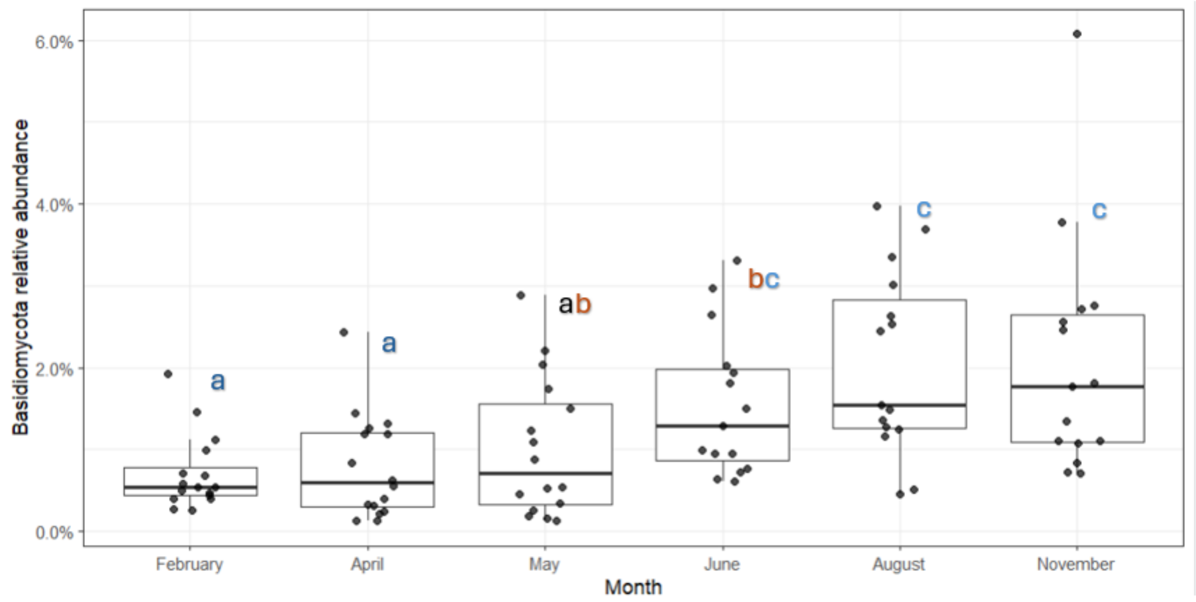

Figure 11: Relative abundance of Basidiomycete endophytes in Douglas-fir needles collected from 16 trees over the 2025 growing season (n = 93). Relative abundance for each sample is shown on the y-axis. Basidiomycete relative abundance is shown on the y-axis. Kruskal-Wallis test and Wilcoxon rank-sum pairwise comparisons were conducted in R. Letters indicate significant differences between months ($p < 0.05$).

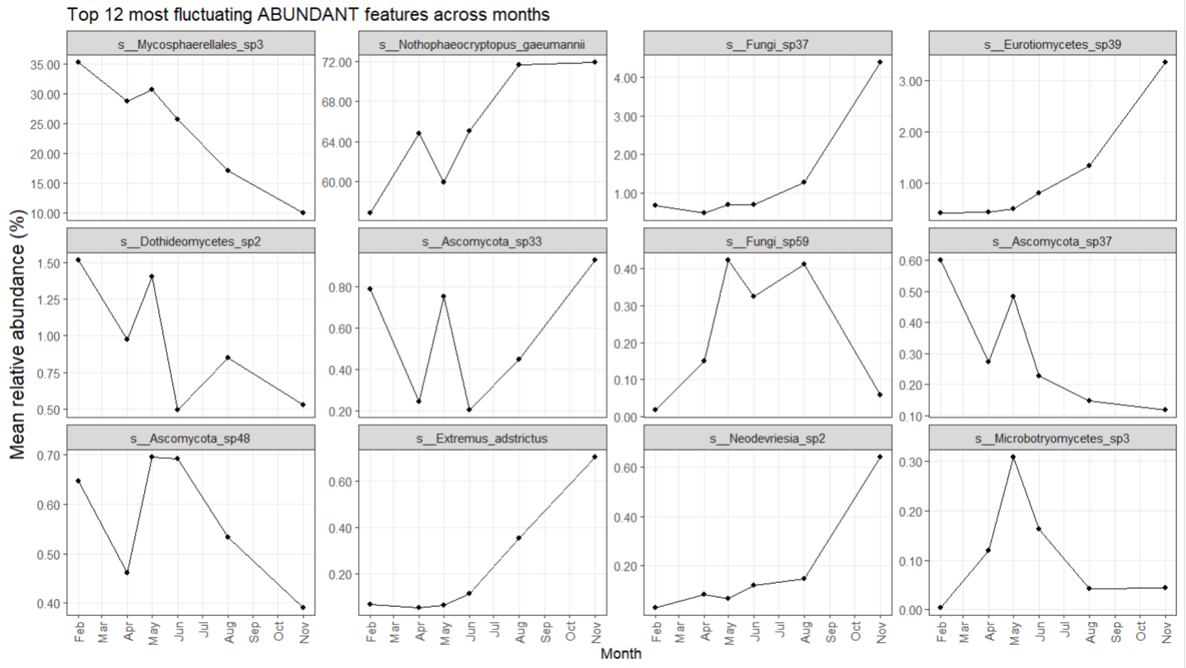

Figure 12: Individual OTUs from Douglas-fir needles collected from 16 trees over a growing season (n = 93) show seasonal fluctuation. Each panel shows one of the top 12 most fluctuating OTUs, with unique y-axes showing mean relative abundance over 2025.

Relative abundances were used to calculate fluctuation over time for each OTU, and the twelve most fluctuating OTUs were retained (Figure 12). *N. gaeumannii* rose over the season (55% → 72%), along with *Fungi sp37* (<1% → 5%)*, Eurotiomycetes sp39* (<1% → 4%)*, Extremus adstrictus* (0.1% → 0.7%)*,* and *Neodevriesia sp2* (<0.1% → 0.5%). *Mycosphaerellales sp3* declined over the season (35% → 10%), as did *Dothideomycetes sp2* (1.5% → 0.5%) and *Ascomycota sp37* (0.6% → 0.1%). Figure 12 again showed that most endophytic fungi, other than *N. gaeumannii* & *Mycosphaerellales sp3*, have consistently low relative abundance.

OTUs with statistically significant differential abundance were calculated using ANCOM (Table 2; Figure 13). ANCOM significance is determined by a set threshold on the W statistic (W = 627), such that only eight taxa exceeded the significance threshold; *Hypholoma capnoides, Ramularia sp4, Fungi_sp59, Helotiales_sp8, Aspergillaceae_sp, Naemateliaceae_sp3, Hypholoma_fasciculare,* and *Chaetothyriales_sp1**. None passed the abundance threshold applied in Figure 12.

Table 2: Fungal OTUs with significant differences in relative abundance between sampling months as determined by ANCOM analysis in Qiime2. W-statistic indicates the number of pairwise log-ratio tests in which that OTU was found to differ significantly between months. OTUs with the highest W values are listed, along with the highest observed read counts for each sampling month (February, April, May, June, August, and November).

		Highest observed read counts for each month					
Species	**W**	**Feb**	**Apr**	**May**	**Jun**	**Aug**	**Nov**
Hypholoma capnoides	696	43	74	32	4	6	1
Ramularia sp4	695	8	4	92	123	34	803
Fungi sp59	694	91	1356	3881	1752	5467	383
Helotiales sp8	668	1	1	6	247	394	167
Aspergillacaea sp	658	14	6	6	6	56	153
Naemateliaceae sp3	644	12	1	177	1	1	1
Hypholoma fasciculare	636	18	8	5	1	1	29
*Chaetothyriales sp1**	635	114	188	601	441	451	1455

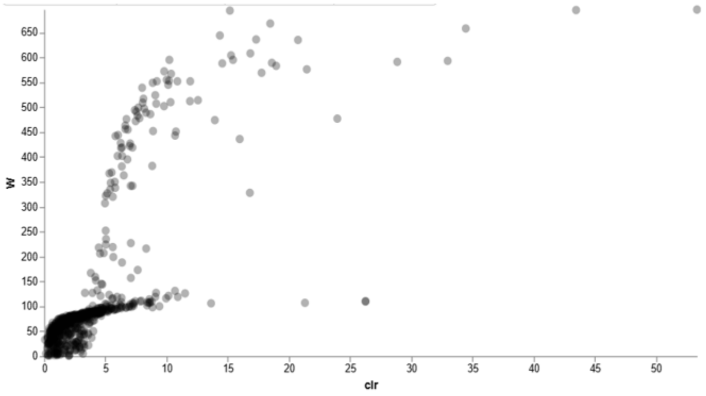

Figure 13: ANCOM volcano plot showing differential abundance of taxa among months. Centered log-ratio (clr) transformed abundances are shown on the x-axis, which express the abundance of each taxon relative to the geometric mean abundance of all taxa in a sample. W-statistic on the y-axis indicates the number of pairwise log-ratio tests in which that OTU was found to differ from other months.

Nothophaeocryptopus gaeumannii & Mycosphaerellales sp3

An interesting trend emerged in these figures wherein the relative abundance of *N. gaeumannii* appeared to increase as the season progressed, and in contrast, *Mycosphaerellales sp3* appeared to decrease in lock-step. Figure 14 explored this relationship further, showing the mean relative abundance per month for the top two OTUs, and indeed this relationship appears to be negatively correlated. *Mycosphaerellales sp3* relative abundance started at 35% in February, steadily decreased throughout the season with 10% abundance in November. In contrast, *N. gaeumannii* had 57% relative abundance in February and steadily increased to 72% abundance in November (Figure 14-A). This relationship was tested using Spearman correlation, and indeed there is a strong significant negative correlation between the two dominant taxa (ρ = - 0.87, p = 6.75e-30, α = 0.05; Figure 14-B).

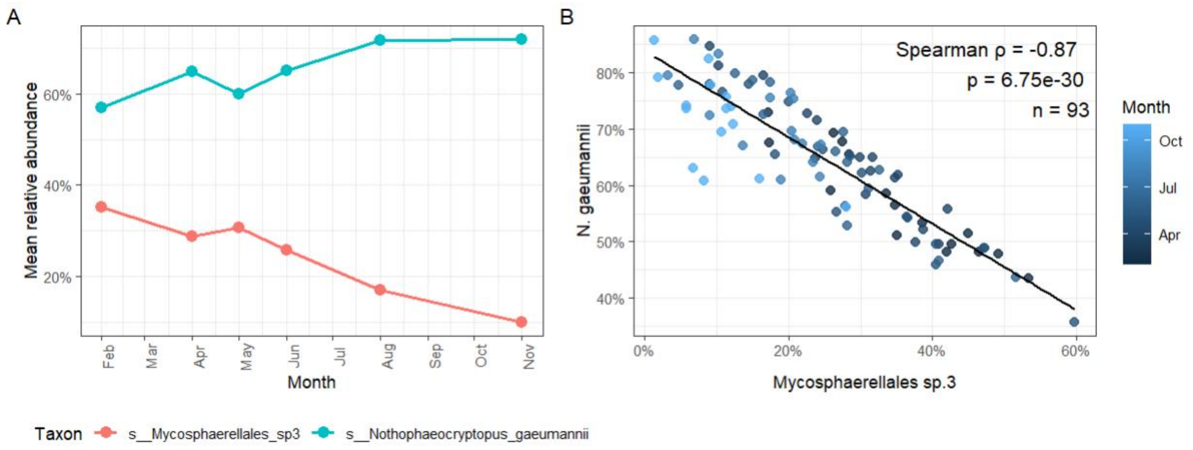

Figure 14: Negative correlation between *Nothophaeocryptopus gaeumannii & Mycosphaerellales sp3* in Douglas-fir needles collected from 16 trees over the 2025 growing season (n = 93). **A)** Relative abundance of *Nothophaeocryptopus gaeumannii & Mycosphaerellales sp3* over the sampling period **B)** Scatterplot showing *N. gaeumannii* relative abundance on the y-axis and *Mycosphaerellales sp3* relative abundance on the x-axis. Spearman correlation results are displayed. Colour scheme represents months; light blue is November and dark blue is February. Each dot represents one sample.

Fungal Trait Assignment

Fungal traits were assigned to OTUs resolved to species and genus levels. Only a small portion of the dataset was assigned to these higher levels, and when compared to the FungalTraits database, 42 matches were found (Appendix C, Table 1). Of these, 25 were Basidiomycetes, and in my dataset the majority of taxa resolved to species and genus levels were Basidiomycetes, despite this phylum representing only 1% of total sequence reads. Figure 15 shows monthly variation in relative abundance for OTUs assigned to specific traits. Most of the assigned fungi were pathogens with abundance highest in November, while saprotrophs appeared to be more common in February. OTUs assigned as pathogens were as follows; *Tremella globispora* was assigned as a fungal pathogen, *Fomitopsis pinicola, Mollisia fuscoparaphysata, Microdochium phragmitis, Cladosporium sp, & Epicoccum nigrum* were assigned as plant pathogens, and *Malassezia sp, Exophiala sp & Cyphellophora gamsii* were assigned as animal pathogens. OTUs assigned as saprotrophs were *Sistotrema sp, Lachnum clandestinum, Hypholoma fasciculare, Hypholoma dispersum, Xenasmatella vaga & Hypholoma capnoides.* OTUs assigned as endophytes were *Epicoccum nigrum, Cladophialophora sp, & Cladophialophora minutissima.* Endophytes assigned as ectomycorrhizal were *Ceratobasidium sp, & Amphinema sp.* Unassigned taxa are likely to contain more fungi of these trophic modes.

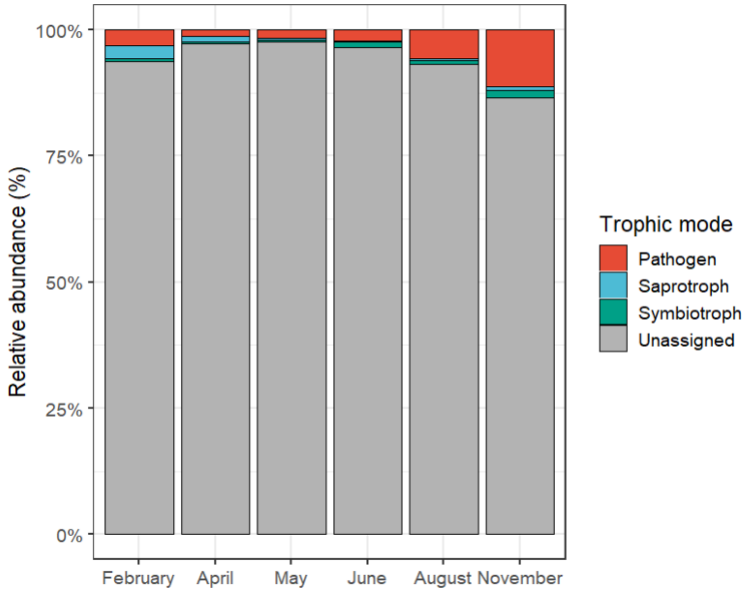

Figure 15: Annotated functional traits for fungal endophytes of Douglas-fir needles collected from 16 trees over the 2025 growing season. OTUs with genus or species level resolution were assigned traits using FungalTraits database. Trophic modes are grouped by month showing relative abundance on the y-axis.

Discussion

This research sought to explore the dynamic seasonal nature of fungal foliar endophyte communities living within Douglas-fir leaf tissue. This was achieved by collecting DNA samples from needles of 16 Douglas-fir trees every one to two months over the 2025 growing season and analysing fungal ITS DNA amplicon sequences generated through next generation meta-barcoding technology. The data strongly support seasonally dynamic fungal community structure by showing relative abundance fluctuations across different months as well as significant variation in diversity between months using both Alpha and Beta Diversity measures. The data also identified a new, highly dominant taxon, *Mycosphaerellales sp3,* which appeared to have a negatively correlated relationship with *Nothophaeocryptopus gaeumannii*, a ubiquitous dominant Douglas-fir foliar endophyte.

Seasonal Drivers of Endo-Mycobiome Diversity

Observed fluctuations in fungal community composition could be influenced by a large variety of factors, although temperature and tree phenology are likely major drivers. Sampling dates (February, April, May, June, August, & November) were selected to cover a full spectrum of seasonal variation, with below freezing temperatures in February, heavy rains in April, drought-like conditions in August coupled with high temperatures nearing 30˚C, and wet fall weather in November. Temperature may play a significant role in endophyte infection and hyphal growth by triggering metabolic/phenological processes and driving seasonal change. *Pinus sylvestris* (Scots pine) in Northern Europe had significant fungal endophyte community differences between seasons, with highest richness in fall (Solheim *et al*., 2021) which is consistent with my results. Szymanski & Miles (2025) saw significant fluctuations in mycobiome alpha diversity coinciding with major phenological events in *Vaccinium corymbosum* (highbush blueberry), yet Redondo *et al*., (2022) found no variation associated with phenology in *Picea abies* (Norway spruce). Endophyte research shows higher fungal DNA concentration during the summer months, often declining over the winter (Fuchs *et al.,* 2017).

In this study, fungal endophyte communities within needles sampled in February experienced sub-zero temperatures associated with a dormancy period. Conifer needles maintain high levels of soluble sugars over the winter (Schoonmaker et al., 2021), which is thought to provide osmoregulation to protect plant tissues against freezing during cold periods (Wong *et al*., 2003). Fungal endophytes obtain nutrients in apoplastic spaces through the uptake of soluble sugars (Lam *et al*., 1994). Increased soluble sugars during dormancy may enable cold hardy fungal endophytes to overwinter in needle tissues. *Mycosphaerellales sp3* and *Dothideomycetes sp2* were 2nd and 5th most abundant OTUs, with relative abundance for both species being highest in February. They are both within the same phylogenetic clade, likely within the family Teratosphaeriaceae, as inferred by the phylogenetic tree constructed using fungal endophyte ITS1 sequences acquired through this research. Teratosphaeriaceae commonly includes extremophile species (Quaedvlieg *et al*., 2014).

At the onset of spring, conifer needles undergo a decline in soluble sugars and an increase in starch in preparation for bud flush (Schoonmaker *et al*., 2021). Bud flush at the West45 site began in May 2025 (Degner, personal communication, 2026), following a small spike in *N. gaeumannii* relative abundance in April and the lowest Shannon diversity observed across all months. April also coincided with the heaviest precipitation events of 2025, and rainfall is known to reduce aerial spore concentrations (Katial *et al*., 1997; Pakpour *et al*., 2015), which may contribute to reduced fungal diversity observed for this sampling date. Preliminary stomatal occlusion data, quantifying the proportion of stomata blocked by *N. gaeumannii* pseudothecia (fruiting bodies), further indicated slightly higher pseudothecial occlusion in April compared to adjacent months (Appendix E, Figure 1). Occlusion decreased in May and June, then increased again in August and remained high later in the season. This pattern aligns with the biology of *N. gaeumannii*: initial sporulation coincides with bud flush to maximize colonization of newly forming needles (Stone *et al*., 2008). Although the needles sampled here were two-year-old needles containing established colonies, internal colonization continues through winter and pseudothecial primordia mature through until sporulation during bud flush (Stone *et al*., 2008). Pseudothecia in later months were likely fully developed and therefore more easily removed by needle surface washing prior to DNA extraction.

A major driver of endophyte infection and community richness is aerial spore concentration (Redondo *et al*., 2022). Previous research found both aerial spore concentration and spore diversity tend to be highest during hot, dry conditions (Katial *et al*., 1997; Pakpour *et al*., 2015). Drought-like conditions occurred at the West45 site through July, August and September 2025 and my data showed increasing fungal endophyte diversity in these later months. Fog is a common feature of late summer along the coast of Vancouver Island, with August conditions sometimes referred to as “Fogust,” reflecting the frequent occurrence of marine fog that often forms overnight and dissipates in the morning (Environment Canada, 2015). These fog events likely impact the West45 site, situated on the West Coast within 2 km of the Salish Sea, by introducing moisture to needle surfaces. Wet leaf surfaces are known to promote fungal infection (Bradley *et al*., 2003). A higher overall concentration and diversity of aerial spores produced by sporulating fungi over the warmer months coupled with late summer fog events likely contributed to an increase in fungal endophyte infection and diversity. Overall foliar Basidiomycete relative abundance increased significantly in the later months (~ 0.3% → 2%), peaking in August. Basidiomycetes relative abundances appeared to level off in November, which is counter-intuitive given that this is peak mushroom season with basidiomycetes producing large fruiting bodies. However, rain is thought to reduce aerial spore concentration by “washing” spores from the air (Katial *et al*., 1997; Pakpour *et al*., 2015), and the West45 site experienced wet, rainy weather starting in late October.

Beta diversity analyses revealed clear seasonal differences in fungal community structure. Bray-Curtis and weighted UniFrac indicated higher dissimilarity between samples grouped into later months, while unweighted UniFrac indicated dissimilarity between fungal communities of every month, reflecting its sensitivity to rare and low abundance OTUs. PERMDISP applied to the unweighted UniFrac distance matrix showed significantly greater dispersion in early months compared to late months, indicating higher within-month heterogeneity in community composition. These dispersion differences suggest that early-season communities are more variable and likely shaped by stochastic colonization processes, coupled with lower Shannon diversity. In contrast, later months exhibited lower dispersion and higher Shannon diversity, reflecting more even and stable fungal assemblages across trees. Thus, seasonal differences in community structure appeared to be driven by both changes in season specific taxonomic composition and a progressive reduction in fungal community heterogeneity (more similar community structure across trees in later months compared to earlier months).

Basidiomycetes

Despite representing only 1% of all sequence reads, Basidiomycetes represented 38% of OTUs resolved to phylum or higher which is consistent with other research (Gonan, 2020;

Solheim, *et al.*, 2021). Gervers (2024) reported Basidiomycota as representing only 8% of OTUs, while Hayward (2024), whose study site was also located near Jordan river, reported 14%, likely reflecting the season wherein the sampling took place. Most Basidiomycete OTUs in my data were resolved to the genus or species level while most Ascomycete OTUs were only resolved to class, order, or family. This may reflect a research bias towards the charismatic fruiting bodies (mushrooms) and ectomycorrhizal species. Ascomycetes tend to be less annotated in fungal reference databases.

Prior to the removal of tree 555 June sample from the dataset, Basidiomycetes represented 2% of all fungal reads. This sample was removed because tree 555 had died and the needles were brown in June, which created skewed data. Once that sample was removed from analyses, Basidiomycetes representation decreased by half in overall reads. This insinuates that Basidiomycetes spores can better colonize dying needles, and therefore only specific Basidiomycete species can overcome living plant defenses, and/or compete with established communities. Basidiomycetes include diverse trophic strategies, with a large proportion being saprotrophs. Tree canopies prone to desiccation are considered to be high-stress habitats for Basidiomycete saprotrophs (Boddy & Hiscox, 2016). Colonization of plant tissue by decomposers depends on the endophyte community already in place, therefor arrival time is key for many saprotrophs. Successful establishment hinges on a fungi's enzymatic arsenal with which to fend off competition and secure resources (Boddy & Hiscox, 2016).

Nothophaeocryptopus gaeumannii & Mycosphaerellales sp3

Ascomycota were represented by the vast majority of read counts (98%), which is consistent with endophyte research (Gervers, 2024; Hayward, 2024). *Nothophaeocryptopus gaeumannii* represented 66% of overall sequence reads & *Mycosphaerellales sp3* represented 23% of overall sequence reads which, combined, represented ~ 90% of all reads. The remaining rare and relatively low abundance features accounted for 99.71% of OTUs, but only ~ 10% of overall reads. *N. gaeumannii* is a well studied Douglas-fir endophyte best known for being the causal agent of Swiss Needle Cast (Stone *et al.*, 2008). This fungus becomes pathogenic when pseudothecia grow through stomata blocking gas exchange, and causing eventual needle senescence when pseudothecia block a critical number of stomata (Stone *et al.*, 2008). The West45 research site was assessed by BC Ministry of Forests staff for Swiss needle cast in 2025 and was found to have high severity (Degner, personal communication, 2026). Other metabarcoding surveys of Douglas-fir foliar fungal endophytes found *N. gaeumannii* to be the most dominant species (Gervers, 2024; Hayward, 2024). This fungus is both endophyte and epiphyte, with hyphae emerging from pseudothecial primordia, and re-infecting through un-occupied stomata. Pseudothecial growth continues from mid-summer on (Stone *et al*., 2008). Manter *et al*. (2005) found that increased heat and sun exposure coupled with reduced humidity experimentally increased *N. gaeumannii* in Douglas-fir needles. This is consistent with my data, which shows a steady increase in *N. gaeumannii* over the dry, hot months. Occlusion data gathered from this study also indicated that the percent of stomata occluded by pseudothecia increased as the season progressed (Appendix E, Figure 1).

Attempts to further define *Mycosphaerellales sp3* were unsuccessful. Possibly this taxon belongs to the family Teratosphaeriaceae as inferred by the phylogenetic tree constructed from fungal endophyte ITS1 sequences acquired through this research. In this reconstruction, members of the family Teratosphaeriaceae are split between several clades. Teratosphaeriaceae is a newly formed family, recently split from the family Mycosphaerellaceae. The clade containing *Mycosphaerellales sp3* also contains families Dissoconiaceae and Cladosporiaceae, and it is therefor possible that *Mycosphaerellales sp3* could be within those families. Relative abundance data infers a negative relationship between *Mycosphaerellales sp3* and *N. gaeumannii*, confirmed by a strong negative Spearman correlation. As the primary symbiont of Douglas-fir needles, *N. gaeumannii* may be highly capable of outcompeting other abundant occupants of this niche.

Fungal Traits

Fungal traits were assigned to OTUs resolved to genus or species level. Of those that were matched to the FungalTraits database, several were classified as pathogens of fungi and animals. Finding animal and fungi pathogens in plant tissue may represent complex lifestyles wherein multiple hosts and life stages exist (Redman *et al*., 2001). *Tremella globispora,* a Basidiomycete in the family Tremellaceae, was listed as a pathogen of fungi in my dataset. Tremella species must grow associated with other fungi (Diederich *et al*., 2022), and *Tremella globispora* is known as a parasite of *Valsa* and *Diaporthe* species (Brough, 1974). Neither *Valsa* nor *Diaporthe* species were found in my data set, insinuating greater host diversity for *Tremella globispora*. An animal pathogen found was *Malassezia restricta,* a Basidiomycete in the family Malasseziaceae, which is common and ubiquitous on human skin, often causing dandruff or eczema (Xu *et al.,* 2007). This suggests that this OTU was actually a contaminant introduced during DNA extraction. No *Malassezia* species were found in my negative control, which omitted needle tissue, therefor this species may have been introduced through needle handling. Cryptococcus, a well-known animal pathogen being the causal agent of meningitis (BC Centre for Disease Control, n.d.), was also present in my data, yet, it was not included in the FungalTraits database, indicating the limitations of this service. One endophyte from my data assigned as plant pathogen was a *Fomitopsis pinicola,* a Basidiomycete of the family Fomitopsidaceae. These fungi form large conspicuous fruiting bodies on standing trees, often causing heart rot in living trees, also known as Brown Crumbly Rot (Natural Resources Canada, n.d.). Of the plant pathogens listed, there was no mention of Douglas-fir pathogens *Nothophaeocryptopus gaeumannii* which causes Swiss Needle Cast*,* or *Rhabdocline pseudotsugae* which causes Rhabdocline Needle Cast (Natural Resources Canada, n.d.). Both of these were present in my data.

Hypholoma fasciculare, Hypholoma dispersum, and *Hypholoma capnoides*, which are Basidiomycetes in the family Strophariaceae, were assigned as saprotrophs. These are common mushrooms on the West Coast often associated with Douglas-fir stands. While *H. capnoides* is considered a choice edible, *H. fasciculare,* or Sulphur Tuft, is poisonous (Kuo, M., n.d.). Both *Hypholoma fasciculare* and *Hypholoma capnoides* were also found to have significant differential abundance between sampling months. Assigning traits to endophytic fungi is formidable and complex, as fungi life histories are cryptic and elusive. It has been theorised that most endophytes are saprobes seeking refuge until plant senescence (Promputtha, 2010; Tanney, 2017). Conversely, many endophytes may be latent pathogens (Redman *et al*., 2001) triggered by subtle environmental cues or opportunistically awaiting transfer to susceptible hosts.

The OTUs Driving Seasonal Community Variation

To better understand how months differ in mycobiome composition, individual fluctuating taxa were identified and ranked from highest to lowest fluctuation, and the top 12 are shown in Figure 10. *N. gaeumannii, Fungi sp37, Eurotiomycetes sp39, Extremus adstrictus,* and *Neodevriesia sp2* rise progressively from February to November, while *Mycosphaerellales sp3, Dothideomycetes sp2*, and *Ascomycota sp37* decline in relative abundance over the season. *Fungi* *sp37, Eurotiomycetes sp39*, *Dothideomycetes sp2* had 3rd, 4th, and 5th most abundant sequence read counts. More detailed taxonomy can be inferred using the phylogenetic tree constructed from sequences of this study. *Fungi sp37* is situated among members of Teratosphaeriaceae. *Eurotiomycetes sp39* is within a clade occupied OTUs in the Order Chaetothyriales (Data not shown). *Dothideomycetes sp2* is within the same clade as *Mycosphaerellales sp3,* also within the family Teratosphaeriaceae.

Extremus adstrictus, an Ascomycete of the family Extremaceae, has been described as a rock dwelling melanized fungus found in European locations, and the only other species of this genus was found on Antarctic rock (Pem *et al*., 2019). The Genus *Extremus* is of the Order Capnodiales according to most sources, but is labelled as Mycosphaerellales by UNITE reference database, and is located among members of Mycosphaerellaceae on my phylogenetic tree. The Genus *Neodevriesia,* an Ascomycete of the family Neodevriesiaceae, is distributed globally and has been found associated with marine algae, corals, and high elevation terrestrial limestone (Lee *et al*., 2022). *Neodevriesia knoxdaviesii* is a fungus associated with leaf spots on *Persoonia* (also known as snottygobbles) in South Africa (Crous *et al*., 2008). *Fungi sp37, Dothideomycetes sp2* and *Mycosphaerellales sp3* are likely within the Family Teratosphaeriacae. This family was recently established, along with Extremaceae and Neodevresiaceae, which all previously belonged to Mycosphaerellaceae (Quaedvlieg *et al*., 2014). These families commonly include saprobes, plant pathogens, and extremophiles (Quaedvlieg *et al*., 2014). The order Chaetothyriales of Ascomycota, is primarily represented by melanized fungi capable of inhabiting diverse, extreme, toxic environments, and are known for ant symbioses (Vassa *et al*., 2017).

While the above were described because their abundance fluctuated most across sampling months, statistically significant differentially abundant taxa were identified comparing OTU abundance in each month. These were *Hypholoma capnoides, Ramularia sp4, Fungi sp59, Helotiales sp8, Aspergillaceae sp, Naemateliaceae sp3, Hypholoma fasciculare,* and *Chaetothyriales sp1*. Ramularia sp4* is located in a clade adjacent to that of *N. gaeumannii* in my phylogenetic reconstruction. This is a genus in the family Mycosphaerellaceae and is an important plant pathogen in agriculture (Videira *et al*., 2016). *Fungi sp59* is located within the least derived branches of Ascomycota, very close to *Ritiarus sp* (data not shown), which is a globally distributed genus of pollen parasites also often found on lichen (Huereca *et al*., 2025).

The order Helotiales are Ascomycetes of the class Leotiomycetes, and comprises common Douglas-fir endophytes/pathogens such as *Rhabdocline parkerii* and *Rhabdocline pseudotsuga.* Aspergillaceae is an Ascomycete family in the order Eurotiales and contains ubiquitous and important genera such as *Aspergillus* and *Penicillium* (Houbraken *et al*., 2014). The family *Naemateliaceae* are Basidiomycota in the order Tremelles and contains only two genera, one of which is an important Chinese medicinal fungus (Tang & Yang, 2024).

It is interesting to think of where this diversity might come from, considering the global distribution of some of the taxa present. Many fungal spores are airborne (Meng *et al*., 2009; Pakpour *et al*., 2015) and can be picked up by air currents. The West45 site is located within 2 kilometers of the Salish Sea which receives strong winds from the Pacific Ocean and the North Pacific Gyre (Ocean Tracks, n.d.). These major air currents circulate the North Pacific Ocean clockwise, and have the potential to import spores by mingling with the South Pacific Gyre or Subpolar Gyre, or from the coasts of Asia. Spores landing on needle surfaces often enter inner leaf tissue by penetrating the stomata, although ability to colonize is not guaranteed. Co-evolution has honed plant-endophyte relationships (Zipfel & Oldroyd, 2017) resulting in host, and even lineage, specificity (Redondo *et al*., 2022), conversely plant defence systems may not be in place for the exclusion of novel fungi.

The fungi described in the preceding paragraphs were only a portion of the taxa seen to fluctuate in relative abundance throughout the season, driving endo-mycobiome community structure diversity when comparing different months. Inter-microbe interactions may be credited for the dynamic nature of these communities, as fungal secondary metabolite production changes with multiple endophytes present (Kusari *et al*., 2013; Soliman & Raizada, 2013), often to gain competitive advantage and secure resources within plant tissue (Boddy & Hiscox, 2016), and many fungal endophytes can inhibit or suppress the growth of competitors (Graham *et al*., 2025). It appears that the inner tissues of plant hosts are busy microcosms wherein opportunistically dispersed spores are attempting to gain and secure entry into occupied habitat, and many appear to succeed in small numbers, suggesting complex interactions based on community structure.

Filtering

For this dataset, I chose a conservative filtering approach, proposing that variation in community composition would be largely driven by low abundance taxa. Workflows suggest filtering out all features with a mean sample depth of < 0.1% (Comeau *et al*., 2017), because Illumina bleed-through is reported to introduce ~ 0.1% contamination (Illumina, 2017). This level of filtering would have required the removal of all OTUs with read counts <142 for my dataset, cutting out the vast majority. Instead, I removed all OTUs with < 25 sequence reads overall and all OTUs with reads found in only one sample, as well as 3 OTUs present in the negative control. This "conservative" filtering still removed 2/3 of all OTUs. Of the rare and low abundance OTUs removed, a considerable number of them were corticoid and crust-like fungi, as well as lichen associated fungi, and interestingly there was also a high number of marine algae species such as kelps and diatoms (data not shown). My immediate intuition was that these sequences resulted from Illumina bleed-through due to library multiplexing, but one cannot rule out Type II error. The West45 site is located close to the ocean, receiving heavy winds loaded with ocean spray, and it may be possible for marine algae DNA to end up in fir needle tissue. Also, lichen and corticoid fungi are ubiquitous, therefore these could be genuine biological results and should not be wholly dismissed.

Future outlook

The results reported here only begin to scratch the surface of what this dataset can tell us. Here I reported on only the most statistically significant results, which were consistent with my original hypothesis that fungal endophyte communities shift in composition over the course of the growing season. However, I also compared fungal communities between tree families, as well as some initial statistics on Swiss needle cast signs and symptoms, but chose to omit these results due to time and space constraints. Future research would include a more in-depth account of these variables, as well as revising the statistics seen here with methods modified for compositional data such as this. Bray-Curtis, UniFrac and Spearman correlation analyses are controversial measures for compositional data, and Gloor *et al*. (2017) suggest more suitable tools, including centered log ratio (clr) transformation coupled with Aitchison distance for Beta-diversity comparisons, and SPARCC or SPieCeasi for correlational analyses. In addition, compositional data such as this cannot accurately represent taxon abundance due to the nature of the sequencing technology, therefore qPCR could be employed to adequately quantify taxa of interest (Comeau, personal communication). Importantly, future attempts to identify *Mycosphaerellales sp3* using culturing methods should be prioritised, along with construction of a phylogenetic tree using reliable Dothidiomycetes species sequences. Multivariate analyses should be conducted to include metadata collected, such as soil type and pH, tree size, tree growth, and brush competition. It would also be interesting to track the changes in endo-mycobiome structure within tree 555 needles, which was healthy at the beginning of the sampling period, yet was dead by July. One could attempt to parse the cause of death in this manner, and I suspect one would see a steep transition to saprotrophic species.

Conclusion

This research is the first to confirm the seasonally dynamic nature of foliar fungal endophyte communities in Douglas-fir needles throughout a growing season. Although consistent taxa exist in these spheres, it is evident that one cannot assume static community structure when parsing microbial foliar ecology. The dynamic nature of these communities coupled with inter-microbial interactions and secondary metabolite production could have implications in implementation of fungal endophyte assemblage inoculation as biocontrol agents or for crop enhancement. Furthering this work will deepen our knowledge of plant endophytes and strengthen efforts to improve food security, forestry practices, and conservation efforts, all of which require critical attention to ensure a sustainable future.

References

Abdelfattah, A., Malacrinò, A., Wisniewski, M., Cacciola, S. O., & Schena, L. (2018). Metabarcoding: A powerful tool to investigate microbial communities and shape future plant protection strategies. *Biological Control*, *120*, 1-10. https://doi.org/10.1016/j.biocontrol.2017.07.009

Abarenkov, K., Zirk, A., Piirmann, T., Pöhönen, R., Ivanov, F., Nilsson, R. H., Kõljalg, U. (2025). UNITE QIIME release for eukaryotes 2. Version 19.02.2025. UNITE Community. https://doi.org/10.15156/BIO/3301244

Aghai, M., Khan, Z., Joseph, M., Stoda, A., Sher, A., Ettl, G., & Doty, S. (2019). The effect of microbial endophyte consortia on Pseudotsuga menziesii and Thuja plicata survival, growth, and physiology across edaphic gradients. *Frontiers in Microbiology*, *10*, 1353.https://doi.org/10.3389/fmicb.2019.01353

Andlar, M., Rezić, T., Marđetko, N., Kracher, D., Ludwig, R., & Šantek, B. (2018). Lignocellulose degradation: An overview of fungi and fungal enzymes involved in lignocellulose degradation. *Engineering in life sciences*, *18*(11), 768-778. doi: 10.1002/elsc.201800039

BC Centre for Disease Control. (n.d.). *Cryptococcus gattii*. Retrieved March 11, 2026, from https://www.bccdc.ca/health-info/diseases-conditions/cryptococcus-gattii

BC Ministry of Forests (2024, May 23). *Coastal Douglas-fir tree breeding program*. Province of British Columbia. https://www2.gov.bc.ca/gov/content/industry/forestry/managing-our-forest-resources/tree-seed/forest-genetics/tree-breeding-improvement/coastal-douglas-fir

Berbee, M. L., & Taylor, J. W. (2007). Rhynie chert: a window into a lost world of complex plant-fungus interactions. *The New phytologist*, *174*(3), 475–479. https://doi.org/10.1111/j.1469-8137.2007.02080.x

Berbee, M.L., Strullu-Derrien, C., Delaux, PM. *et al* (2020). Genomic and fossil windows into the secret lives of the most ancient fungi. *Nat Rev Microbiol* **18**, 717–730. https://doi.org/10.1038/s41579-020-0426-8

Boddy, L., & Hiscox, J. (2016). Fungal Ecology: Principles and mechanisms of colonization and competition by saprotrophic fungi. *Microbiology Spectrum*, *4*(6). https://doi.org/10.1128/microbiolspec.FUNK-0019-2016

Bolyen, E., Rideout, J.R., Dillon, M.R. *et al.* (2019). Reproducible, interactive, scalable and extensible microbiome data science using QIIME 2. *Nat Biotechnol* **37**, 852–857 https://doi.org/10.1038/s41587-019-0209-9

Bowman, E. A., & Arnold, A. E. (2021). Drivers and implications of distance decay differ for ectomycorrhizal and foliar endophytic fungi across an anciently fragmented landscape. *The ISME Journal*, *15*(12), 3437–3454. https://doi.org/10.1038/s41396-021-01006-9

Brader, G., Compant, S., Vescio, K., Mitter, B., Trognitz, F., Ma, L. J., & Sessitsch, A. (2017). Ecology and genomic insights into plant-pathogenic and plant-nonpathogenic endophytes. *Annual Review of Phytopathology*, *55*(1), 61-83. https://doi.org/10.1146/annurev-phyto-080516-035641

Bradley, D. J., Gilbert, G. S., & Parker, I. M. (2003). Susceptibility of clover species to fungal infection: the interaction of leaf surface traits and environment. *American Journal of Botany*, *90*(6), 857-864.

Brodski, M., Tullus, A., Agan, A., Adamson, K., Drenkhan, R., Rosenvald, K., & Sellin, A. (2025). The effects of humidity and seasonality on foliar and root mycobiomes of *Betula pendula*. *Environmental Microbiology Reports*, *17*(4), e70145. https://doi.org/10.1111/1758-2229.70145

Brough, S. G. (1974). *Tremella globospora*, in the field and in culture. *Canadian Journal of Botany*, *52*(8), 1853–1859. https://doi.org/10.1139/b74-238

Camacho, C., Coulouris, G., Avagyan, V., Ma, N., Papadopoulos, J., Bealer, K., and Madden, T.L. 2009. BLAST+: architecture and applications. *BMC Bioinformatics*, 10, 421.

Carroll, G. C., & Carroll, F. E. (1978). Studies on the incidence of coniferous needle endophytes in the Pacific Northwest. *Canadian Journal of Botany*, *56*(24), 3034–3043. https://doi.org/10.1139/b78-367

Chen, C. C., Chen, Y. N., Liou, J. M., Wu, M. S., & Taiwan Gastrointestinal Disease and Helicobacter Consortium. (2019). From germ theory to germ therapy. *The Kaohsiung journal of medical sciences*, *35*(2), 73-82. https://doi.org/10.1002/kjm2.12011

Chow, C., Padda, K. P., Puri, A., & Chanway, C. P. (2022). An archaic approach to a modern issue: endophytic archaea for sustainable agriculture. *Current Microbiology*, *79*(11), Article 322. https://doi.org/10.1007/s00284-022-03016-y

Comeau, A. M., Douglas, G. M., & Langille, M. G. I. (2017). *Microbiome Helper: a custom and streamlined workflow for microbiome research*. mSystems, 2(1), e00127-16. https://doi.org/10.1128/mSystems.00127-16

Cosner, J., Pandharikar, G., Tremble, K., Nash, J., Rush, T. A., Vilgalys, R., & Veneault-Fourrey, C. (2025). Fungal endophytes. *Current Biology*, *35*(19), R904–R910. https://doi.org/10.1016/j.cub.2025.08.058

Crous, P. W., Summerell, B. A., Mostert, L., & Groenewald, J. Z. (2008). Host specificity and speciation of Mycosphaerella and Teratosphaeria species associated with leaf spots of Proteaceae. *Persoonia*, *20*, 59–86. https://doi.org/10.3767/003158508X323949

Diederich, P., Millanes, A. M., & Wedin, M. (2022). Class Tremellomycetes, order Tremellales. *Flora of Lichenicolous Fungi*, *1*, 105-282.

Edgar RC. 2004. MUSCLE: multiple sequence alignment with high accuracy and high throughput. *Nucleic Acids Research* 32(5):1792–1797. https://doi.org/10.1093/nar/gkh340

Environment Canada. (2015). *National marine weather guide: British Columbia regional guide*. Government of Canada. https://publications.gc.ca/site/eng/9.630051/publication.html

Field, C. B., Behrenfeld, M. J., Randerson, J. T., & Falkowski, P. (1998). Primary production of the biosphere: integrating terrestrial and oceanic components. *Science (American Association for the Advancement of Science)*, *281*(5374), 237–240. https://doi.org/10.1126/science.281.5374.237

Fitzpatrick, C. R., Salas-González, I., Conway, J. M., Finkel, O. M., Gilbert, S., Russ, D., ... & Dangl, J. L. (2020). The plant microbiome: from ecology to reductionism and beyond. *Annual review of microbiology*, *74*(1), 81-100. https://doi.org/10.1146/annurev-micro-022620-014327

Flynn, S. (1999). *Coastal Douglas-fir ecosystems*. British Columbia Ministry of Environment, Lands and Parks. https://www.env.gov.bc.ca/wld/documents/douglasfir.pdf

Freeman, S., Shtienberg, D., Maymon, M., Levin, A. G., & Ploetz, R. C. (2014). New insights into mango malformation disease epidemiology lead to a new integrated management strategy for subtropical environments. *Plant disease*, *98*(11), 1456-1466.

Fuchs, B., Krischke, M., Mueller, M. J., & Krauss, J. (2017). Plant age and seasonal timing determine endophyte growth and alkaloid biosynthesis. *Fungal Ecology*, *29*, 52-58.

Gardes, M., & Bruns, T. D. (1993). ITS primers with enhanced specificity for basidiomycetes—Application to the identification of mycorrhizae and rusts. *Molecular Ecology*, 2(2), 113-118.https://doi.org/10.1111/j.1365-294x.1993.tb00005.x

Geetha Thanuja, K., Annadurai, B., Thankappan, S., & Uthandi, S. (2020). Non-rhizobial endophytic (NRE) yeasts assist nodulation of Rhizobium in root nodules of blackgram

(Vigna mungo L.). *Archives of Microbiology*, *202*(10), 2739-2749. https://doi-org.ezproxy.library.uvic.ca/10.1007/s00203-020-01983-z

Gervers, K. A. (2024). Host and environmental drivers of foliar fungal abundance and composition in coastal Douglas-fir. *Oregon State University Libraries and Press*. https://ir.library.oregonstate.edu/concern/graduate_thesis_or_dissertations/dv1403169

Gloor, G. B., Macklaim, J. M., Pawlowsky-Glahn, V., & Egozcue, J. J. (2017). Microbiome datasets are compositional: and this is not optional. *Frontiers in Microbiology*, 8:2224.

Goh, C. H., Veliz Vallejos, D. F., Nicotra, A. B., & Mathesius, U. (2013). The impact of beneficial plant-associated microbes on plant phenotypic plasticity. *Journal of chemical ecology*, *39*(7), 826-839. https://doi.org/10.1007/s10886-013-0326-8

Gonen, L. (2020). Community ecology of foliar fungi and Oomycetes of *Pseudotsuga menziesii* on the Pacific Northwest Coast. *Oregan State University*. https://ir.library.oregonstate.edu/concern/graduate_thesis_or_dissertations/z316q844f

Gould, P. J., Harrington, C. A., & Clair, J. B. S. (2012). Growth phenology of coast Douglas-fir seed sources planted in diverse environments. *Tree Physiology*, *32*(12), 1482–1496. https://doi.org/10.1093/treephys/tps106

Graham, H., Hayward, E., Ehlting, J., de la Bastide, P., Avis, T., Feau, N., Hamelin, R., Bérubé, J., McMullin, D., & Tanney, J. (2025). In vitro suppression of the Swiss needle cast pathogen *Nothophaeocryptopus gaeumannii* by metabolite extracts from endophytes of Douglas-Fir. *PhytoFrontiers*, *5*(3), 366–378. https://doi.org/10.1094/PHYTOFR-07-24-0085-R

Hardoim, P. R., van Overbeek, L. S., Berg, G., Pirttilä, A. M., Compant, S., Campisano, A., Döring, M., & Sessitsch, A. (2015). The hidden world within plants: ecological and evolutionary considerations for defining functioning of microbial endophytes. *Microbiology and Molecular Biology Reviews*, *79*(3), 293–320. https://doi.org/10.1128/MMBR.00050-14

Hawkins, H. J., Cargill, R. I., Van Nuland, M. E., Hagen, S. C., Field, K. J., Sheldrake, M., ... & Kiers, E. T. (2023). Mycorrhizal mycelium as a global carbon pool. *Current Biology*, *33*(11), R560-R573. https://doi.org/10.1016/j.cub.2023.02.027

Hayward, E. (2024). Swiss needle cast and the foliar mycobiome of coastal Douglas-fir (*Pseudotsuga menziesii*). *University of Victoria.*

Houbraken, J., Vries, R., & Samson, R. (2014). Chapter Four - Modern taxonomy of biotechnologically important Aspergillus and Penicillium species. *Advances in Applied Microbiology*, *86*, 199–249. https://doi.org/10.1016/B978-0-12-800262-9.00004-4

Huereca, A., Allen, G., McMullin, T., Simon, A., Belosokhov, A., & Spribille, T. (2025). Evidence for extensive diversity in the pollen-parasitic genus *Retiarius* in western North America, including two new species associated with lichens. *Mycologia*, *117*(6), 1148–1174. https://doi.org/10.1080/00275514.2025.2513197

Illumina, Inc. (2017). Effects of index misassignment on multiplexing and downstream analysis (White paper No. 770-2017-004). https://www.illumina.com/content/dam/illumina-marketing/documents/products/whitepapers/index-hopping-white-paper-770-2017-004.pdf

Katial, R. K., Zhang, Y., Jones, R. H., & Dyer, P. D. (1997). Atmospheric mold spore counts in relation to meteorological parameters. *International journal of biometeorology*, *41*(1), 17-22. https://doi.org/10.1007/s004840050048

Katoh K, Standley DM. 2013. MAFFT multiple sequence alignment software version 7: improvements in performance and usability. *Molecular Biology and Evolution* 30(4):772–780. https://doi.org/10.1093/molbev/mst010

Kiser, J., Daniels, H., and Scrivani, J., (2019). Isolation of endophytic fungi from Douglas-fir (Pseudotsuga menziesii) foliage with bioprospecting potential for Natural Pharmaceuticals. *Current Trends in Forest Research*, *3*(01). https://doi.org/10.29011/2638-0013.100035

Kumar, S., Stecher, G., Suleski, M., Sanderford, M., Sharma, S., Tamura, K. (2024). Molecular evolutionary genetics analysis version 12 for adaptive and green computing. *Molecular Biology and Evolution 41: 1-9*

Kuo, M. (n.d.). *Hypholoma fasciculare*. MushroomExpert.Com. Retrieved March 10, 2026, from https://www.mushroomexpert.com/hypholoma_fasciculare.html

Kusari, S., Pandey, S. P., & Spiteller, M. (2013). Untapped mutualistic paradigms linking host plant and endophytic fungal production of similar bioactive secondary metabolites. *Phytochemistry (Oxford)*, *91*, 81–87. https://doi.org/10.1016/j.phytochem.2012.07.021

Lam, C. K., Belanger, F. C., White Jr, J. J., & Daie, J. (1994). Mechanism and rate of sugar uptake by *Acremonium typhinum*, an endophytic fungus infecting *Festuca rubra*: evidence for presence of a cell wall invertase in endophytic fungi. *Mycologia*, *86*(3), 408-415.

Le May, C., Potage, G., Andrivon, D., Tivoli, B., & Outreman, Y. (2009). Plant disease complex: Antagonism and synergism between pathogens of the Ascochyta blight complex on pea. *Journal of Phytopathology*, *157*(11-12), 715-721.

Lee, L. C., Rizman-Idid, M., Alias, S. A., Palaniveloo, K., & Gu, H. (2022). First record of the fungal genus Neodevriesia Quaedvl. & Crous (Ascomycota, Dothideomycetes, Neodevriesiaceae) isolated from scleractinian corals of Perhentian Islands, Malaysia. *Biodiversity Data Journal*, *10*(6), e81533. https://doi.org/10.3897/BDJ.10.e81533

Letunic I, Bork P. (2021). Interactive Tree of Life (iTOL) v5: an online tool for phylogenetic tree display and annotation. *Nucleic Acids Research*. 49(W1):W293-W296. doi: 10.1093/nar/gkab301. PMID: 33885785; PMCID: PMC8265157.

Liao, C., Doilom, M., Jeewon, R., Hyde, K. D., Manawasinghe, I. S., Chethana, K. W. T., Balasuriya, A., Thakshila, S. A. D., Luo, M., Mapook, A., Htet, Z. H., Koodalugodaarachchi, V., Wijekoon, N., Saxena, R. K., Senanayake, I. C., Kularathnage, N. D., Alrefaei, A. F., & Dong, W. (2025). Challenges and update on fungal endophytes: classification, definition, diversity, ecology, evolution and functions. *Fungal Diversity*, *131*(1), 301–367. https://doi.org/10.1007/s13225-025-00550-5

Ligon, B. L. (2004). Penicillin: its discovery and early development. In *Seminars in pediatric infectious diseases* (Vol. 15, No. 1, pp. 52-57). WB Saunders. https://doi.org/10.1053/j.spid.2004.02.001

Ludwig-Müller, J. (2015). Plants and endophytes: equal partners in secondary metabolite production? *Biotechnology Letters*, *37*(7), 1325–1334. https://doi.org/10.1007/s10529-015-1814-4

Mandal, S., Van Treuren, W., White, R. A., Eggesbø, M., Knight, R., & Peddada, S. D. (2015). Analysis of composition of microbiomes: a novel method for studying microbial composition. *Microbial Ecology in Health and Disease*, 26, 27663. https://doi.org/10.3402/mehd.v26.27663

Manter, D., Reeser, P., & Stone, J. (2005). climate-based model for predicting geographic variation in Swiss needle cast severity in the Oregon Coast Range. *Phytopathology*, *95*(11), 1256–1265. https://doi.org/10.1094/PHYTO-95-1256

Martin, M. (2011). Cutadapt removes adapter sequences from high-throughput sequencing reads. *Embnet journal*, 17, 10-12. https://doi.org/10.14806/ej.17.1.200

Masson-Boivin, C., & Sachs, J. L. (2018). Symbiotic nitrogen fixation by rhizobia—the roots of a success story. *Current Opinion in Plant Biology*, *44*, 7-15. https://doi.org/10.1016/j.pbi.2017.12.001

Massoni, J., Bortfeld-Miller, M., Jardillier, L., Salazar, G., Sunagawa, S., & Vorholt, J. A. (2020). Consistent host and organ occupancy of phyllosphere bacteria in a community of wild herbaceous plant species. *The ISME journal*, *14*(1), 245-258. https://doi.org/10.1038/s41396-019-0531-8

Meng, S., Torto-Alalibo, T., Chibucos, M. C., Tyler, B. M., & Dean, R. A. (2009). Common processes in pathogenesis by fungal and oomycete plant pathogens, described with Gene Ontology terms. *BMC Microbiology*, *9*(Suppl 1), Article S7. https://doi.org/10.1186/1471-2180-9-S1-S7

Natural Resources Canada. (n.d.). *Trees, insects and diseases of Canada's forests: Factsheet 18*. Government of Canada. https://tidcf.nrcan.gc.ca/en/diseases-caused-by-pathogens/factsheet/18, https://tidcf.nrcan.gc.ca/en/diseases-caused-by-pathogens/factsheet/1000043

Natural Resources Canada (n.d.) *Trees, insects and diseases of Canada's forests: Factsheet 122*. Government of Canada. Available at: https://tidcf.nrcan.gc.ca/en/trees/factsheet/122

Newcombe, G., Harding, A., Ridout, M., & Busby, P. E. (2018). A hypothetical bottleneck in the plant microbiome. *Frontiers in microbiology*, *9*, 1645. https://doi.org/10.3389/fmicb.2018.01645

Ocean Tracks. (n.d.). *Major currents*. Ocean Tracks. https://oceantracks.org/library/the-north-pacific-ocean/major-currents

Ondov D, Bergman H, Phillippy M. (2011). Interactive metagenomic visualization in a Web browser. *BMC Bioinformatics* 12:385. https://doi.org/10.1186/1471-2105-12-385

Pakpour, S., Li, D. W., & Klironomos, J. (2015). Relationships of fungal spore concentrations in the air and meteorological factors. *Fungal Ecology*, *13*, 130-134. https://doi.org/10.1016/j.funeco.2014.09.008

Partida-Martinez, L., Hertweck, C. (2005). Pathogenic fungus harbours endosymbiotic bacteria for toxin production. *Nature* **437**, 884–888 https://doi.org/10.1038/nature03997

Partida-Martínez, L. P., & Heil, M. (2011). The microbe-free plant: fact or artifact? *Frontiers in plant science*, *2*, 100. https://doi.org/10.3389/fpls.2011.00100

Perry, d. A. (1996) A brief overview of coastal Douglas-fir ecosystems. *Ecology and management of interior Douglas-fir (Pseudotsuga menziesii var glauca) at the northern extreme of its range*, 3.

Phillips, R. (2014). *Alcohol: a history*. UNC Press Books.

Põlme, S., Abarenkov, K., Nilsson, R.H., Lindahl, B.D., Clemmensen, K.E., Kauserud, H., Nguyen, N., Kjøller, R., Bates, S.T., Baldrian, P., et al. (2020). FungalTraits: a user-friendly traits database of fungi. *Fungal Diversity*, 105, 1–16. https://doi.org/10.1007/s13225-020-00466-2

Posit Team. 2024. RStudio: Integrated Development Environment for R. Posit Software, PBC, Boston, MA, USA. http://www.posit.co/

Price N, Dehal S, Arkin P. (2010). FastTree 2 – approximately maximum-likelihood trees for large alignments. *PLoS ONE* 5(3):e9490. https://doi.org/10.1371/journal.pone.0009490

Promputtha, I., Hyde, K. D., McKenzie, E. H., Peberdy, J. F., & Lumyong, S. (2010). Can leaf degrading enzymes provide evidence that endophytic fungi becoming saprobes? *Fungal Diversity*, *41*(1), 89-99. https://doi.org/10.1007/s13225-010-0024-6

Quaedvlieg, W., Binder, M., Groenewald, J. Z., Summerell, B. A., Carnegie, A. J., Burgess, T. I., & Crous, P. W. (2014). Introducing the Consolidated Species Concept to resolve species in the Teratosphaeriaceae. *Persoonia*, *33*, 1–40. https://doi.org/10.3767/003158514X681981

Quiring, D., Flaherty, L., Adams, G., McCartney, A., Miller, J. D., & Edwards, S. (2019). An endophytic fungus interacts with crown level and larval density to reduce the survival of eastern spruce budworm, *Choristoneura fumiferana* (Lepidoptera: Tortricidae), on white spruce (Picea glauca). *Canadian Journal of Forest Research*, *49*(3), 221-227. https://doi.org/10.1139/cjfr-2018-0194

R Core Team. 2024. R: A language and environment for statistical computing. R Foundation for Statistical Computing, Vienna, Austria. https://www.R-project.org//

Rana, K. L., Kour, D., Kaur, T., Devi, R., Yadav, A. N., Yadav, N., ... & Saxena, A. K. (2020). Endophytic microbes: biodiversity, plant growth-promoting mechanisms and potential applications for agricultural sustainability. *Antonie Van Leeuwenhoek*, *113*(8), 1075-1107.

Raza, W., Jiang, G., Eisenhauer, N., Huang, Y., Wei, Z., Shen, Q., ... & Jousset, A. (2024). Microbe-induced phenotypic variation leads to overyielding in clonal plant populations. *Nature Ecology & Evolution*, *8*(3), 392-399. https://doi.org/10.1038/s41559-023-02297-1

Redman, R. S., Dunigan, D. D., & Rodriguez, R. J. (2001). Fungal symbiosis from mutualism to parasitism: who controls the outcome, host or invader? *New Phytologist*, *151*(3), 705-716. https://doi-org.ezproxy.library.uvic.ca/10.1046/j.0028-646x.2001.00210.x

Redman, R. S., Sheehan, K. B., Stout, R. G., Rodriguez, R. J., & Henson, J. M. (2002). Thermotolerance generated by plant/fungal symbiosis. *Science (American Association for the Advancement of Science)*, *298*(5598), 1581. https://doi.org/10.1126/science.1072191

Redondo, M. A., Oliva, J., Elfstrand, M., Boberg, J., Capador-Barreto, H. D., Karlsson, B., & Berlin, A. (2022). Host genotype interacts with aerial spore communities and influences the needle mycobiome of Norway spruce. *Environmental Microbiology*, *24*(8), 3640-3654. doi:10.1111/1462-2920.15974

Rognes T, Flouri T, Nichols B, Quince C, Mahé F. (2016) VSEARCH: A versatile open-source tool for metagenomics. *PeerJ* 4:e2584. doi: 10.7717/peerj.2584

Santoyo, G., del Carmen Orozco-Mosqueda, M., & Babalola, O. O. (2025). How protists contribute to plant growth and health: exploring new interactions with the plant microbiome. *The Microbe*, 100361. https://doi.org/10.1016/j.microb.2025.100361

Schoonmaker, A. L., Hillabrand, R. M., Lieffers, V. J., Chow, P. S., & Landhäusser, S. M. (2021). Seasonal dynamics of non-structural carbon pools and their relationship to growth in two boreal conifer tree species. *Tree Physiology*, *41*(9), 1563–1582. https://doi.org/10.1093/treephys/tpab013

Sherwood-Pike, M., Stone, J. K., & Carroll, G. C. (1986). Rhabdocline parkeri, a ubiquitous foliar endophyte of Douglas-fir. *Canadian Journal of Botany*, *64*(9), 1849–1855. https://doi.org/10.1139/b86-245

Sieber, T. N. (2007). Endophytic fungi in forest trees: are they mutualists? *Fungal Biology Reviews*, *21*(2), 75–89. https://doi.org/10.1016/j.fbr.2007.05.004

Simard, S., Roach, W., Defrenne, C., Pickles, B., Snyder, E., Robinson, A., & Lavkulich, L. (2020). Harvest intensity effects on carbon stocks and biodiversity are dependent on regional climate in Douglas-fir forests of British Columbia. *Frontiers in Forests and Global Change*, *3*, 88. https://doi.org/10.3389/ffgc.2020.00088

Solheim, H., Agan, A., Hietala, A. M., Drenkhan, R., Adamson, K., & Tedersoo, L. (2021). Seasonal dynamics of fungi associated with healthy and diseased *Pinus sylvestris* needles in Northern Europe. *Microorganisms (Basel)*, *9*(8), 1757. https://doi.org/10.3390/microorganisms9081757

Soliman, S. S., & Raizada, M. N. (2013). Interactions between co-habitating fungi elicit synthesis of Taxol from an endophytic fungus in host Taxus plants. *Frontiers in microbiology*, *4*, 3. https://doi.org/10.3389/fmicb.2013.00003

Stierle, A., Strobel, G., & Stierle, D. (1993). Taxol and taxane production by Taxomyces andreanae, an endophytic fungus of Pacific yew. *Science*, *260*(5105), 214-216. DOI: 10.1126/science.8097061

Stone, J., Capitano, B., & Kerrigan, J. (2008). The histopathology of *Phaeocryptopus gaeumannii* on Douglas-fir needles. *Mycologia*, *100*(3), 431–444. https://doi.org/10.3852/07-170R1

Szymanski, S., & Miles, T. (2025). Temporal dynamics and tissue-specific variations of the blueberry phyllosphere mycobiome. *Horticulture Research*, *12*(5), uhaf042. https://doi.org/10.1093/hr/uhaf042

Tang, J., & Yang, Z. (2024). Phylogeny and taxonomy of the *Naematelia aurantialba* complex in southwestern China. *Journal of fungi (Basel, Switzerland)*, *10*(12), 845. https://doi.org/10.3390/jof10120845

Tang, Y., Tian, C., Yao, D., Yang S., Shi L., Yi L. (2024). Community assembly and potential function analysis of the endophyte in *Eucommia ulmoides*. *BMC Microbiol* 24, 460 https://doi.org/10.1186/s12866-024-03601-0

Tanney, J. (2017). A taxonomic and phylogenetic investigation of conifer endophytes of Eastern Canada (Doctoral dissertation, Carleton University).

Toju, H., Tanabe, A. S., Yamamoto, S., & Sato, H. (2012). High-coverage ITS primers for the DNA-based identification of ascomycetes and basidiomycetes in environmental samples. *PloS One*,7(7), e40863. https://doi.org/10.1371/journal.pone.0040863

Vasse M., Voglmayr H., Mayer V., Gueidan C., Nepel M., Moreno L., de Hoog S., Selosse M., McKey D., Blatrix R. (2017). A phylogenetic perspective on the association between ants (Hymenoptera: Formicidae) and black yeasts (Ascomycota: Chaetothyriales). *Proc Biol Sci* 1; 284 (1850): 20162519. https://doi.org/10.1098/rspb.2016.2519

Videira, S., Groenewald, J., Braun, U., Shin, H., & Crous, P. (2016). All that glitters is not Ramularia. *Studies in mycology*, *83*, 49–163. https://doi.org/10.1016/j.simyco.2016.06.001

Watts, D., Palombo, E. A., Jaimes Castillo, A., & Zaferanloo, B. (2023). Endophytes in agriculture: potential to improve yields and tolerances of agricultural crops. *Microorganisms*, *11*(5), 1276. https://doi.org/10.3390/microorganisms11051276

White, T., Bruns, T., Lee, S., & Taylor, J. (1990). Amplification and direct sequencing of fungal ribosomal RNA genes for phylogenetics. In Sninsky J and White T. San Diego: CA *Academic Press* (Vol. 38, pp. 315–322). https://doi.org/10.1016/B978-0-12-372180-8.50042-1

Wong, B. L., Baggett, K., & Rye, A. (2003). Seasonal patterns of reserve and soluble carbohydrates in mature sugar maple (*Acer saccharum*). *Canadian Journal of Botany*, *81*(8), 780-788.Abdelfattah, A., Malacrinò, A., Wisniewski, M., Cacciola, S. O., & Schena, L. (2018).

Xu, J., Saunders, W., Hu, P., Grant, A., Boekhout, T., Kuramae, E., Kronstad, W., Deangelis, M., Reeder, L., Johnstone, R., Leland, M., Fieno, M., Begley, M., Sun, Y., Lacey, P., Chaudhary, T., Keough, T., Chu, L., Sears, R., Yuan, B., … Dawson, L., (2007). Dandruff-associated Malassezia genomes reveal convergent and divergent virulence traits shared with plant and human fungal pathogens. *Proceedings of the National Academy of Sciences of the United States of America*, *104*(47), 18730–18735. https://doi.org/10.1073/pnas.07067561

Zipfel, C., & Oldroyd, G. E. (2017). Plant signalling in symbiosis and immunity. *Nature*, *543*(7645), 328-336. https://doi.org/10.1038/nature22009

Appendices

Appendix A: Metadata

Table 1: Brush species and composition adjacent 16 trees at the West45 research site collected over the 2025 growing season. Crown closure (cc) and heights (cm) are listed for each brush species at each tree.
The ✓ icon indicates plant species present, x indicates absent. See plant code legend for species names.

Tree	GASH	CC	Height	VAPA	CC	Height	RUSP	CC	Height	RUSU	CC	Height	EPAN	CC	Height	LOIN	CC	Height	PREM	CC	Height
323	✓	2	100	✓	2	150	✓	8	120	✓	1	50	✓	1	190	x	x	x	x	x	x
201	✓	30	50	✓	1	120	✓	1	100	✓	2	50	✓	1	180	x	x	x	x	x	x
199	✓	5	100	✓	1	120	✓	3	120	✓	1	50	✓	1	200	x	x	x	✓	1	300
283	✓	5	50	✓	1	150	✓	5	200	✓	1	50	✓	1	130	x	x	x	✓	8	300
196	✓	1	50	✓	2	150	✓	1	100	✓	1	50	x	x	x	✓	1	50	✓	10	250
287	✓	5	50	✓	3	120	✓	1	100	✓	1	50	x	x	x	x	x	x	✓	20	300
408	✓	30	50	✓	1	100	x	x	x	x	x	x	✓	1	100	x	x	x	✓	10	250
68	✓	40	80	✓	1	1.8	✓	1	150	✓	1	50	✓	1	120	x	x	x	✓	20	300
662	✓	30	50	✓	1	120	x	x	x	✓	1	50	✓	1	200	x	x	x	✓	7	250
544	✓	40	50	✓	1	120	x	x	x	✓	30	50	✓	1	200	x	x	x	✓	7	250
793	✓	30	50	✓	2	150	✓	1	150	x	x	x	x	x	x	x	x	x	✓	15	300
1047	✓	20	50	✓	1	120	x	x	x	✓	1	60	✓	1	200	x	x	x	✓	1	300
808	✓	5	50	✓	2	150	✓	2	170	✓	1	60	✓	1	200	x	x	x	✓	10	300
555	x	x	x	✓	1	120	x	x	x	✓	1	50	✓	1	200	x	x	x	x	x	x
689	x	x	x	✓	5	150	✓	5	150	✓	1	60	x	x	x	x	x	x	✓	15	350
276	✓	1	50	✓	1	120	✓	5	150	✓	2	50	✓	1	220	x	x	x	✓	25	350

	BLSP	CC	Height	POMU	CC	Height	RUAR	CC	Height	RULA	CC	Height	PTAQ	CC	Height	RUPA	CC	Height
323	✓	1	100	✓	1	100	x	x	x	x	x	x	x	x	x	x	x	x
201	✓	1	100	✓	1	100	x	x	x	x	x	x	x	x	x	✓	1	120
199	✓	1	50	✓	1	50	x	x	x	✓	3	300	x	x	x	x	x	x
283	✓	1	50	x	x	x	x	x	x	✓	3	200	x	x	x	x	x	x

196	x	x	x	x	x	x	x	x	x	x	x	x	x	x	x	x	x	x
287	✓	1	50	x	x	x	x	x	x	x	x	x	x	x	x	x	x	x
408	x	x	x	x	x	x	x	x	x	✓	1	200	x	x	x	x	x	x
68	✓	1	50	✓	1	80	x	x	x	x	x	x	x	x	x	x	x	x
662	x	x	x	✓	1	90	x	x	x	x	x	x	✓	5	200	x	x	x
544	x	x	x	✓	1	90	x	x	x	x	x	x	✓	1	120	x	x	x
793	x	x	x	x	x	x	x	x	x	x	x	x	✓	4	200	x	x	x
1047	x	x	x	x	x	x	x	x	x	x	x	x	✓	15	250	x	x	x
808	x	x	x	x	x	x	x	x	x	x	x	x	x	x	x	x	x	x
555	✓	1	50	x	x	x	✓	1	300	x	x	x	x	x	x	x	x	x
689	x	x	x	✓	1	70	x	x	x	x	x	x	x	x	x	x	x	x
276	✓	1	50	✓	1	70	x	x	x	x	x	x	x	x	x	✓	5	150

Plant Code:

Salal (*Gaultheria shallon*) = GASH
Red Huckleberry (*Vaccinium Parvifolium) = VAPA*
Bracken fern (*Pteridium aquilinum*) = PTAQ
Cherry (*Prunus emarginata*) = PREM
Fireweed (*Epilobium angustifolium*) = EPAN
Deer Fern (*Blechnum spican*t) = BLSP
Sword Fern (*Polystichum munitum*) = POMU
Trailing Blackberry (*Rubus sursinus*) = RUSU
Himalayan Blackberry (*Rubus armeniacus*) = RUAR
Cut-Leaf Blackberry (*Rubus laciniatus*) = RULA
Salmon Berry (*Rubus spectabilis*) = RUSP
Thimble Berry (*Rubus parviflorus*) = RUPA
Twin Berry (*Lonicera involucrata*) = LOIN

<u>Table 2</u>: Metadata collected from year 2 needles of 16 trees at the West45 research site over 2025 growing season.

Tree ID	**Family**	**Height Apr (cm)**	**Height Nov (cm)**	**Growth Height (cm)**	**DBH Apr (cm)**	**DBH Nov (cm)**	**Growth Diameter (cm)**	**Needle Loss Sep (%)**	**Average Occlusion (proportion)**	**Soil pH**
323	64	370	452	82	3.9	5.1	1.2	80	0.222318	5.13
201	14	518	629	111	4.9	6.4	1.5	80	0.402226	4.79
199	34	610	736	126	7.6	10.1	2.5	70	0.256073	4.7
283	14	513	650	137	5	7.6	2.6	40	0.274173	4.8
196	64	518	660	142	6.1	7.5	1.4	20	0.296502	4.96
287	46	577	678	101	7.5	9.3	1.8	70	0.36048	4.98
408	64	348	462	114	5.8	6.1	0.3	60	0.352471	5.15
68	34	572	703	131	6.3	8.5	2.2	70	0.206283	5.08
662	14	358	449	91	3.8	4.9	1.1	30	0.246294	5.7
544	64	210	259	149	1.2	2.7	1.5	60	0.37742	5
793	46	478	619	141	6.8	8.5	1.7	20	0.190883	4.74
1047	46	541	622	81	6.5	8.2	1.7	100	0.42617	5.03
808	34	635	749	114	7.7	9.6	1.9	30	0.213559	4.85
555	14	374			3.1			100	0.169445	5.37
689	34	320	416	96	3.2	3.8	0.6	40	0.405733	4.48
276	46	546	675	129	6.8	8.3	1.5	50	0.233781	6.24

Appendix B: Culture Based Taxonomy

Table 1: Douglas-fir needle fungal endophyte taxonomy acquired through culture-based methods using Sanger sequencing to compare against fungal endophyte taxonomy acquired through Illumina sequencing.

Culture-Based Taxonomy Assignments from Sanger Sequencing	Match or closest to OTUs from High Throughput Meta-Barcoding
Biscogniauxia sp.	*No*
Ceratostomella melanospora	*No*
Cladosporium sp	*Yes*
Coniochaeta sp	*No*
Coniochaeta velutina	*No*
Desmazierella acicola	*No*
Diaporthe rudis	*No*
Fomitopsis ochraceae	*Fomitopsis pinicola*
Geopysix carbonaria	*No*
Humicolopsis cephalosporioides	*No*
Jackrogersella multiformis	*No*
Juxtiphoma eupyrena	*No*
Leptobacillium leptobactrum	*No*
Nemania serpens	*No*
Nothophaeocryptopus gaeumannii	*No*
Oidiodendron sp	*No*
Penicillium angulare	*Penicillium penicilloides*
Penicillium cf. glaucoalbidum	*No*
Penicillium rubens	*No*
Peziza nivalis	*No*
Physalospora sp.	*No*
Plectania melastoma	*No*

Priestia sp	*No*
Pseudoplecantia melaena	*No*
Pseudoplectania sp.	*No*
Pulvinula archeri	*No*
Rhabdocline parkeri	*No*
Rosellinia thelena/Rosellinia mycophila	*No*
Sydowia polyspora	*Sydowia fenestrans*
Tricharina cretea	*No*
Xylaria hypoxylon	*No*
Zasmidium sp	*Yes*

Appendix C: Fungal Traits Assignments

Table 1: Annotated functional traits for fungal endophytes of Douglas-fir needles collected from 16 trees over the 2025 growing season. Only a small portion of the total OTUs were resolved to genus or species levels. OTUs with genus or species level resolution were assigned traits using FungalTraits database in RStudio. Taxa matched with a trait are listed.

Phylum	**Class**	**Order**	**Family**	**Genus**	**Species**	**trophic_final**	**guild_final**
Basidiomycota	Agaricomycetes	Atheliales	Atheliaceae	Amphinema	Amphinema_sp	Symbiotroph	Ectomycorrhizal
Basidiomycota	Agaricomycetes	Cantharellales	Ceratobasidiaceae	Ceratobasidium	Ceratobasidium_sp	Symbiotroph	Ectomycorrhizal
Ascomycota	Eurotiomycetes	Chaetothyriales	Herpotrichiellaceae	Cladophialophora	Cladophialophora_minutissima	Symbiotroph	Endophyte
Ascomycota	Eurotiomycetes	Chaetothyriales	Herpotrichiellaceae	Cladophialophora	NA	Symbiotroph	Endophyte
Ascomycota	Eurotiomycetes	Chaetothyriales	Herpotrichiellaceae	Cladophialophora	NA	Symbiotroph	Endophyte
Ascomycota	Eurotiomycetes	Chaetothyriales	Herpotrichiellaceae	Cladophialophora	NA	Symbiotroph	Endophyte
Ascomycota	Eurotiomycetes	Chaetothyriales	Herpotrichiellaceae	Cladophialophora	NA	Symbiotroph	Endophyte
Ascomycota	Eurotiomycetes	Chaetothyriales	Herpotrichiellaceae	Cladophialophora	NA	Symbiotroph	Endophyte
Ascomycota	Dothideomycetes	Cladosporiales	Cladosporiaceae	Cladosporium	NA	Pathotroph	Plant Pathogen
Ascomycota	Dothideomycetes	Cladosporiales	Cladosporiaceae	Cladosporium	NA	Pathotroph	Plant Pathogen
Ascomycota	Eurotiomycetes	Chaetothyriales	Cyphellophoraceae	Cyphellophora	Cyphellophora_gamsii	Pathotroph	Animal Pathogen
Ascomycota	Dothideomycetes	Pleosporales	Didymellaceae	Epicoccum	Epicoccum_nigrum	Pathotroph-Symbiotroph	Endophyte-Plant Pathogen
Ascomycota	Eurotiomycetes	Chaetothyriales	Herpotrichiellaceae	Exophiala	Exophiala_sp	Pathotroph	Animal Pathogen
Basidiomycota	Agaricomycetes	Polyporales	Fomitopsidaceae	Fomitopsis	Fomitopsis_pinicola	Pathotroph-Saprotroph	Plant Pathogen-Wood Saprotroph
Basidiomycota	Agaricomycetes	Agaricales	Strophariaceae	Hypholoma	Hypholoma_capnoides	Saprotroph	Wood Saprotroph
Basidiomycota	Agaricomycetes	Agaricales	Strophariaceae	Hypholoma	Hypholoma_dispersum	Saprotroph	Wood Saprotroph
Basidiomycota	Agaricomycetes	Agaricales	Strophariaceae	Hypholoma	Hypholoma_fasciculare	Saprotroph	Wood Saprotroph
Ascomycota	Eurotiomycetes	Chaetothyriales	Trichomeriaceae	Knufia	Knufia_sp	Pathotroph	Lichen Parasite
Ascomycota	Leotiomycetes	Helotiales	Lachnaceae	Lachnum	Lachnum_clandestinum	Saprotroph	Undefined Saprotroph
Ascomycota	Leotiomycetes	Helotiales	Lachnaceae	Lachnum	Lachnum_sp	Saprotroph	Undefined Saprotroph
Basidiomycota	Malasseziomycetes	Malasseziales	Malasseziaceae	Malassezia	Malassezia_restricta_var1	Pathotroph	Animal Pathogen
Basidiomycota	Malasseziomycetes	Malasseziales	Malasseziaceae	Malassezia	Malassezia_restricta_var2	Pathotroph	Animal Pathogen

Basidiomycota	Malasseziomycetes	Malasseziales	Malasseziaceae	Malassezia	Malassezia_sp	Pathotroph	Animal Pathogen
Ascomycota	Sordariomycetes	Xylariales	Microdochiaceae	Microdochium	Microdochium_phragmitis	Pathotroph	Plant Pathogen
Ascomycota	Leotiomycetes	Helotiales	Mollisiacea	Mollisia	Mollisia_fuscoparaphysata	Pathotroph	Plant Pathogen
Ascomycota	Eurotiomycetes	Chaetothyriales	Chaetothyriales_fam_Incertae_sedis	Sarcinomyces	Sarcinomyces_crustaceus	Symbiotroph	Endophyte
Basidiomycota	Agaricomycetes	Cantharellales	Hydnaceae	Sistotrema	Sistotrema_sp1*	Saprotroph-Symbiotroph	Ectomycorrhizal-Wood Saprotroph
Basidiomycota	Agaricomycetes	Cantharellales	Hydnaceae	Sistotrema	Sistotrema_sp1*	Saprotroph-Symbiotroph	Ectomycorrhizal-Wood Saprotroph
Basidiomycota	Agaricomycetes	Cantharellales	Hydnaceae	Sistotrema	NA	Saprotroph-Symbiotroph	Ectomycorrhizal-Wood Saprotroph
Basidiomycota	Agaricomycetes	Cantharellales	Hydnaceae	Sistotrema	NA	Saprotroph-Symbiotroph	Ectomycorrhizal-Wood Saprotroph
Basidiomycota	Agaricomycetes	Cantharellales	Hydnaceae	Sistotrema	NA	Saprotroph-Symbiotroph	Ectomycorrhizal-Wood Saprotroph
Basidiomycota	Agaricomycetes	Cantharellales	Hydnaceae	Sistotrema	NA	Saprotroph-Symbiotroph	Ectomycorrhizal-Wood Saprotroph
Basidiomycota	Tremellomycetes	Tremellales	Tremellaceae	Tremella	Tremella_globispora_var1	Pathotroph	Fungal Parasite
Basidiomycota	Tremellomycetes	Tremellales	Tremellaceae	Tremella	Tremella_globispora_var2	Pathotroph	Fungal Parasite
Basidiomycota	Tremellomycetes	Tremellales	Tremellaceae	Tremella	Tremella_globispora_var3	Pathotroph	Fungal Parasite
Basidiomycota	Tremellomycetes	Tremellales	Tremellaceae	Tremella	Tremella_globispora_var4	Pathotroph	Fungal Parasite
Basidiomycota	Tremellomycetes	Tremellales	Tremellaceae	Tremella	Tremella_globispora_var5	Pathotroph	Fungal Parasite
Basidiomycota	Tremellomycetes	Tremellales	Tremellaceae	Tremella	Tremella_globispora_var6	Pathotroph	Fungal Parasite
Basidiomycota	Tremellomycetes	Tremellales	Tremellaceae	Tremella	Tremella_globispora_var7	Pathotroph	Fungal Parasite
Basidiomycota	Agaricomycetes	Russulales	Xenasmataceae	Xenasmatella	NA	Saprotroph	Undefined Saprotroph
Basidiomycota	Agaricomycetes	Russulales	Xenasmataceae	Xenasmatella	NA	Saprotroph	Undefined Saprotroph
Basidiomycota	Agaricomycetes	Russulales	Xenasmataceae	Xenasmatella	Xenasmatella_vaga	Saprotroph	Undefined Saprotroph

Appendix D: Full OTU Taxonomy List

Table 1: Full list of OTU taxonomic assignments for fungal endophytes found in Douglas-fir needles collected from 16 trees at the West 45 research site over the 2025 growing season (n = 94). Table represents 679 OTUs and 639 BUFs. Taxon strings show kingdom_phylum_class_order_family_genus_species. Taxon multiples were collapsed and represented as sp1, sp2, etc., or var1, var2, etc. BUFs are identified with an asterisk (*). Full OTU list with sequences and monthly totals (non-normalized & normalized) can be accessed through the icon link.

feature_taxonomy_se
quence_counts_by_mc

k__kingdom:p__phylum:c__class:o__order:f__family:g__genus:s__species
k__Fungi;p__Ascomycota;c__Lecanoromycetes;o__Unknown;f__Unknown;g__Unknown;s__*Lecanoromycetes_sp1 & sp2*
k__Fungi;p__Ascomycota;c__Archaeorhizomycetes;o__Archaeorhizomycetales;f__Archaeorhizomycetaceae;g__Archaeorhizomyces;s__*Archaeorhizomyces_sp*
k__Fungi;p__Ascomycota;c__Arthoniomycetes;o__Arthoniales;f__Arthoniaceae;g__Arthonia;s__*Arthonia_dispersa*
k__Fungi;p__Ascomycota;c__Arthoniomycetes;o__Lichenostigmatales;f__Phaeococcomycetaceae;g__Phaeococcomyces;s__*Phaeococcomyces_mexicanus*
k__Fungi;p__Ascomycota;c__Arthoniomycetes;o__Unknown;f__Unknown;g__Unknown;s__*Arthoniomycetes_sp*
k__Fungi;p__Ascomycota;c__Dothideomycetes;o__Botryosphaeriales;f__Botryosphaeriaceae;g__Sphaeropsis;s__*Sphaeropsis porosa*
k__Fungi;p__Ascomycota;c__Dothideomycetes;o__Botryosphaeriales;f__Botryosphaeriaceae;g__Unknown;s__*Botryosphaeriaceae_sp*
k__Fungi;p__Ascomycota;c__Dothideomycetes;o__Botryosphaeriales;f__Unknown;g__Unknown;s__*Botryosphaeriales_sp1 - sp10*
k__Fungi;p__Ascomycota;c__Dothideomycetes;o__Capnodiales;f__Unknown;g__Unknown;s__*Capnodiales_sp1 - sp4*
k__Fungi;p__Ascomycota;c__Dothideomycetes;o__Cladosporiales;f__Cladosporiaceae;g__Cladosporium;s__*Cladosporium_sp1 & sp2*
k__Fungi;p__Ascomycota;c__Dothideomycetes;o__Cladosporiales;f__Cladosporiaceae;g__Rachicladosporium;s__*Rachicladosporium_pennatum*
k__Fungi;p__Ascomycota;c__Dothideomycetes;o__Cladosporiales;f__Cladosporiaceae;g__Rachicladosporium;s__*Rachicladosporium_pini*
k__Fungi;p__Ascomycota;c__Dothideomycetes;o__Cladosporiales;f__Cladosporiaceae;g__Rachicladosporium;s__*Rachicladosporium_sp1**
k__Fungi;p__Ascomycota;c__Dothideomycetes;o__Cladosporiales;f__Cladosporiaceae;g__Rachicladosporium;s__*Rachicladosporium_sp2 - sp8*
k__Fungi;p__Ascomycota;c__Dothideomycetes;o__Dothideales;f__Dothideaceae;g__Rhizosphaera;s__*Rhizosphaera sp**

k__Fungi;p__Ascomycota;c__Dothideomycetes;o__Dothideales;f__Unknown;g__Unknown;s__*Dothideales_sp1*
k__Fungi;p__Ascomycota;c__Dothideomycetes;o__Unknown;f__Micropeltidaceae;g__Stomiopeltis;s__*Stomiopeltis_sp*
k__Fungi;p__Ascomycota;c__Dothideomycetes;o__Unknown;f__Unknown;g__Peltaster;s__*Peltaster_sp*
k__Fungi;p__Ascomycota;c__Dothideomycetes;o__Mycosphaerellales;f__Dissoconiaceae;g__Dissoconium;s__*Dissoconium_sp1*
k__Fungi;p__Ascomycota;c__Dothideomycetes;o__Mycosphaerellales;f__Dissoconiaceae;g__Unknown;s__*Dissoconiaceae_sp1*
k__Fungi;p__Ascomycota;c__Dothideomycetes;o__Mycosphaerellales;f__Dissoconiaceae;g__Uwebraunia;s__*Uwebraunia_musae*
k__Fungi;p__Ascomycota;c__Dothideomycetes;o__Mycosphaerellales;f__Extremaceae;g__Extremopsis;s__*Extremopsis_radicicola*
k__Fungi;p__Ascomycota;c__Dothideomycetes;o__Mycosphaerellales;f__Extremaceae;g__Extremus;s__*Extremus_adstrictus*
k__Fungi;p__Ascomycota;c__Dothideomycetes;o__Mycosphaerellales;f__Extremaceae;g__Paradevriesia;s__*Paradevriesia_pseudoamericana_var1 & var2*
k__Fungi;p__Ascomycota;c__Dothideomycetes;o__Mycosphaerellales;f__Mycosphaerellaceae;g__Chuppomyces;s__*Chuppomyces_handelii*
k__Fungi;p__Ascomycota;c__Dothideomycetes;o__Mycosphaerellales;f__Mycosphaerellaceae;g__Nothophaeocryptopus;s__*Nothophaeocryptopus_gaeumannii*
k__Fungi;p__Ascomycota;c__Dothideomycetes;o__Mycosphaerellales;f__Mycosphaerellaceae;g__Pachyramichloridium;s__*Pachyramichloridium_sp*
k__Fungi;p__Ascomycota;c__Dothideomycetes;o__Mycosphaerellales;f__Mycosphaerellaceae;g__Ramularia;s__*Ramularia_digitalis-ambiguae*
k__Fungi;p__Ascomycota;c__Dothideomycetes;o__Mycosphaerellales;f__Mycosphaerellaceae;g__Ramularia;s__*Ramularia_sp1 - sp5*
k__Fungi;p__Ascomycota;c__Dothideomycetes;o__Mycosphaerellales;f__Mycosphaerellaceae;g__Sphaerulina;s__*Sphaerulina_pelargonii*
k__Fungi;p__Ascomycota;c__Dothideomycetes;o__Mycosphaerellales;f__Mycosphaerellaceae;g__Unknown;s__*Mycosphaerellaceae_sp1 - sp12*
k__Fungi;p__Ascomycota;c__Dothideomycetes;o__Mycosphaerellales;f__Mycosphaerellaceae;g__Zasmidium;s__*Zasmidium_sp1*
k__Fungi;p__Ascomycota;c__Dothideomycetes;o__Mycosphaerellales;f__Mycosphaerellaceae;g__Zymoseptoria;s__*Zymoseptoria_ardabiliae*
k__Fungi;p__Ascomycota;c__Dothideomycetes;o__Mycosphaerellales;f__Neodevriesiaceae;g__Neodevriesia;s__*Neodevriesia_knoxdaviesii*
k__Fungi;p__Ascomycota;c__Dothideomycetes;o__Mycosphaerellales;f__Neodevriesiaceae;g__Neodevriesia;s__*Neodevriesia_sp1 & sp2*
k__Fungi;p__Ascomycota;c__Dothideomycetes;o__Mycosphaerellales;f__Teratosphaeriaceae;g__Acrodontium;s__*Acrodontium_crateriforme*
k__Fungi;p__Ascomycota;c__Dothideomycetes;o__Mycosphaerellales;f__Teratosphaeriaceae;g__Acrodontium;s__*Acrodontium_luzulae*
k__Fungi;p__Ascomycota;c__Dothideomycetes;o__Mycosphaerellales;f__Teratosphaeriaceae;g__Bryochiton;s__*Bryochiton_sp*
k__Fungi;p__Ascomycota;c__Dothideomycetes;o__Mycosphaerellales;f__Teratosphaeriaceae;g__Capnobotryella;s__*Capnobotryella_sp1 & sp2*
k__Fungi;p__Ascomycota;c__Dothideomycetes;o__Mycosphaerellales;f__Teratosphaeriaceae;g__Catenulostroma;s__*Catenulostroma_hermanusense_var1 & var2*
k__Fungi;p__Ascomycota;c__Dothideomycetes;o__Mycosphaerellales;f__Teratosphaeriaceae;g__Constantinomyces;s__*Constantinomyces_sp*
k__Fungi;p__Ascomycota;c__Dothideomycetes;o__Mycosphaerellales;f__Teratosphaeriaceae;g__Meristemomyces;s__*Meristemomyces_arctostaphyli*
k__Fungi;p__Ascomycota;c__Dothideomycetes;o__Mycosphaerellales;f__Teratosphaeriaceae;g__Microcyclospora;s__*Microcyclospora_tardicrescens*
k__Fungi;p__Ascomycota;c__Dothideomycetes;o__Mycosphaerellales;f__Teratosphaeriaceae;g__Neocatenulostroma;s__*Neocatenulostroma_sp*
k__Fungi;p__Ascomycota;c__Dothideomycetes;o__Mycosphaerellales;f__Teratosphaeriaceae;g__Penidiella;s__*Penidiella_ellipsoidea*

k__Fungi;p__Ascomycota;c__Dothideomycetes;o__Mycosphaerellales;f__Teratosphaeriaceae;g__Teratosphaeria;s__*Teratosphaeria_sp1*
k__Fungi;p__Ascomycota;c__Dothideomycetes;o__Mycosphaerellales;f__Teratosphaeriaceae;g__Unknown;s__*Teratosphaeriaceae_sp1 - sp13*
k__Fungi;p__Ascomycota;c__Dothideomycetes;o__Mycosphaerellales;f__Teratosphaeriaceae;g__Xenoteratosphaeria;s__*Xenoteratosphaeria_jonkershoekensis*
k__Fungi;p__Ascomycota;c__Dothideomycetes;o__Mycosphaerellales;f__Unknown;g__Unknown;s__*Mycosphaerellales_sp1 - sp6*
k__Fungi;p__Ascomycota;c__Dothideomycetes;o__Myriangiales;f__Myriangiaceae;g__Anhellia;s__*Anhellia_sp*
k__Fungi;p__Ascomycota;c__Dothideomycetes;o__Myriangiales;f__Unknown;g__Unknown;s__*Myriangiales_sp1*
k__Fungi;p__Ascomycota;c__Dothideomycetes;o__Mytilinidiales;f__Unknown;g__Unknown;s__*Mytilinidiales_sp2*
k__Fungi;p__Ascomycota;c__Dothideomycetes;o__Pleosporales;f__Didymellaceae;g__Epicoccum;s__*Epicoccum_nigrum*
k__Fungi;p__Ascomycota;c__Dothideomycetes;o__Pleosporales;f__Didymosphaeriaceae;g__Paraphaeosphaeria;s__*Paraphaeosphaeria_michotii*
k__Fungi;p__Ascomycota;c__Dothideomycetes;o__Pleosporales;f__Leptosphaeriaceae;g__Leptosphaeria;g__*Leptosphaeria_sp*
k__Fungi;p__Ascomycota;c__Dothideomycetes;o__Pleosporales;f__Leptosphaeriaceae;g__Plenodomus;s__*Plenodomus_sp*
k__Fungi;p__Ascomycota;c__Dothideomycetes;o__Pleosporales;f__Lophiostomataceae;g__Lophiostoma;s__*Lophiostoma_corticola*
k__Fungi;p__Ascomycota;c__Dothideomycetes;o__Pleosporales;f__Phaeosphaeriaceae;g__Phaeosphaeria;s__*Phaeosphaeria_sp*
k__Fungi;p__Ascomycota;c__Dothideomycetes;o__Pleosporales;f__Pleosporaceae;g__Hendersonia;s__*Hendersonia_pinicola*
k__Fungi;p__Ascomycota;c__Dothideomycetes;o__Pleosporales;f__Sporormiaceae;g__Preussia;s__*Preussia_sp*
k__Fungi;p__Ascomycota;c__Dothideomycetes;o__Unknown;f__Unknown;g__Unknown;s__*Dothideomycetes_sp1 - sp19*
k__Fungi;p__Ascomycota;c__Dothideomycetes;o__Unknown;f__Unknown;g__Unknown;s__*Dothideomycetes_sp20**
k__Fungi;p__Ascomycota;c__Dothideomycetes;o__Venturiales;f__Sympoventuriaceae;g__Unknown;s__*Sympoventuriaceae_sp*
k__Fungi;p__Ascomycota;c__Dothideomycetes;o__Venturiales;f__Unknown;g__Unknown;s__Venturiales_sp1 & sp2
k__Fungi;p__Ascomycota;c__Eurotiomycetes;o__Chaetothyriales;f__Chaetothyriaceae;g__Ceramothyrium;s__*Ceramothyrium_carniolicum*
k__Fungi;p__Ascomycota;c__Eurotiomycetes;o__Chaetothyriales;f__Chaetothyriales_fam_Incertae_sedis;g__Sarcinomyces;s__*Sarcinomyces_crustaceus*
k__Fungi;p__Ascomycota;c__Eurotiomycetes;o__Chaetothyriales;f__Cyphellophoraceae;g__Cyphellophora;s__*Cyphellophora_gamsii*
k__Fungi;p__Ascomycota;c__Eurotiomycetes;o__Chaetothyriales;f__Herpotrichiellaceae;g__Cladophialophora;s__*Cladophialophora_minutissima*
k__Fungi;p__Ascomycota;c__Eurotiomycetes;o__Chaetothyriales;f__Herpotrichiellaceae;g__Cladophialophora;s__*Cladophialophora_sp1 - sp5*
k__Fungi;p__Ascomycota;c__Eurotiomycetes;o__Chaetothyriales;f__Herpotrichiellaceae;g__Exophiala;s__*Exophiala_sp*
k__Fungi;p__Ascomycota;c__Eurotiomycetes;o__Chaetothyriales;f__Herpotrichiellaceae;g__Unknown;s__*Herpotrichiellaceae_sp1 - sp5*
k__Fungi;p__Ascomycota;c__Eurotiomycetes;o__Chaetothyriales;f__Trichomeriaceae;g__Knufia;s__*Knufia_sp*
k__Fungi;p__Ascomycota;c__Eurotiomycetes;o__Chaetothyriales;f__Unknown;g__Unknown;s__*Chaetothyriales_sp1**
k__Fungi;p__Ascomycota;c__Eurotiomycetes;o__Chaetothyriales;f__Unknown;g__Unknown;s__*Chaetothyriales_sp2 - sp17*
k__Fungi;p__Ascomycota;c__Eurotiomycetes;o__Eurotiales;f__Aspergillaceae;g__Penicillium;s__*Penicillium_penicillioides*

k__Fungi;p__Ascomycota;c__Eurotiomycetes;o__Eurotiales;f__Aspergillaceae;g__Unknown;s__*Aspergillaceae_sp*
k__Fungi;p__Ascomycota;c__Eurotiomycetes;o__Unknown;f__Unknown;g__Unknown;s__Eurotiomycetes_sp1* - sp5*
k__Fungi;p__Ascomycota;c__Eurotiomycetes;o__Unknown;f__Unknown;g__Unknown;s__*Eurotiomycetes_sp6 - sp42*
k__Fungi;p__Ascomycota;c__Lecanoromycetes;o__Baeomycetales;f__Xylographaceae;g__Xylographa;s__*Xylographa_hians*
k__Fungi;p__Ascomycota;c__Lecanoromycetes;o__Baeomycetales;f__Xylographaceae;g__Xylographa;s__*Xylographa_rubescens*
k__Fungi;p__Ascomycota;c__Lecanoromycetes;o__Lecanorales;f__Lecanoraceae;g__Lecanora;s__*Lecanora_farinaria*
k__Fungi;p__Ascomycota;c__Lecanoromycetes;o__Lecanorales;f__Scoliciosporaceae;g__Scoliciosporum;s__*Scoliciosporum_curvatum*
k__Fungi;p__Ascomycota;c__Lecanoromycetes;o__Lecanorales;f__Scoliciosporaceae;g__Scoliciosporum;s__*Scoliciosporum_sarothamni*
k__Fungi;p__Ascomycota;c__Lecanoromycetes;o__Lecanorales;f__Unknown;g__Unknown;s__*Lecanorales_sp1 - sp3*
k__Fungi;p__Ascomycota;c__Leotiomycetes;o__Helotiales;f__Cenangiaceae;g__Rhabdocline;s__*Rhabdocline_parkeri*
k__Fungi;p__Ascomycota;c__Leotiomycetes;o__Helotiales;f__Cenangiaceae;g__Rhabdocline;s__*Rhabdocline_pseudotsugae*
k__Fungi;p__Ascomycota;c__Leotiomycetes;o__Helotiales;f__Discinellaceae;g__Articulospora;s__*Articulospora_tetracladia*
k__Fungi;p__Ascomycota;c__Leotiomycetes;o__Helotiales;f__Drepanopezizaceae;g__Blumeriella;s__*Blumeriella_jaapii*
k__Fungi;p__Ascomycota;c__Leotiomycetes;o__Helotiales;f__Hamatocanthoscyphaceae;g__Ciliolarina;s__*Ciliolarina_ligniseda*
k__Fungi;p__Ascomycota;c__Leotiomycetes;o__Helotiales;f__Hamatocanthoscyphaceae;g__Infundichalara;s__*Infundichalara microchona*
k__Fungi;p__Ascomycota;c__Leotiomycetes;o__Helotiales;f__Helotiaceae;g__Hymenoscyphus;s__*Hymenoscyphus_sp*
k__Fungi;p__Ascomycota;c__Leotiomycetes;o__Helotiales;f__Helotiaceae;g__Unknown;s__*Helotiaceae_sp*
k__Fungi;p__Ascomycota;c__Leotiomycetes;o__Helotiales;f__Hyaloscyphaceae;g__Eupezizella;s__*Eupezizella britannica*
k__Fungi;p__Ascomycota;c__Leotiomycetes;o__Helotiales;f__Hyaloscyphaceae;g__Hyaloscypha;s__*Hyaloscypha_sp1*
k__Fungi;p__Ascomycota;c__Leotiomycetes;o__Helotiales;f__Hyaloscyphaceae;g__Scolecolachnum;s__*Scolecolachnum_sp*
k__Fungi;p__Ascomycota;c__Leotiomycetes;o__Helotiales;f__Hyaloscyphaceae;g__Unknown;s__*Hyaloscyphaceae_sp*
k__Fungi;p__Ascomycota;c__Leotiomycetes;o__Helotiales;f__Lachnaceae;g__Lachnum;s__*Lachnum_clandestinum*
k__Fungi;p__Ascomycota;c__Leotiomycetes;o__Helotiales;f__Lachnaceae;g__Lachnum;s__*Lachnum_sp*
k__Fungi;p__Ascomycota;c__Leotiomycetes;o__Helotiales;f__Lachnaceae;g__Unknown;s__*Lachnaceae_sp*
k__Fungi;p__Ascomycota;c__Leotiomycetes;o__Helotiales;f__Mollisiacea;g__Mollisia;s__*Mollisia_fuscoparaphysata*
k__Fungi;p__Ascomycota;c__Leotiomycetes;o__Helotiales;f__Mollisiaceae;g__Phialocephala;s__*Phialocephala_sp*
k__Fungi;p__Ascomycota;c__Leotiomycetes;o__Helotiales;f__Pezizellaceae;g__Calycellina;s__*Calycellina_leucella*
k__Fungi;p__Ascomycota;c__Leotiomycetes;o__Helotiales;f__Pezizellaceae;g__Calycina;s__*Calycina_marina*
k__Fungi;p__Ascomycota;c__Leotiomycetes;o__Helotiales;f__Pezizellaceae;g__Calycina;s__*Calycina_sp*
k__Fungi;p__Ascomycota;c__Leotiomycetes;o__Helotiales;f__Pezizellaceae;g__Xenopolyscytalum;s__*Xenopolyscytalum_pinea*

k__Fungi;p__Ascomycota;c__Leotiomycetes;o__Helotiales;f__Ploettnerulaceae;g__Pyrenopeziza;s__*Pyrenopeziza_revincta*
k__Fungi;p__Ascomycota;c__Leotiomycetes;o__Helotiales;f__Sclerotiniaceae;g__Ciboria;s__*Ciboria_sp*
k__Fungi;p__Ascomycota;c__Leotiomycetes;o__Helotiales;f__Tricladiaceae;g__Tricladium;s__*Tricladium biappendiculatum*
k__Fungi;p__Ascomycota;c__Leotiomycetes;o__Helotiales;f__Unknown;g__Unknown;s__*Helotiales_sp1 - sp18*
k__Fungi;p__Ascomycota;c__Leotiomycetes;o__Phacidiales;f__Phacidiaceae;g__Unknown;s__*Phacidiaceae_sp*
k__Fungi;p__Ascomycota;c__Leotiomycetes;o__Thelebolales;f__Pseudeurotiaceae;g__Geomyces;s__*Geomyces_sp*
k__Fungi;p__Ascomycota;c__Leotiomycetes;o__Thelebolales;f__Unknown;g__Unknown;s__*Thelebolales_sp*
k__Fungi;p__Ascomycota;c__Leotiomycetes;o__Unknown;f__Unknown;g__Unknown;s__*Leotiomycetes_sp1 - sp9*
k__Fungi;p__Ascomycota;c__Orbiliomycetes;o__Orbiliales;f__Orbiliaceae;g__Retiarius;s__*Retiarius_sp*
k__Fungi;p__Ascomycota;c__Sordariomycetes;o__Amphisphaeriales;f__Sporocadaceae;g__Seimatosporium;s__*Seimatosporium_sp*
k__Fungi;p__Ascomycota;c__Sordariomycetes;o__Diaporthales;f__Sydowiellaceae;g__Sydowiella;s__*Sydowiella_fenestrans*
k__Fungi;p__Ascomycota;c__Sordariomycetes;o__Hypocreales;f__Nectriaceae;g__Cylindromonium;s__*Cylindromonium_eugeniicola*
k__Fungi;p__Ascomycota;c__Sordariomycetes;o__Hypocreales;f__Niessliaceae;g__Niesslia;s__*Niesslia_endophytica*
k__Fungi;p__Ascomycota;c__Sordariomycetes;o__Hypocreales;f__Niessliaceae;g__Niesslia;s__*Niesslia_sp*
k__Fungi;p__Ascomycota;c__Sordariomycetes;o__Xylariales;f__Microdochiaceae;g__Microdochium;s__*Microdochium_phragmitis*
k__Fungi;p__Ascomycota;c__Sordariomycetes;o__Xylariales;f__Unknown;g__Unknown;s__*Xylariales_sp*
k__Fungi;p__Ascomycota;c__Sordariomycetes;o__Xylariales;f__Xylariaceae;g__Unknown;s__*Xylariaceae_sp1 & sp2*
k__Fungi;p__Ascomycota;c__Taphrinomycetes;o__Taphrinales;f__Taphrinaceae;g__Taphrina;s__*Taphrina_betulina_var1 - var5*
k__Fungi;p__Ascomycota;c__Taphrinomycetes;o__Taphrinales;f__Taphrinaceae;g__Taphrina;s__*Taphrina_carpini*
k__Fungi;p__Ascomycota;c__Taphrinomycetes;o__Taphrinales;f__Taphrinaceae;g__Taphrina;s__*Taphrina_flavorubra*
k__Fungi;p__Ascomycota;c__Taphrinomycetes;o__Taphrinales;f__Taphrinaceae;g__Taphrina;s__*Taphrina_sp1 - sp7*
k__Fungi;p__Ascomycota;c__Taphrinomycetes;o__Taphrinales;f__Taphrinaceae;g__Taphrina;s__*Taphrina_vestergrenii*
k__Fungi;p__Ascomycota;c__Taphrinomycetes;o__Taphrinales;f__Taphrinaceae;g__Unknown;s__*Taphrinaceae_sp*
k__Fungi;p__Ascomycota;c__Unknown;o__Unknown;f__Unknown;g__Unknown;s__*Ascomycota_sp1 - sp53*
k__Fungi;p__Basidiomycota;c__ Cystobasidiomycetes;o__Erythrobasidiales;f__Erythrobasidiaceae;g__Unknown;s__ *Erythrobasidiaceae_sp2 & sp2*
k__Fungi;p__Basidiomycota;c__ Cystobasidiomycetes;o__Unknown;f__Unknown;g__Unknown;s__ *Cystobasidiomycetes_sp1 & sp2*
k__Fungi;p__Basidiomycota;c__Agaricomycetes;o__Agaricales;f__Hydnangiaceae;g__Laccaria:s__*Laccaria_sp*
k__Fungi;p__Basidiomycota;c__Agaricomycetes;o__Agaricales;f__Mycenaceae;g__Roridomyces;s__*Roridomyces_roridus*
k__Fungi;p__Basidiomycota;c__Agaricomycetes;o__Agaricales;f__Strophariaceae;g__Deconica;s__*Deconica_horizontalis*
k__Fungi;p__Basidiomycota;c__Agaricomycetes;o__Agaricales;f__Strophariaceae;g__Hypholoma;s__*Hypholoma_capnoides*

k__Fungi;p__Basidiomycota;c__Agaricomycetes;o__Agaricales;f__Strophariaceae;g__Hypholoma;s__*Hypholoma_dispersum*
k__Fungi;p__Basidiomycota;c__Agaricomycetes;o__Agaricales;f__Strophariaceae;g__Hypholoma;s__*Hypholoma_fasciculare*
k__Fungi;p__Basidiomycota;c__Agaricomycetes;o__Agaricales;f__Typhulaceae;g__Unknown;s__*Typhulaceae_sp*
k__Fungi;p__Basidiomycota;c__Agaricomycetes;o__Atheliales;f__Atheliaceae;g__Amphinema;s__*Amphinema_sp*
k__Fungi;p__Basidiomycota;c__Agaricomycetes;o__Boletales;f__Serpulaceae;g__Serpula;s__*Serpula_himantioides*
k__Fungi;p__Basidiomycota;c__Agaricomycetes;o__Boletales;f__Tapinellaceae;g__Tapinella;s__*Tapinella_atrotomentosa*
k__Fungi;p__Basidiomycota;c__Agaricomycetes;o__Cantharellales;f__Botryobasidiaceae;g__Botryobasidium;s__*Botryobasidium_candicans*
k__Fungi;p__Basidiomycota;c__Agaricomycetes;o__Cantharellales;f__Botryobasidiaceae;g__Botryobasidium;s__*Botryobasidium_sp*
k__Fungi;p__Basidiomycota;c__Agaricomycetes;o__Cantharellales;f__Botryobasidiaceae;g__Botryobasidium;s__*Botryobasidium_subcoronatum*
k__Fungi;p__Basidiomycota;c__Agaricomycetes;o__Cantharellales;f__Botryobasidiaceae;g__Botryobasidium;s__*Botryobasidium_tubulicystidium*
k__Fungi;p__Basidiomycota;c__Agaricomycetes;o__Cantharellales;f__Ceratobasidiaceae;g__Ceratobasidium;s__*Ceratobasidium_sp*
k__Fungi;p__Basidiomycota;c__Agaricomycetes;o__Cantharellales;f__Ceratobasidiaceae;g__Unknown;s__*Ceratobasidiaceae_sp1 & sp2*
k__Fungi;p__Basidiomycota;c__Agaricomycetes;o__Cantharellales;f__Clavulinaceae;g__Unknown;s__*Clavulinaceae_sp1 & sp2*
k__Fungi;p__Basidiomycota;c__Agaricomycetes;o__Cantharellales;f__Hydnaceae;g__Burgoa;s__*Burgoa_sp*
k__Fungi;p__Basidiomycota;c__Agaricomycetes;o__Cantharellales;f__Hydnaceae;g__Sistotrema;s__*Sistotrema_sp**
k__Fungi;p__Basidiomycota;c__Agaricomycetes;o__Cantharellales;f__Hydnaceae;g__Sistotrema;s__*Sistotrema_sp1 - sp4*
k__Fungi;p__Basidiomycota;c__Agaricomycetes;o__Cantharellales;f__Unknown;g__Unknown;s__*Cantharellales_sp1 & sp2*
k__Fungi;p__Basidiomycota;c__Agaricomycetes;o__Corticiales;f__Corticiaceae;g__Unknown;s__*Corticiaceae_sp*
k__Fungi;p__Basidiomycota;c__Agaricomycetes;o__Hymenochaetales;f__Hymenochaetaceae;g__Fuscoporia;s__*Fuscoporia_ferrea*
k__Fungi;p__Basidiomycota;c__Agaricomycetes;o__Hymenochaetales;f__Hymenochaetaceae;g__Tubulicrinis;s__*Tubulicrinis_glebulosus*
k__Fungi;p__Basidiomycota;c__Agaricomycetes;o__Hymenochaetales;f__Unknown;g__Skvortzovia;s__*Skvortzovia_furfuracea*
k__Fungi;p__Basidiomycota;c__Agaricomycetes;o__Polyporales;f__Dacryobolaceae;g__Postia;s__*Postia_guttulata*
k__Fungi;p__Basidiomycota;c__Agaricomycetes;o__Polyporales;f__Fomitopsidaceae;g__Fomitopsis;s__*Fomitopsis_pinicola*
k__Fungi;p__Basidiomycota;c__Agaricomycetes;o__Polyporales;f__Ganodermataceae;g__Ganoderma;s__*Ganoderma_applanatum*
k__Fungi;p__Basidiomycota;c__Agaricomycetes;o__Polyporales;f__Gelatoporiaceae;g__Cinereomyces;s__*Cinereomyces_lindbladii*
k__Fungi;p__Basidiomycota;c__Agaricomycetes;o__Polyporales;f__Polyporaceae;g__Perenniporia;s__*Perenniporia_subacida*
k__Fungi;p__Basidiomycota;c__Agaricomycetes;o__Polyporales;f__Polyporaceae;g__Trametes;s__*Trametes_versicolor*
k__Fungi;p__Basidiomycota;c__Agaricomycetes;o__Russulales;f__Bondarzewiaceae;g__Heterobasidion;s__*Heterobasidion_parviporum*
k__Fungi;p__Basidiomycota;c__Agaricomycetes;o__Russulales;f__Peniophoraceae;g__Dichostereum;s__*Dichostereum_pallescens*
k__Fungi;p__Basidiomycota;c__Agaricomycetes;o__Russulales;f__Peniophoraceae;g__Peniophora;s__*Peniophora_incarnata*

k__Fungi;p__Basidiomycota;c__Agaricomycetes;o__Russulales;f__Stereaceae;g__Acanthobasidium;s__*Acanthobasidium_sp*
k__Fungi;p__Basidiomycota;c__Agaricomycetes;o__Russulales;f__Stereaceae;g__Aleurodiscus;s__*Aleurodiscus_sp*
k__Fungi;p__Basidiomycota;c__Agaricomycetes;o__Russulales;f__Stereaceae;g__Amylostereum;s__*Amylostereum_chailletii*
k__Fungi;p__Basidiomycota;c__Agaricomycetes;o__Russulales;f__Xenasmataceae;g__Xenasmatella;s__*Xenasmatella_sp1 & sp2*
k__Fungi;p__Basidiomycota;c__Agaricomycetes;o__Thelephorales;f__Thelephoraceae;g__Thelephora;s__*Thelephora_terrestris*
k__Fungi;p__Basidiomycota;c__Agaricomycetes;o__Trechisporales;f__Hydnodontaceae;g__Luellia;s__*Luellia_sp*
k__Fungi;p__Basidiomycota;c__Agaricomycetes;o__Trechisporales;f__Hydnodontaceae;g__Trechispora;s__*Trechispora_sp1 & sp2*
k__Fungi;p__Basidiomycota;c__Agaricomycetes;o__Trechisporales;f__Unknown;g__Unknown;s__*Trechisporales_sp*
k__Fungi;p__Basidiomycota;c__Agaricomycetes;o__Unknown;f__Unknown;g__Unknown;s__*Agaricomycetes_sp1 - sp9*
k__Fungi;p__Basidiomycota;c__Agaricostilbomycetes;o__Agaricostilbales;f__Agaricostilbaceae;g__Pseudobensingtonia;s__*Pseudobensingtonia_fusiformis*
k__Fungi;p__Basidiomycota;c__Agaricostilbomycetes;o__Agaricostilbales;f__Chionosphaeraceae;g__Ballistosporomyces;s__*Ballistosporomyces_sasicola*
k__Fungi;p__Basidiomycota;c__Agaricostilbomycetes;o__Agaricostilbales;f__Chionosphaeraceae;g__Ballistosporomyces;s__*Ballistosporomyces_taupoensis*
k__Fungi;p__Basidiomycota;c__Agaricostilbomycetes;o__Agaricostilbales;f__Chionosphaeraceae;g__Kurtzmanomyces;s__*Kurtzmanomyces_sp*
k__Fungi;p__Basidiomycota;c__Agaricostilbomycetes;o__Agaricostilbales;f__Chionosphaeraceae;g__Unknown;s__*Chionosphaeraceae_sp*
k__Fungi;p__Basidiomycota;c__Agaricostilbomycetes;o__Agaricostilbales;f__Kondoaceae;g__Bensingtonia;s__*Bensingtonia_naganoensis*
k__Fungi;p__Basidiomycota;c__Agaricostilbomycetes;o__Agaricostilbales;f__Kondoaceae;g__Bensingtonia;s__*Bensingtonia_pseudonaganoensis*
k__Fungi;p__Basidiomycota;c__Agaricostilbomycetes;o__Agaricostilbales;f__Kondoaceae;g__Bensingtonia;s__*Bensingtonia_sp1 - sp3*
k__Fungi;p__Basidiomycota;c__Agaricostilbomycetes;o__Agaricostilbales;f__Ruineniaceae;g__Ruinenia;s__*Ruinenia_dracophylli_var1 & var2*
k__Fungi;p__Basidiomycota;c__Cystobasidiomycetes;o__Cystobasidiales;f__Microsporomycetaceae;g__Occultifur;s__*Occultifur_cladoniae*
k__Fungi;p__Basidiomycota;c__Cystobasidiomycetes;o__Cystobasidiales;f__Unknown;g__Unknown;s__*Cystobasidiales_sp*
k__Fungi;p__Basidiomycota;c__Cystobasidiomycetes;o__Erythrobasidiales;f__Erythrobasidiaceae;g__Erythrobasidium;s__*Erythrobasidium_sp*
k__Fungi;p__Basidiomycota;c__Cystobasidiomycetes;o__Unknown;f__Symmetrosporaceae;g__Symmetrospora;s__*Symmetrospora_sp*
k__Fungi;p__Basidiomycota;c__Cystobasidiomycetes;o__Unknown;f__Unknown;g__Unknown;s__*Cystobasidiomycetes_sp1 - sp8*
k__Fungi;p__Basidiomycota;c__Dacrymycetes;o__Dacrymycetales;f__Dacrymycetaceae;g__Unknown;s__*Dacrymycetaceae_sp1*
k__Fungi;p__Basidiomycota;c__Exobasidiomycetes;o__Exobasidiales;f__Exobasidiaceae;g__Exobasidium;s__*Exobasidium_maculosum*
k__Fungi;p__Basidiomycota;c__Exobasidiomycetes;o__Exobasidiales;f__Exobasidiaceae;g__Exobasidium;s__*Exobasidium_sp1 - sp3*
k__Fungi;p__Basidiomycota;c__Exobasidiomycetes;o__Georgefischeriales;f__Gjaerumiaceae;g__Gjaerumia;s__*Gjaerumia_minor*
k__Fungi;p__Basidiomycota;c__Exobasidiomycetes;o__Golubeviales;f__Golubeviaceae;g__Golubevia;s__*Golubevia_pallescens*
k__Fungi;p__Basidiomycota;c__Exobasidiomycetes;o__Unknown;f__Unknown;g__Unknown;s__*Exobasidiomycetes_sp*
k__Fungi;p__Basidiomycota;c__Malasseziomycetes;o__Malasseziales;f__Malasseziaceae;g__Malassezia;s__*Malassezia_restricta_var1 & var2*

k__Fungi;p__Basidiomycota;c__Malasseziomycetes;o__Malasseziales;f__Malasseziaceae;g__Malassezia;s__*Malassezia_sp*
k__Fungi;p__Basidiomycota;c__Microbotryomycetes;o__Kriegeriales;f__Kriegeriaceae;g__Yamadamyces;s__*Yamadamyces_rosulatus*
k__Fungi;p__Basidiomycota;c__Microbotryomycetes;o__Leucosporidiales;f__Leucosporidiaceae;g__Leucosporidium;s__*Leucosporidium_intermedium*
k__Fungi;p__Basidiomycota;c__Microbotryomycetes;o__Sporidiobolales;f__Sporidiobolaceae;g__Rhodotorula;s__*Rhodotorula_sp*
k__Fungi;p__Basidiomycota;c__Microbotryomycetes;o__Sporidiobolales;f__Sporidiobolaceae;g__Sporobolomyces;s__*Sporobolomyces_sp1 & sp2*
k__Fungi;p__Basidiomycota;c__Microbotryomycetes;o__Sporidiobolales;f__Unknown;g__Unknown;s__*Sporidiobolales_sp*
k__Fungi;p__Basidiomycota;c__Microbotryomycetes;o__Unknown;f__ Colacogloeaceae;g__Colacogloea;s__*Colacogloea_sp*
k__Fungi;p__Basidiomycota;c__Microbotryomycetes;o__Unknown;f__Chrysozymaceae;g__Bannozyma;s__*Bannozyma_yamatoana*
k__Fungi;p__Basidiomycota;c__Microbotryomycetes;o__Unknown;f__Chrysozymaceae;g__Fellozyma;s__*Fellozyma_cerberi*
k__Fungi;p__Basidiomycota;c__Microbotryomycetes;o__Unknown;f__Chrysozymaceae;g__Fellozyma;s__*Fellozyma_inositophila*
k__Fungi;p__Basidiomycota;c__Microbotryomycetes;o__Unknown;f__Chrysozymaceae;g__Unknown;s__*Chrysozymaceae_sp1 & sp2*
k__Fungi;p__Basidiomycota;c__Microbotryomycetes;o__Unknown;f__Colacogloeaceae;g__Colacogloea;s__*Colacogloea_eucalyptica*
k__Fungi;p__Basidiomycota;c__Microbotryomycetes;o__Unknown;f__Colacogloeaceae;g__Colacogloea;s__*Colacogloea_falcata*
k__Fungi;p__Basidiomycota;c__Microbotryomycetes;o__Unknown;f__Unknown;g__Curvibasidium;s__*Curvibasidium_sp*
k__Fungi;p__Basidiomycota;c__Microbotryomycetes;o__Unknown;f__Unknown;g__Oberwinklerozyma;s__*Oberwinklerozyma_silvestris*
k__Fungi;p__Basidiomycota;c__Microbotryomycetes;o__Unknown;f__Unknown;g__Pseudohyphozyma;s__*Pseudohyphozyma_buffonii_var1 & var2*
k__Fungi;p__Basidiomycota;c__Microbotryomycetes;o__Unknown;f__Unknown;g__Unknown;s__*Microbotryomycetes_sp1 - sp9*
k__Fungi;p__Basidiomycota;c__Microbotryomycetes;o__Unknown;f__Unknowns;g__Curvibasidium;s__*Curvibasidium_cygneicollum_var1 & var2*
k__Fungi;p__Basidiomycota;c__Tremellomycetes;o__Cystofilobasidiales;f__Cystofilobasidiaceae;g__Cystofilobasidium;s__*Cystofilobasidium_capitatum*
k__Fungi;p__Basidiomycota;c__Tremellomycetes;o__Cystofilobasidiales;f__Mrakiaceae;g__Itersonilia;s__*Itersonilia_pannonica*
k__Fungi;p__Basidiomycota;c__Tremellomycetes;o__Cystofilobasidiales;f__Mrakiaceae;g__Krasilnikovozyma;s__*Krasilnikovozyma_huempii*
k__Fungi;p__Basidiomycota;c__Tremellomycetes;o__Cystofilobasidiales;f__Mrakiaceae;g__Krasilnikovozyma;s__*Krasilnikovozyma_sp*
k__Fungi;p__Basidiomycota;c__Tremellomycetes;o__Cystofilobasidiales;f__Mrakiaceae;g__Tausonia;s__*Tausonia_pamirica*
k__Fungi;p__Basidiomycota;c__Tremellomycetes;o__Cystofilobasidiales;f__Mrakiaceae;g__Udeniomyces;s__*Udeniomyces_pyricola*
k__Fungi;p__Basidiomycota;c__Tremellomycetes;o__Filobasidiales;f__Filobasidiaceae;g__Filobasidium;s__*Filobasidium_chernovii*
k__Fungi;p__Basidiomycota;c__Tremellomycetes;o__Filobasidiales;f__Filobasidiaceae;g__Filobasidium;s__*Filobasidium_wieringae*
k__Fungi;p__Basidiomycota;c__Tremellomycetes;o__Filobasidiales;f__Filobasidiaceae;g__Heterocephalacria;s__*Heterocephalacria_arrabidensis*
k__Fungi;p__Basidiomycota;c__Tremellomycetes;o__Filobasidiales;f__Filobasidiaceae;g__Heterocephalacria;s__*Heterocephalacria_sp*
k__Fungi;p__Basidiomycota;c__Tremellomycetes;o__Filobasidiales;f__Filobasidiaceae;g__Unknown;s__*Filobasidiaceae_sp*
k__Fungi;p__Basidiomycota;c__Tremellomycetes;o__Filobasidiales;f__Piskurozymaceae;g__Piskurozyma;s__*Piskurozyma_fildesensis*

k__Fungi;p__Basidiomycota;c__Tremellomycetes;o__Filobasidiales;f__Piskurozymaceae;g__Piskurozyma;s__*Piskurozyma_sp1 - sp4*
k__Fungi;p__Basidiomycota;c__Tremellomycetes;o__Filobasidiales;f__Piskurozymaceae;g__Piskurozyma;s__*Piskurozyma_taiwanensis*
k__Fungi;p__Basidiomycota;c__Tremellomycetes;o__Filobasidiales;f__Piskurozymaceae;g__Unknown;s__*Piskurozymaceae_sp*
k__Fungi;p__Basidiomycota;c__Tremellomycetes;o__Filobasidiales;f__Unknown;g__Unknown;s__*Filobasidiales_sp1 & sp2*
k__Fungi;p__Basidiomycota;c__Tremellomycetes;o__Tremellales;f__Bulleraceae;g__Genolevuria;s__*Genolevuria_sp*
k__Fungi;p__Basidiomycota;c__Tremellomycetes;o__Tremellales;f__Bulleribasidiaceae;g__Dioszegia;s__*Dioszegia_butyracea*
k__Fungi;p__Basidiomycota;c__Tremellomycetes;o__Tremellales;f__Bulleribasidiaceae;g__Dioszegia;s__*Dioszegia_patagonica*
k__Fungi;p__Basidiomycota;c__Tremellomycetes;o__Tremellales;f__Bulleribasidiaceae;g__Vishniacozyma;s__*Vishniacozyma_victoriae*
k__Fungi;p__Basidiomycota;c__Tremellomycetes;o__Tremellales;f__Cryptococcaceae;g__Cryptococcus;s__*Cryptococcus_sp11**
k__Fungi;p__Basidiomycota;c__Tremellomycetes;o__Tremellales;f__Cryptococcaceae;g__Cryptococcus;s__*Cryptococcus_sp3 - sp10*
k__Fungi;p__Basidiomycota;c__Tremellomycetes;o__Tremellales;f__Cuniculitremaceae;g__Kockovaella;s__*Kockovaella_sp1 & sp2*
k__Fungi;p__Basidiomycota;c__Tremellomycetes;o__Tremellales;f__Naemateliaceae;g__Unknown;s__*Naemateliaceae_sp1 - sp12*
k__Fungi;p__Basidiomycota;c__Tremellomycetes;o__Tremellales;f__Rhynchogastremaceae;g__Papiliotrema;s__*Papiliotrema_sp1 - sp5*
k__Fungi;p__Basidiomycota;c__Tremellomycetes;o__Tremellales;f__Tremellaceae;g__Tremella;s__*Tremella_globispora_var1 - var7*
k__Fungi;p__Basidiomycota;c__Tremellomycetes;o__Tremellales;f__Unknown;g__Unknown;s__*Tremellales_sp1 - sp28*
k__Fungi;p__Basidiomycota;c__Tremellomycetes;o__Tremellales;f__Unknown;g__Unknown;s__*Tremellales_sp29**
k__Fungi;p__Basidiomycota;c__Tremellomycetes;o__Unknown;f__Unknown;g__Unknown;s__*Tremellomycetes_sp1 - sp19*
k__Fungi;p__Basidiomycota;c__Unknown;o__Unknown;f__Unknown;g__Unknown;s__*Basidiomycota_sp1 - sp18*
k__Fungi;p__Unknown;c__Unknown;o__Unknown;f__Unknown;g__Unknown;s__*Fungi_sp**
k__Fungi;p__Unknown;c__Unknown;o__Unknown;f__Unknown;g__Unknown;s__Fungi_*sp1 - sp67*

Appendix E: Stomatal Occlusion by Month

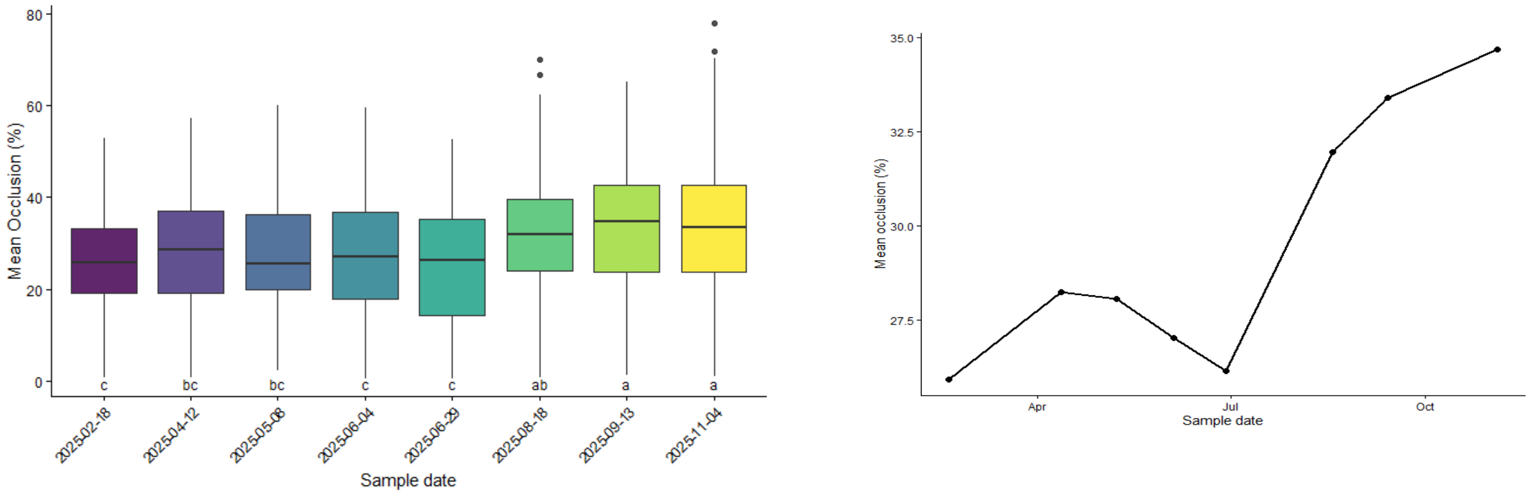

Figure 1: Monthly average of percentage of stomata occluded by N. gaeumannii pseudothecia. Data were acquired from needles of 16 Douglas-fir trees collected eight times over the 2025 growing season. Letters indicate significant differences in average occlusion between months ($p < 0.05$).